Research Department

Technical Report No. 63

A verification study of the global WAM model

December 1987 - November 1988

by

Liana Zambresky(*)
GKSS Forschungszentrum
Federal Republic of Germany

* *Currently a consultant at the European Centre for Medium-Range Weather Forecasts, Reading, U.K.*

May 1989

Abstract

The global ocean wave prediction model, called the WAM model, has been verified against moored buoys for a period of one year in four parts of the world: the Gulf of Alaska, Hawaii, the east coast of the United States and in the Atlantic Ocean north of the United Kingdom.

The WAM model has in general been found to make a good estimate of wave height, but rather often has a tendency to underpredict the extreme waves. This problem was evident in each of the four areas.

A detailed analysis of time series has revealed that the underprediction of peak wave heights appears related to a mechanism limiting the total wave energy in a growing situation when the combination of sea and swell should be substantially exceeding the Pierson-Moskowitz equilibrium wave height.

Peak periods were not available in the northeast Atlantic, but in the remaining three areas, the WAM model makes a good estimate of the shorter peak periods (short wavelengths), but underpredicts the higher peak periods (long wavelengths). In the Hawaiian area, the model, more often than the buoy, has the swell peak to be of higher energy.

The ECMWF 10m surface winds used to drive the WAM model were also verified against the moored buoy observations. In the Gulf of Alaska, the winds were found to be good below 8 m/s, but above 8 m/s, they have a slight positive bias. In the vicinity of the Hawaiian Islands, the trade winds were well estimated at low wind speeds, but underestimated by about 1 m/s for the higher wind speeds. Off the east coast of the United States, there were no biases evident in wind speeds, although the scatter is large. In the northeast Atlantic the winds were biased systematically about .5 m/s too low.

In order to assess the impact of coarse geographical resolution on the quality of wave height estimates made by the WAM model, coarse and fine mesh hindcasts were made for a severe storm in the north Atlantic. It is concluded that the fine mesh implementation is of little or no additional benefit for moderate to large wave systems. However, smaller wave systems, land masses and coastal effects will be resolved better by a fine mesh grid.

CONTENTS

1. INTRODUCTION

Since spring 1987, the third generation wave model, called the WAM model (WAMDIG, 1988; Komen and Zambresky, 1986), has been executing daily at the European Centre for Medium Range Weather Forecasts (ECMWF). This routine execution of the model has allowed near real time verification software to be implemented. The results of this verification will be presented here.

The verification has been carried out in three areas where National Oceanic and Atmospheric Administration (NOAA) moored buoys are available on the Global Telecommunications System (GTS). These areas are the Gulf of Alaska, the Hawaiian Islands and the eastern seaboard of the United States. A fourth area is located in the Atlantic Ocean north of the United Kingdom. Other moored buoys are available, such as in the North Sea, but the coarse 3° resolution of the global WAM model grid rendered verification there useless. Also buoys near to coastlines have not been used, for instance, many along the California coast, because the coarse grid resolution could not resolve coastal effects, if there were any. It is hoped that the buoys chosen will allow the identification of both successes and failures in WAM model physics and will minimize shortcomings due to sub-grid scale effects.

The buoy observations are available hourly over the GTS. They are retrieved from the ECMWF GETDATA automatic ship archive. As the WAM model is driven by instantaneous 10 m winds held constant for 6 hours, the hourly buoy observations have been averaged in time over three hours to make a better temporal comparison. Also, wave heights on the model grid have been linearly interpolated to the buoy location using the four neighboring points. The buoy wave height is reported to the nearest .1 m.

The verification presented here will be only for the 'analysed' D+0 or tau 0 wave height, peak wave period and wind fields. The WAM model has not been forecasting daily beyond 24 hours, so it is not possible to present a verification of forecast fields, at least beyond 24 hours. Also, it should be noted that the analysed wind fields driving the WAM model are not entirely independent of the observations which are used for verification.

The peak period is defined as the inverse of the frequency of peak energy in the frequency domain of the spectrum. The NOAA buoys report the peak period. The WAM model computes it as well as the mean period. Where $E(f,\theta)$ is the energy density, $\Delta\theta$ the directional bandwidth and Δf the frequency bandwidth, the mean period is defined as:

$$T_m = \frac{\sum_f (\Delta\theta \Delta f \frac{1}{f} \sum_\theta E(f,\theta))}{\sum_f (\Delta\theta \Delta f \sum_\theta E(f,\theta))}$$

Some researchers prefer the mean period to the peak period, as the mean period is a more stable measure of the frequency distribution of the spectrum. When a frequency spectrum has more than one peak, the peak period can at times be ambiguous. This is occasionally the case in the Hawaiian area, where the spectra can be bi-modal due to a moderate wind sea and the distinct arrival of long period swell from the southern hemisphere. The swell can have a peak energy which is greater than the local wind sea, but the variance of the wind sea may be greater than that of the swell. This situation is most likely the source of some of the scatter in the plot of peak periods for the Hawaiian area. Unfortunately, mean periods are not available for any of the buoys used in this study.

The four buoys maintained by the United Kingdom report a third measure of the period, called the zero upcrossing period. This is defined as:

$$T_0 = \left[\frac{\sum_f (\Delta\theta \Delta f \sum_\theta E(f,\theta))}{\sum_f (f^2 \Delta\theta \Delta f \sum_\theta E(f,\theta))} \right]^{1/2}$$

As the WAM model does not compute the zero upcrossing period, it is not possible to provide a verification of period in the northeast Atlantic area.

Thus, wave height, peak period and wind statistics will be shown for the first three areas. Only wave height and wind statistics will be presented for the northeast Atlantic. In addition, monthly time series of significant wave height, wind speed, wind direction and the observed air-sea temperature difference will be given at selected buoy locations. Wind and wave statistics for individual buoys will be shown at the bottom of the page.

2. STATISTICS

In this section, an overview of the various statistics presented in this paper is given. The X_i are always the observed values and the Y_i the modeled values.

Mean

$$\overline{X} = \frac{1}{N} \Sigma X_i$$

Standard deviation about the mean

$$\sigma_m = [\frac{1}{N-1} \Sigma (X_i - \overline{X})^2]^{1/2}$$

Standard deviation of the dataset

$$\sigma_d = [\frac{1}{N-1} \Sigma ((X_i - \overline{X}) - (Y_i - \overline{Y}))^2]^{1/2}$$

Bias

$$\text{Bias} = \overline{Y} - \overline{X}$$

Root-mean-square error

$$\text{RMSE} = [\frac{1}{N} \Sigma (Y_i - X_i)^2]^{1/2}$$

Systematic root-mean-square error

$$\text{RMSE}_s = [\frac{1}{N} \Sigma (\hat{Y}_i - X_i)^2]^{1/2}$$

Unsystematic root-mean-square error

$$\text{RMSE}_u = [\frac{1}{N} \sum_i (Y_i - \hat{Y}_i)^2]^{1/2}$$

Least squares fit

The $\hat{Y}_i$ of $RMSE_s$ and $RMSE_u$ are defined in terms of the slope (m) and intercept (b) of the least squares regression.

$$\hat{Y}_i = mX_i + b$$

$$m = \frac{n \Sigma X_i Y_i - (\Sigma X_i)(\Sigma Y_i)}{n \Sigma X_i^2 - (\Sigma X_i)^2}$$

$$b = \overline{Y} - m\overline{X}$$

The least squares regression has been computed in the traditional way, model values versus observations, as well as in the reverse sense, observations versus model values.

Correlation coefficient

$$r = \frac{\Sigma (X_i - \overline{X})(Y_i - \overline{Y})}{[[\Sigma (X_i - \overline{X})^2][\Sigma (Y_i - \overline{Y})^2]]^{1/2}}$$

Scatter index

$$SI = RMSE/\overline{X}$$

The wind statistics include the mean, bias, standard deviation, root-mean-square error, correlation coefficient and scatter index computed both for wind speed and the wind vector. The vector statistics are obtained in the following way:

$$\overline{V}_{mean} = [\overline{u}^2 + \overline{v}^2]^{1/2}$$

$$\text{RMSE}\,(\overline{V}) = [[\text{rmse}(u)]^2 + [\text{rmse}(v)]^2]^{1/2}$$

$$\text{Bias}\,(\overline{V}) = [[\text{bias}(u)]^2 + [\text{bias}(v)]^2]^{1/2}$$

$$\text{Stdev}\,(\overline{V}) = [[\text{stdev}(u)]^2 + [\text{stdev}(v)]^2]^{1/2}$$

$$\text{corr}\,r(\overline{V}) \cong [\tfrac{1}{2} * [r(u)^2 + r(v)^2]]^{1/2}$$

$$\text{SI}\,(\overline{V}) = \text{RMSE}\,(\overline{V})\,/\overline{X}$$

The following is also true:

$$\text{RMSE}\,(\overline{V}) = [[\text{bias}(\overline{V})]^2 + [\text{stdev}(\overline{V})]^2]^{1/2}$$

The mast height of nearly all of the NOAA buoys supplying observations for this study is 5 m. The two exceptions are 46006 in the gulf of Alaska with an anemometer height of 10 m and 44008 off the eastern seaboard of the US with a height of 13.8 m. As the buoys bob up and down on a moving surface, the difference in height of these observations from the 10 m model wind fields was not considered great enough to attempt a height correction via the logarithmic wind profile. If this calculation had been done, a profile for a neutrally stable atmosphere would have been assumed. However, the atmosphere is often unstable, implying a different wind profile than the neutrally stable one, so this adjustment would also have had errors.

3. REGIONAL VERIFICATION

3.1 Gulf of Alaska

3.1.1 Introduction

This is the most favourable of the four areas for verification purposes for several reasons. The dynamic range in wave height is high. Also coastal effects and wave-current interactions (which are not modeled) are minimized. Fetches are essentially infinite as storm systems sweep west to east across the North Pacific. Also of interest is the arrival of very long period swell from the southern hemisphere, on the order of 18-22 sec, which is readily detectable, especially during summer and can give rise to double peaked wave spectra. Fig. 3.1 shows the location of the buoys in the Gulf of Alaska used for this study. In this figure, the wave height chart of 23 Nov 1988 was selected. The contours are wave height in meters. The arrows point in the mean wave direction.

3.1.2 Wave heights and winds

In Fig. 3.2(a) can be seen a plot of the logarithm of the number of collocations of modeled wave heights and buoy wave heights in the Gulf of Alaska. The total number of points plotted is 4657. Both the contour origin and contour interval are .2. The bin width is .25 m. It is clear from this plot that the buoys prefer to report wave height to the nearest .5 m and less frequently to the nearest .25 m. The wave model, in contrast, computes a continuum of wave heights. At low values, in particular, at .5 and 1.0 m, the WAM model appears biased high, while at higher wave heights it is biased low.

In Fig. 3.2(b) can be seen a plot of the log of the number of collocations of ECMWF 10 m winds and wind observations made by buoys. The number of data points is 4451. The contour origin and contour interval are .2. The bin width is .5 m/s. There are no strong biases present in the modeled winds except that above 8 m/s, they may be slightly high. This is in direct contrast to the tendency of the wave model to underpredict the higher waves.

In Table 3.1 are the wind and wave statistics described in Section 2 which have been computed for the Gulf of Alaska.

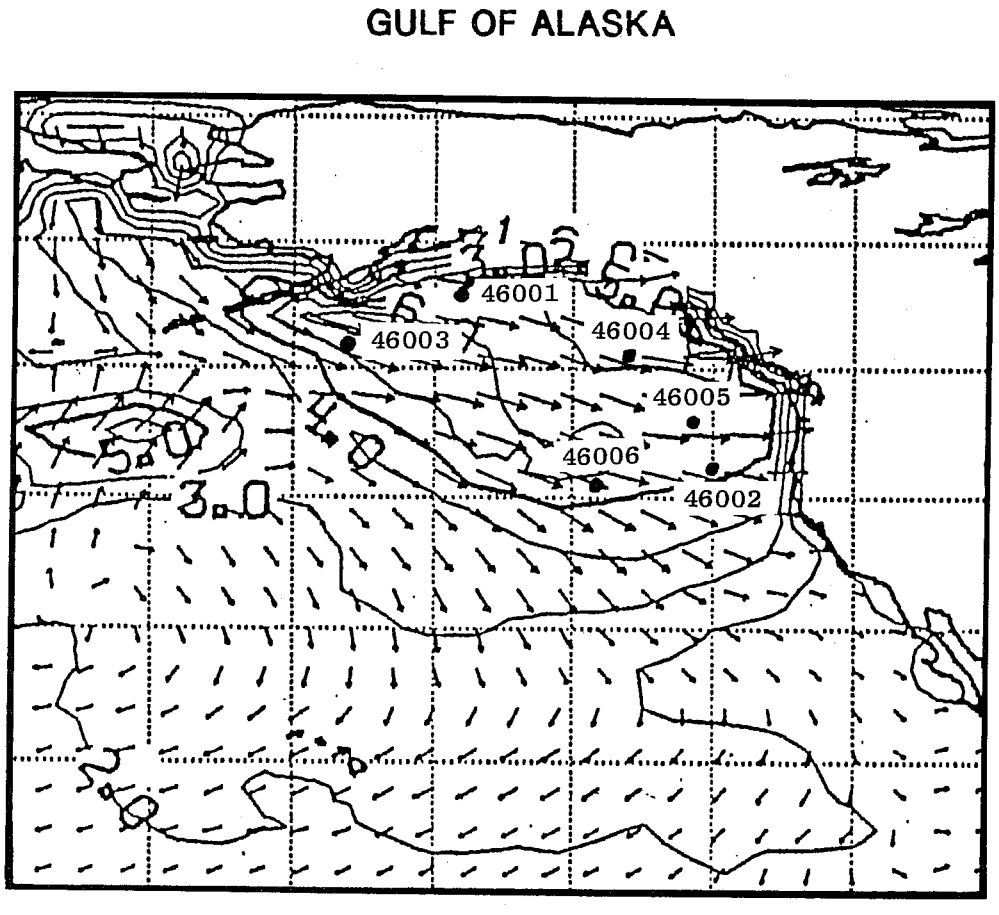

Fig. 3.1 Location of buoys in the Gulf of Alaska.

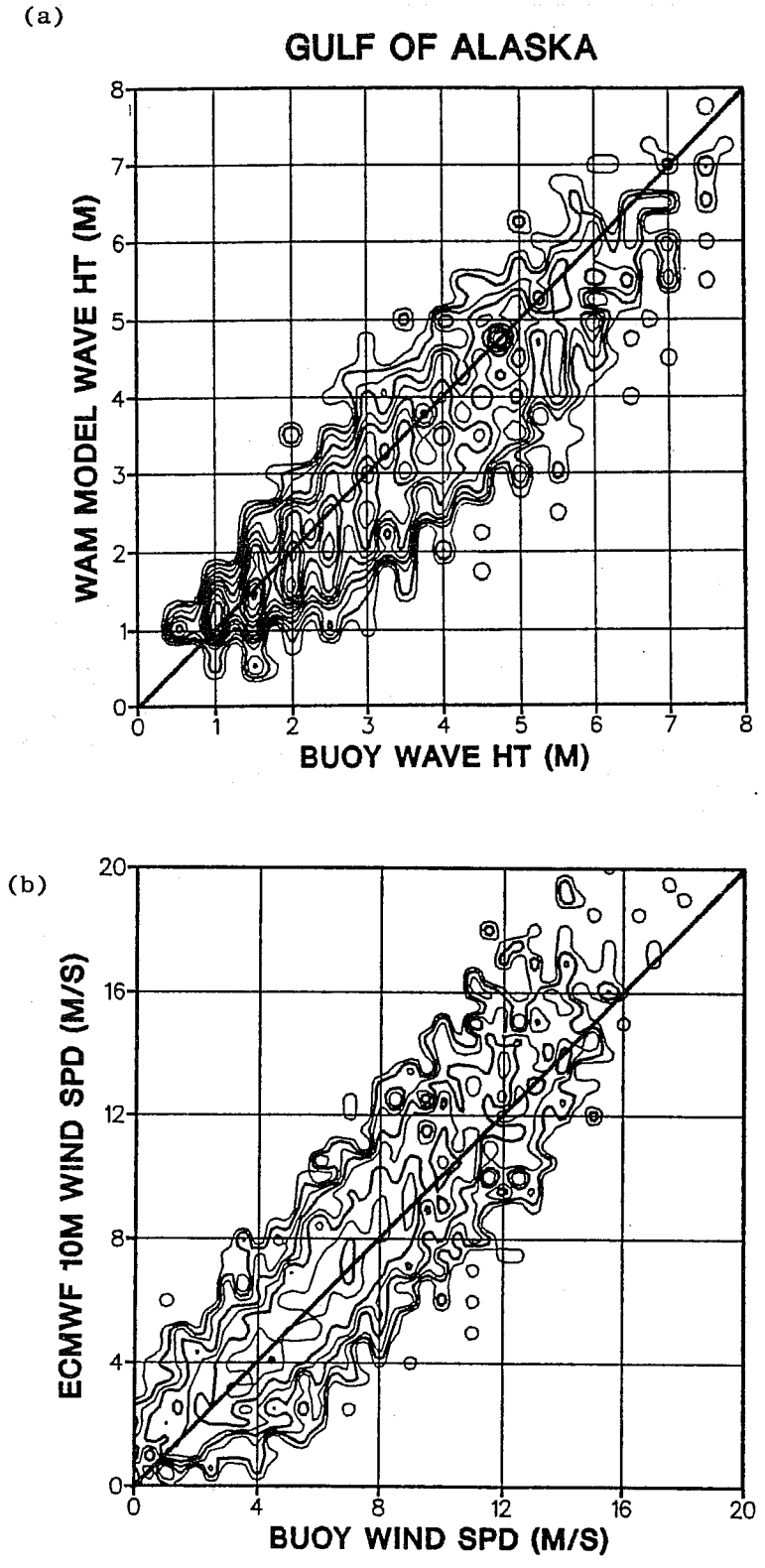

Fig. 3.2 Contour plot of the log of the number of collocations of (a) modeled wave heights and buoy wave heights (b) modeled wind speeds and buoy wind speeds in the Gulf of Alaska.

Table 3.1

Annual wave height and wind field verification statistics in the Gulf of Alaska

Area: Gulf of Alaska		
Buoys: 46001 46003 46004 46005 46006		
Wave height (meters)		
Number of reports 4657		
	OBS	MODEL
Mean	3.03	2.81
Stdev about mean	1.53	1.38
Max value	11.20	12.00
Bias	-0 .22	
Stdev	0.63	
Rmse	0.67	
Rmse sys	0.35	
Rmse unsys	0.57	
Corr coef	0.91	
Scat index	0.22	
Least squares fit		
(Y=model X=obs)	Y-ON-X	X-ON-Y
Slope	0.82	1.01
Intercept	0.31	0.72
Wind speed (m/s)		
Number of reports 4551		
	VECTOR	SCALAR
Mean obs	2.36	7.35
Mean model	2.61	7.83
Bias	0.45	0.49
Stdev	2.74	1.89
Rmse	2.78	1.96
Corr coef	0.94	0.87
Scat index	0.38	0.27

The first two statistics, the mean and standard deviation about the mean, identify a tendency which will be seen throughout this report. The observed numbers are higher than the modeled numbers. This is also true on a monthly basis, though these results are not explicitly shown here. Also, excluding November, the maximum observed wave is always higher than the maximum modeled wave. This means the modeled values consistently have a negative bias, a smaller dynamic range than those observed and that there is a tendency to underpredict the higher waves. However, the bias is only -.22 m. The RMS error of .67 m includes a systematic RMS error of .35 m and an unsystematic RMS error of .57 m. The correlation coefficient is high at .91 and the scatter index is respectable at .22.

The wind statistics show the ECMWF 10 m winds to have a slight positive bias in the vector wind of .45 m/s. The RMS of the wind vector is 2.78 m/s compared to 1.96 m/s RMS in wind speed. The correlation coefficients of .94 and .87 are very good. The scalar scatter index of .27 is also reasonable.

Because of the preference for buoys to report wave height to the nearest .5 m, while the wave model reports a continuum of wave heights, it was felt that this might have some impact on the statistics. To determine if this was the case, the modeled wave heights were rounded off to the nearest .5 m and the statistics were recomputed. The results are presented in Table 3.2. It is readily seen that rounding has nearly no effect whatsoever on the statistics. In fact, rather than reducing errors, they increase slightly. Rounding had the greatest, though still relatively insignificant effect, in the Hawaiian area, where the waves are lower and .5 m is a larger fraction of the average wave height. Rounding was of no advantage in any area.

Table 3.2

The effect on statistics of rounding the modeled wave height to the nearest .5m in the Gulf of Alaska

	No Roundoff	Roundoff to nearest .5 m
BIAS	-.22	-.22
STDEV	.63	.65
RMSE	.67	.68
RMSE SYS	.35	.35
RMSE UNSYS	.57	.58
CORR COEF	.91	.91
SCAT INDEX	.22	.23

3.1.3 Peak periods

In Fig. 3.3 can be seen a plot of the log of the number of collocations of modeled and observed peak periods in the Gulf of Alaska. Both the contour origin and contour interval are again .2. The bin width is .5 s. There were 505 observations available during 1 1/2 months, the latter half of October and November.

This plot shows a strong tendency for the WAM model peak periods to be too short. The higher the observed period, the more aggravated is this condition. For instance, when the buoy observes a peak period of 13 s, the WAM model period is 11 s. This constitutes a substantial difference between the observed (264 m) and modeled (189 m) deep water wavelengths. At shorter periods, there is no strong bias present for the model, although for an observation of 8 s (100 m), there can be quite a spread from 6 - 9 s (56 - 126 m) in the model prediction.

In Table 3.3, the statistics for the peak periods confirm the previous discussion. The bias is -.70 s and the RMS error is 1.92 s. The slope of .55 of the Y-on-X least squares regression is flat.

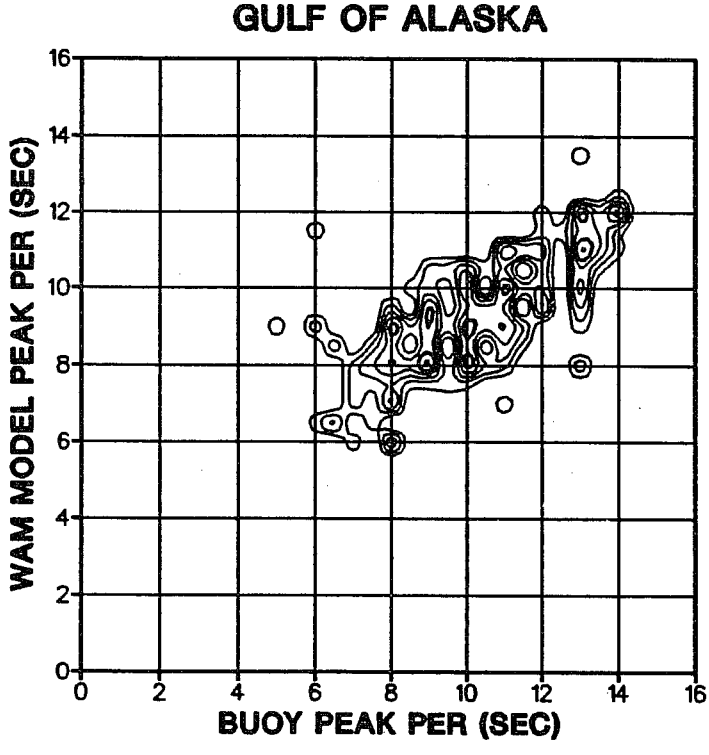

Fig. 3.3 Contour plot of the log of the number of collocations of modeled and observed peak periods in the Gulf of Alaska.

Table 3.3

Peak period statistics for the Gulf of Alaska

Area: Gulf of Alaska Buoys: 46001 46003 46004 46005 46006		
Peak period (sec) Number of reports 505		
	OBS	MODEL
Mean	10.53	9.83
Stdev about mean	2.35	1.94
Max value	17.70	16.40
Bias	-0.70	
Stdev	1.79	
Rmse	1.92	
Rmse sys	1.27	
Rmse unsys	1.44	
Corr coef	0.67	
Scat index	0.18	
Least squares fit		
(Y=model X=obs)	Y-ON-X	X-ON-Y
Slope	0.55	0.81
Intercept	4.04	5.13

3.1.4 Time series

The bulk statistics presented in Table 3.1 tend to hide details of verification which can be seen in monthly time series for individual buoys. For instance, the bias of -.22 m may seem insignificant. However, the time series indicate that the WAM model is exceptional in predicting waves in the lower two thirds of the regime, but often underpredicts peaks in wave height (see Appendix A.1 for January buoys 46001, 46004 and 46005: March buoy 46003: April 46004 and May 46001). Hence, the meaning of the negative bias is that peaks in wave height are underpredicted. As the greatest value of a wave model is to predict the extreme waves, effort will be put into understanding the causes of this underprediction through a careful analysis of individual time series. All of the time series in the Gulf of Alaska may be found in Appendix A.1.

When the wind blows constant in speed and direction for a long enough time over a large enough area, the waves should reach a state of dynamic equilibrium, with a balance between generation, dissipation and nonlinear effects. In the following discussions, reference will often be made to the wave height of the fully developed or equilibrium spectrum for a given wind speed. The significant wave height of the Pierson-Moskowitz equilibrium spectrum is a simple function of wind speed: $H_s=.0212*u^2$.

For buoy 46001 in January, the WAM model well estimated the lower waves, but clearly underpredicted the three major peaks in wave height on the 8th, 13th and 22nd. Fig. 3.1 shows that 46001 lies close to the Alaskan coast. The wind direction on both the 8th and 13th was easterly, so the wind was blowing roughly alongshore. Therefore, these may be viewed as slanting fetch cases which are poorly resolved by the implementation on the coarse grid. As coastal effects cannot be ruled out, it is not worthwhile here to look for another explanation for the underprediction of these peaks. The third peak on the 22nd was underpredicted even though the model winds were on average substantially higher than those observed. The wind direction was southeasterly veering to westerly, so resolution of the shoreline was not an issue here and this was an open ocean case.

At buoy 46004 in January, the modeled wave heights are remarkable in following those which were observed, except for the underestimated peak on the 25th. Although the modeled wind directions for the month agree well with those observed, the modeled wind speeds with a mean value of 9.3 m/s were much higher than the observed winds with a mean value of 7.3 m/s. The positive bias in the winds occurs mainly for the peaks and not for lower values in wind speed. Although the modeled winds were biased high by 2 m/s, the modeled waves have no bias. When the winds drop, the modeled waves decay in close

agreement with the buoy. On the 25th, the modeled winds were much higher than those observed, but the wave model still underpredicted the peak by 2.5 m. The WAM model wave height was very close to the expected equilibrium wave height for the modeled winds during that period. It may also be noticed that 24 - 25 January was a turning wind situation as the wind was backing sharply from southerly to easterly. The observed wind speed accounts for only about 5.4 m of wave energy out of the observed 10 m, so this sharp peak included swell. As the modeled winds were on average substantially higher than the observed winds during this month, an unbiased wave model should have predicted waves with a positive bias, but this was not the case.

At buoy 46005 in January, the comparison between modeled and observed wave heights on the 3rd, 10th, 15th and 20th clearly shows again that the WAM model is underpredicting peaks. On the 3rd, the winds were easterly but for the other three cases they were southerly to westerly or clearly open ocean cases. The observed wind speeds did not account for all of the energy of the observed peak wave heights. Therefore these peaks included swell. Although there was a background sea of about 2.5 m, it is interesting to note that the WAM model never exceeded the equilibrium wave height corresponding to the modeled wind speed.

At buoy 46003 in March on the 3rd, the peak in wave height was again missed by the WAM model. The peak on the 10th appears to have been mostly windsea and was well predicted. On the 14th, the wave model again slightly underestimated the peak wave height, even though the peak in the modeled wind speed was higher than the observation.

For buoy 46004 in March, although the WAM model missed the peaks on the 2nd, 23rd and 25th the remaining comparison between modeled and observed wave heights is good. However, from the wind speed time series, it is clear that the modeled winds had a strong positive bias. This bias was 2.7 m/s. In spite of it, the modeled wave heights were still negatively biased by .3 m. The observed peaks in wave height on the 5th, 11th, 21st, 23rd and 25th cannot be fully explained by the locally observed wind speed, indicating that much of this peak energy was swell energy. The WAM model peak wave heights again correspond well to the expected locally generated windsea with little additional swell present.

The wave height, wind speed and wind direction time series for buoy 46001 in April are remarkably good. Over the month, the wind speeds have only a slight positive bias of .3 m/s and the modeled wave heights are only slightly negatively biased by -.3 m. The peaks in wave height were well estimated by the wave model, but it should also be noticed that the modeled wind speeds were biased high for the major event during the 15th - 17th. The wave height time series are so good for this buoy, that it seems inconsistent with all

of the prior discussions. However, the peak wave heights appear to correspond well to a locally generated windsea with little swell present. This suggests that the WAM model is making a good estimate of windsea and that the underprediction present in other time series indeed results from a failure to exceed the equilibrium wave height in a growing situation when swell should be present.

At buoy 46003 during 11 - 14 April, the peak in wave height lagged behind the peak in the local wind speed, suggesting swell arrival at the buoy. The decay of the windsea by the WAM model was slowed by the overestimated modeled winds, compensating the tendency for underprediction. On the 15th, the observed wind speed was not high enough to generate the peak in wave height, suggesting about half of this energy was swell. The modeled winds were biased high however and again compensated for the underprediction of wave height by the WAM model.

At buoy 46004 in April, the peaks in wind speed on the 3rd, 5th, 9th and 15th were strongly overestimated by about 5 m/s. In spite of this, the first three corresponding peaks in wave height were well estimated, but the fourth peak was severely underpredicted by about 3 m. A glimpse at weather charts on 15 - 16 April (see Fig. 3.4) shows that there was a moderate storm system at this time in the Gulf of Alaska moving due north at roughly the group velocity of the dominant waves. This could cause the abrupt arrival of wave energy as observed by the buoy on 16 April. The peak observed wave height was about 8.5 m, whereas the observed wind speed would account for only about 2 m of wave energy, a substantial difference. The overestimated modeled winds would have accounted for about 4.2 m of wave energy, so the modeled wave height of 5.5 m exceeded the equilibrium wave height slightly, but not excessively. The WAM model behaves as if there was some mechanism for damping waves in excess of the equilibrium wave height. The observed peak wave height on the 4th of 6 m was completely missed by the WAM model. This peak is apparently mainly due to the arrival of swell as the local wind would generate a sea of only about 3.6 m.

The two major peaks in wave height of 5 m and 3.7 m by buoy 46001 on the 2nd and 12th of May went nearly unnoticed by the wave model. The fully developed wave height of 3.3 m and 1.7 m which follows from the observed wind speed implies a significant fraction of the total energy was again swell.

At buoy 46001 on 10 and 13 November, the two peaks in wave height of 5.5 m and 6.2 m were not predicted by the wave model. During and prior to the 10th, the wind was rapidly backing a full 360°. The fully developed wave height of 3.5 m corresponding to the observed wind speed of 12 m/s indicates a significant fraction of the total energy was

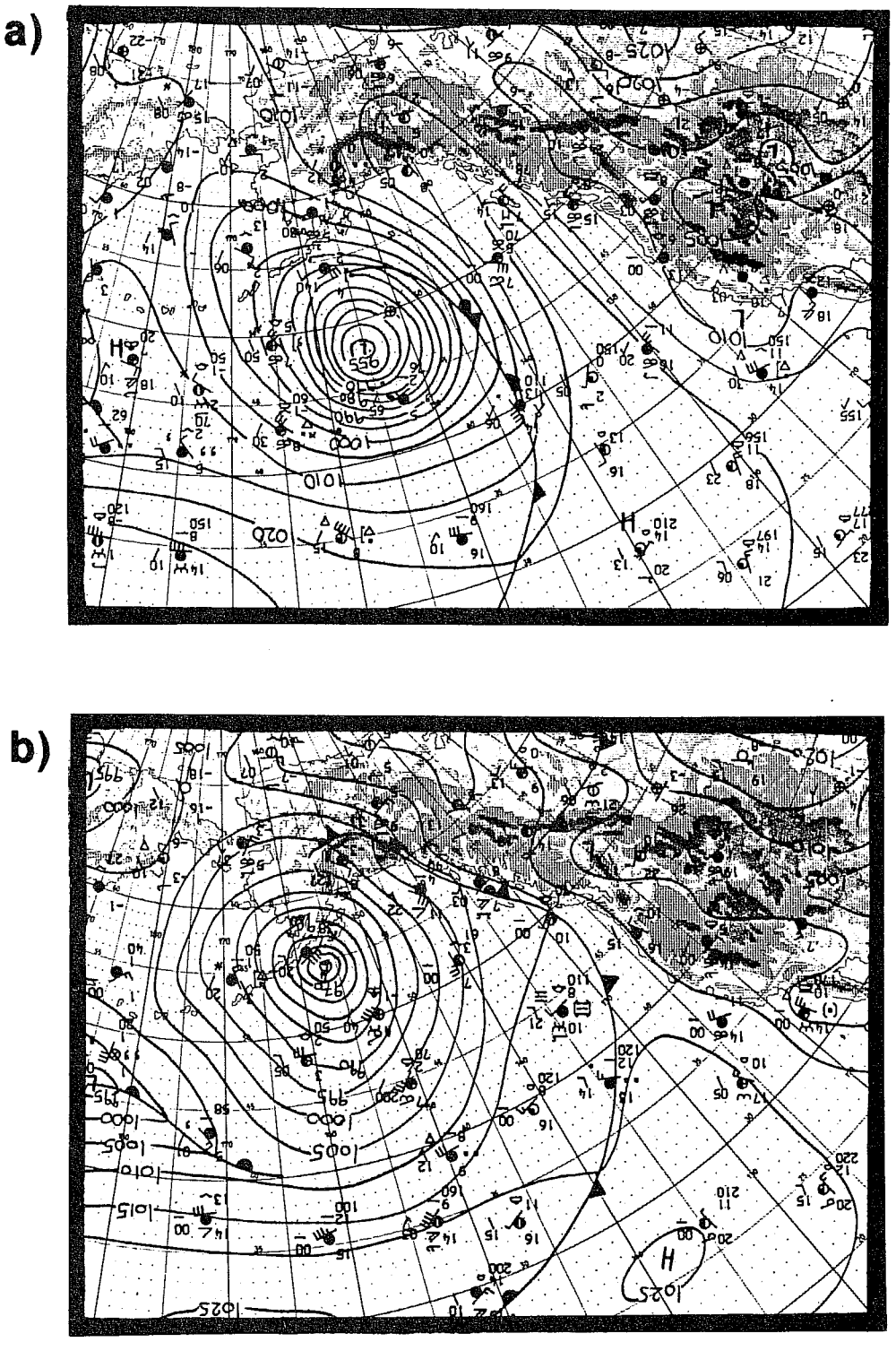

Fig. 3.4 Surface synoptic situation at 00 UT on (a) 15 April 1988 (b) 16 April 1988. Charts are from the European Meteorological Bulletin.

swell. The WAM model completely missed the event. However, the modeled winds in this case were much too low at 7.5 m/s, so the failure does not reside entirely with the wave model. For the peak in wave height on the 13th, the modeled northwesterly winds corresponded well to observations. The equilibrium windsea of 3.0 m indicates that there was about 5.4 m of swell energy present. The WAM model peak wave height corresponded closely to the equilibrium value without any additional swell energy. On the 16th, the WAM model again underpredicted the peak wave height. The modeled peak wave energy is once more equivalent to the equilibrium value without additional swell.

Although the modeled wind speed and directions correspond remarkably well to observations at buoy 46002 in November, the modeled wave heights were underpredicted on average by about 1 m. The peak on the 14th was again missed. This is possibly in part because the background sea was not high enough. As the observed wind speeds are so low on the 20th, the observed peak marked clearly the distinct arrival of swell, but this was not modeled at all. Although the mainly westerly winds during 22 - 24 April were well predicted, the wave model again severely underestimated the peak and appears to have been limited by the equilibrium wave height.

At buoy 46006 in November, the modeled winds were well predicted in both speed and direction. The modeled waves were biased .4 m too low. The observed swell peaks in wave height on the 4th and 20th went unnoticed by the wave model. The peak on the 20th was also present in the time series for 46002. The peak on the 13th was also underpredicted, with the modeled wave height again corresponding closely to the equilibrium wave height. The event during 22 - 25 November appears to be mainly windsea and was only slightly under represented by the wave model.

The conclusions resulting from the discussion of time series in the Gulf of Alaska can be summarized as follows. The modeled background wave energy was often at the right level. When a storm would pass through an area, the modeled peak wave height grew to but seldom exceeded the Pierson-Moskowitz equilibrium value, whereas the peak buoy wave heights often substantially exceeded this wave height. The buoy measurements indicated that the peak wave energy frequently contained energy in addition to the local windsea. Afterwards, when the wind dropped, the modeled wave heights decayed at a rate in good agreement with the buoy to a correct background level. There was one period of one month when the peak wave height observed by the buoy did not exceed the equilibrium value. This was in April at 46001. For this case, the WAM model wave height estimates were accurate.

It is obvious that a full understanding of the physical mechanisms leading to the above results requires detailed analysis of appropriate case studies. With the actual evidence several hypotheses can be considered. The failure of the WAM model to predict peaks in wave height could be related to a mechanism limiting wave heights when the combination of sea and swell exceeds the Pierson-Moskowitz equilibrium wave height. If this is the case, either the modeling of windsea-swell interactions is incorrect or dissipation is too strong.

On a few occasions the buoys observed swell peaks that were completely missed by the WAM model. No explanation can be given at this time for this. Coastal effects were minor in the Gulf of Alaska and noticed only at buoy 46001.

3.2 Hawaiian Islands

3.2.1 Introduction

Buoys in the Hawaiian area provide an opportunity for wave model verification in the subtropics. The origin of the wave climate there will be notably different than in the Gulf of Alaska, where local synoptic scale storm systems generate wind sea. The trade winds are steady in both speed and direction, generating a moderate uni-directional sea. Situated nearly in the center of the Pacific, long period swell can arrive in Hawaii from almost anywhere, from the Gulf of Alaska or the high latitudes of the southern hemisphere. Sub-grid scale effects which would not be resolved properly by the current implementation of the WAM model would include hurricanes and shadowing by the islands. The buoys used in this study and their positioning relative to the Hawaiian Islands can be seen in Fig. 3.5.

3.2.2 Wave heights and winds

In Fig. 3.6(a) can be seen a plot of the logarithm of the number of collocations of modeled wave heights and buoy wave heights in the Hawaiian area. Fewer observations were available than in the Gulf of Alaska, as the buoys were not in continuous operation during the year. There were 2061 observations used here. The buoy wave heights are not evenly distributed over the range, but show a strong preference to report a wave height of either 1.5 or 2.0 m. The WAM model has a strong tendency to underpredict the higher waves. However, this may not be entirely a problem with the WAM model, but may be caused in part by the wind fields driving it.

Fig. 3.6(b) shows a plot of the log of the number of collocations of ECMWF 10 m winds and wind observations made by the buoys. From this, it is clear that the modeled winds are biased low on average by about 1 m/s and that the negative bias is larger at the higher wind speeds.

Table 3.4 presents the Hawaiian wind and wave statistics. The first three statistics, the mean, standard deviation about the mean and the maximum value show the same tendency as those for the Gulf of Alaska. That is, the observed numbers are all higher than the modeled numbers. The bias is -.28 m and the RMS error is .47 m. The correlation coefficient is .78 and the scatter index is .22.

The wind statistics show that the wind speed is biased -.38 m/s low. This could certainly contribute to the negative bias of the wave model. However, apart from this bias, the winds look good, with low RMS errors, high correlation coefficients and a low scatter index in wind speed of .18.

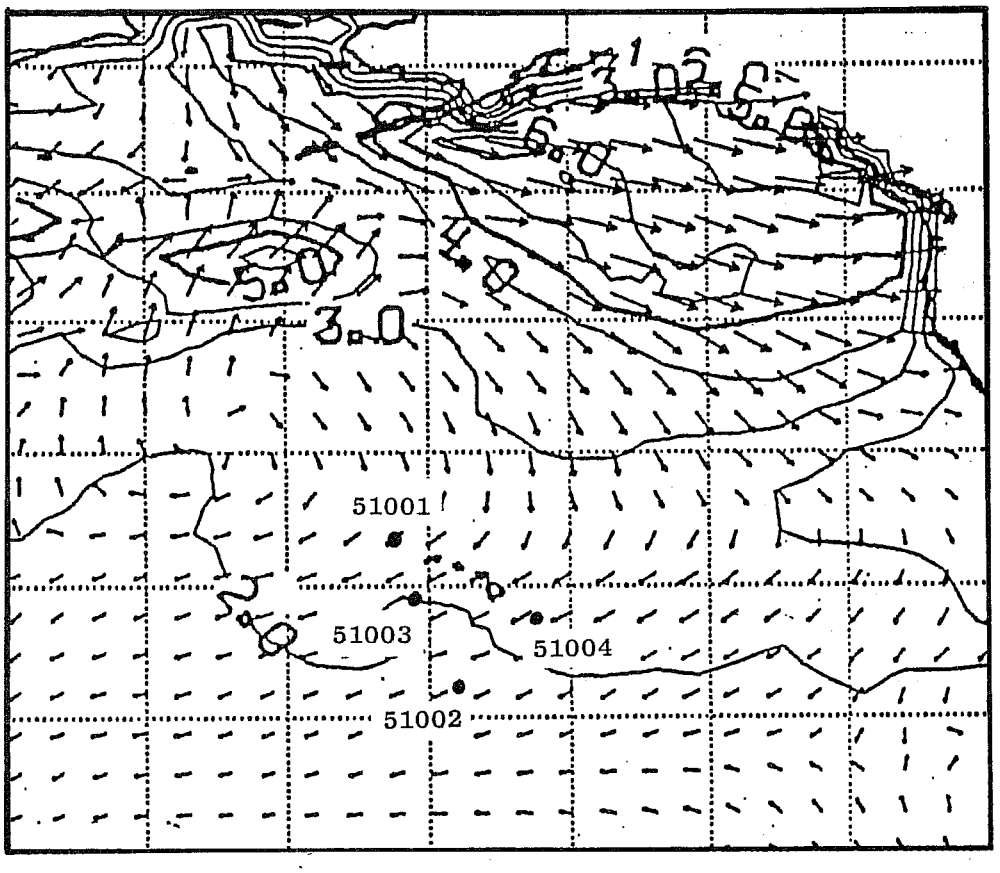

Fig. 3.5 Location of buoys in the Hawaiian Islands.

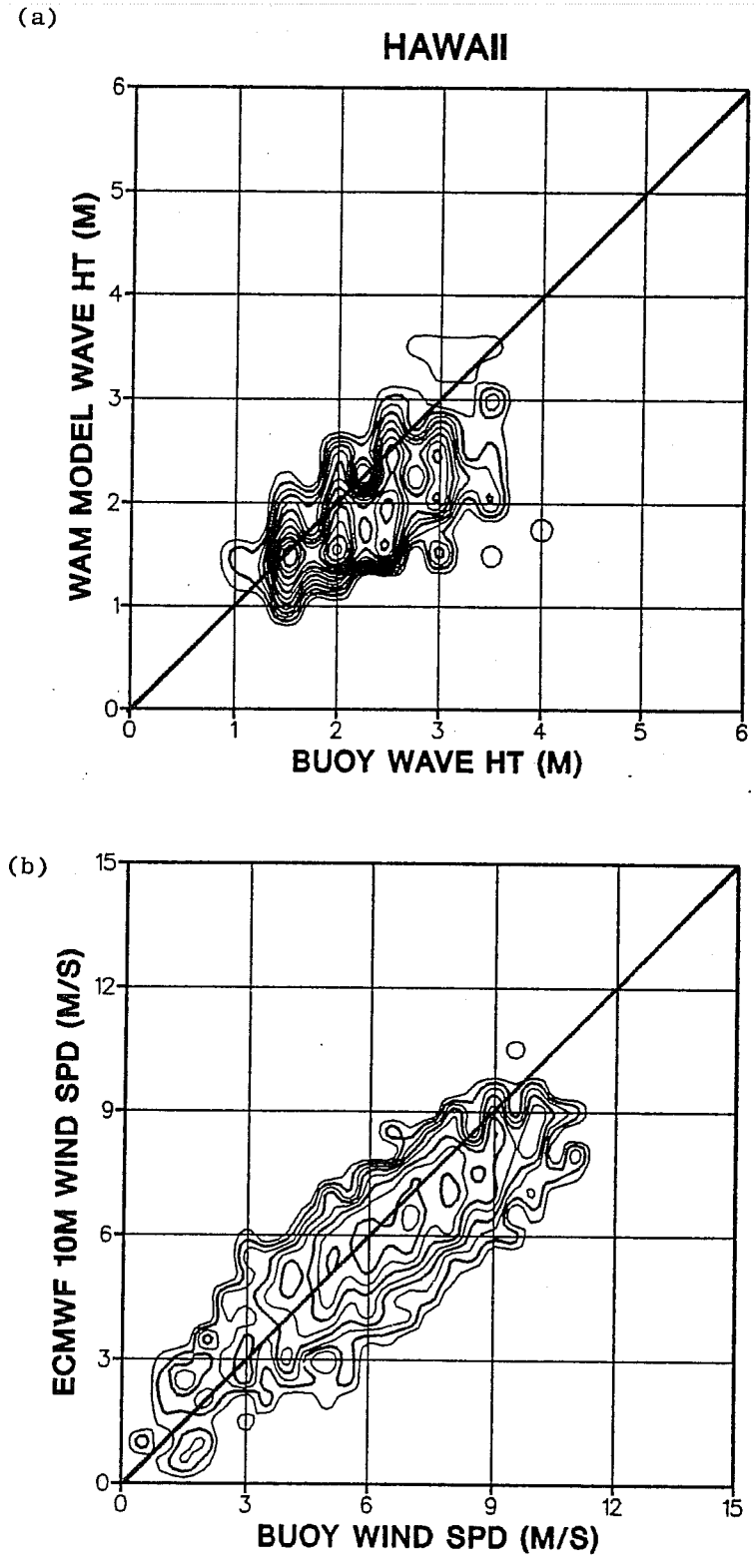

Fig. 3.6 Contour plot of the log of the number of collocations of (a) modeled wave heights and buoy wave heights (b) modeled wind speeds and buoy wind speeds in the Hawaiian area.

Table 3.4

Annual wave height and wind field verification statistics in the vicinity of the Hawaiian Islands

Area: Hawaii		
Buoys: 51001 51002 51003 51004		
Wave height (meters)		
Number of reports 2061		
	OBS	MODEL
Mean	2.14	1.86
Stdev about mean	0.59	0.45
Max value	10.00	6.60
Bias	-0 .28	
Stdev	0.37	
Rmse	0.47	
Rmse sys	0.37	
Rmse unsys	0.28	
Corr coef	0.78	
Scat index	0.22	
Least squares fit		
(Y=model X=obs)	Y-ON-X	X-ON-Y
Slope	0.59	1.03
Intercept	0.61	1.05
Wind speed (m/s)		
Number of reports 2057		
	VECTOR	SCALAR
Mean obs	6.04	6.61
Mean model	5.81	6.23
Bias	0.69	-0.38
Stdev	1.73	1.15
Rmse	1.86	1.21
Corr coef	0.85	0.82
Scat index	0.28	0.18

Because Fig. 3.6(a) shows such a strong preference for the buoys to report wave heights of 1.5, 2.0 or 2.5 m while the wave model reports a continuum of wave heights, it was thought this might have an impact on the statistics. Therefore, the modeled wave heights were rounded off to the nearest .5 m and the statistics were recomputed. The results are shown in Table 3.5. Though each statistic was slightly affected, there were no substantial changes to any of the numbers. It is curious to note that rounding made each statistic worse.

Table 3.5

The effect on statistics of rounding the modeled wave height to the nearest .5m in the Hawaiian area

	No Roundoff	Roundoff to nearest .5 m
BIAS	-.28	-.30
STDEV	.37	.40
RMSE	.47	.50
RMSE SYS	.37	.38
RMSE UNSYS	.28	.32
CORR COEF	.78	.74
SCAT INDEX	.22	.23

3.2.3 Peak periods

The contour plot of the log of the number of collocations of observed and modeled peak periods for the Hawaiian area is shown in Fig. 3.7. The contour origin and contour interval are .2 with a bin width of .5 s, as before. There were 648 observations available.

This plot shows that the observed peak period is often 8 s and that in most cases, the WAM model also has 8 s. However, there is a curious splitting of the 8 s peak by the WAM model into three other longer period peaks. The model is most likely showing arrival of longer period swell in greater proportion to that which is observed. The wave spectrum in the frequency domain at Hawaii is often bi-modal and the wave model is probably showing the swell peak to be higher. Otherwise, at the longer periods, the WAM model has a tendency to be too short, as in the Gulf of Alaska.

The peak period statistics for this area are presented in Table 3.6. The maximum value of 20 s for the peak period shows that at times, very long period swell can be in the region. The model is showing overall no bias in particular and an RMS error of 1.99 s. Largely dominated by the bullseyes at 7, 8 and 9 s, the slope of the Y-on-X least squares regression is flat at .44.

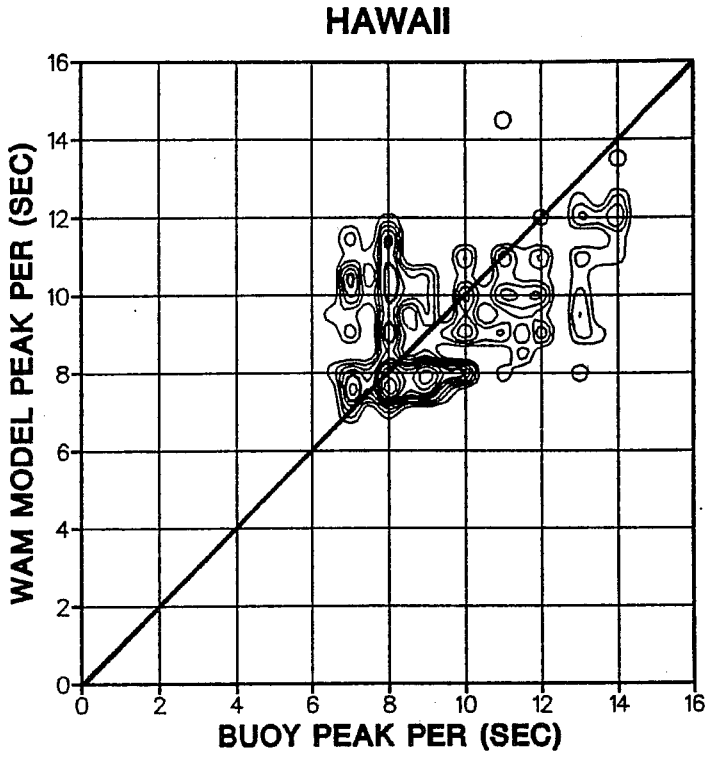

Fig. 3.7 Contour plot of the log of the number of collocations of modeled and observed peak periods in the Hawaiian area.

Table 3.6

Peak period statistics in the Hawaiian area

Area: Hawaii		
Buoys: 51001 51002 51003 51004		
Peak period (sec)		
Number of reports 648		
	OBS	MODEL
Mean	9.45	9.46
Stdev about mean	2.25	1.84
Max value	20.00	16.40
Bias	-0 .01	
Stdev	1.99	
Rmse	1.99	
Rmse sys	1.25	
Rmse unsys	1.55	
Corr coef	0.54	
Scat index	0.21	
Least squares fit		
(Y=model X=obs)	Y-ON-X	X-ON-Y
Slope	0.44	0.66
Intercept	5.28	5.27

3.2.4 Time series

The time series in this region clearly indicate a tendency for the WAM model to again underpredict wave heights. However, the problem is not only with the underprediction of peaks, as was the case in the Gulf of Alaska. This may result in part from a low bias of the modeled trade winds by about .5 m/s. Selected time series for Hawaiian buoys 51001, 51002 and 51003 may be found in Appendix A.2 and a discussion of some individual cases will now be given.

In January, the time series for buoy 51002 shows the differences between observed and modeled waves to be only minor. The average wave height of 2.7 m was not high. The trade winds were mainly northeasterly or easterly in direction. The modeled winds were biased low over the month by 1.3 m/s and this would contribute to the slight underprediction of wave heights by the wave model. During this month, the equilibrium wave height corresponding to the modeled wind speed was always substantially lower than the total modeled wave energy. The modeled combination of background sea and swell energy was approximately correct.

At buoys 51001 and 51003 in May, the differences between modeled and observed waves is again small, but the wave model is clearly underpredicting the waves. This may be caused in part by the modeled winds which have a low bias. During the first week of May, the wind speeds dropped nearly to zero. Any waves in the area would have been mainly swell. The WAM model was more successful at 51003 than at 51001 for this period.

The time series in July for buoys 51001 and 51003 shows that the trade winds blew steadily from the east. The modeled winds are in good agreement with the observed winds in both speed and direction. In spite of this, the modeled waves are too low, and are in approximate agreement to the equilibrium wave height for those wind speeds. As the southern hemisphere winter occurs in July, the discrepancy most likely arises from a failure to account properly for long period swell from this distant region.

During the period 4 - 8 November, an interesting event occurred which was a dramatic change to the usual Hawaiian weather pattern. The prevailing northeasterly trade winds were interrupted by strong southwesterlies because of a cut-off vortex in the upper atmosphere which led to a stationary surface depression. Two wave height charts are shown on November 4 and 5 in Fig. 3.8. On the 4th, the WAM model predicts a 5 m wave system to the northwest of Hawaii and a strong northerly flow has generated a moderate 5 m sea further to the north. Over the next 24 hours, the wave system near to Hawaii remains stationary and grows to 11 m. The waves generated in the source region to the north should be arriving in the Hawaiian area.

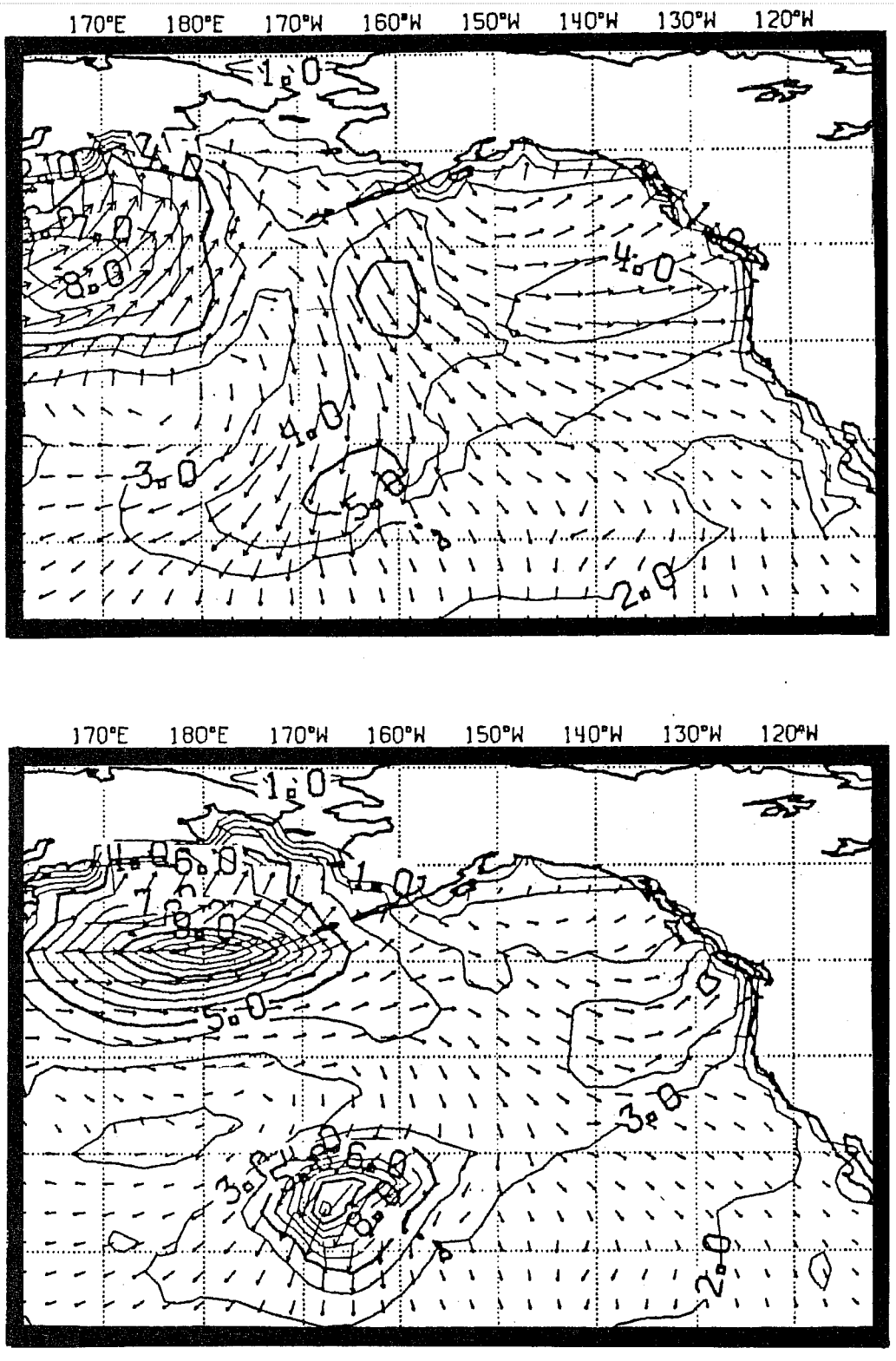

Fig. 3.8 Wave height charts in the Hawaiian area. Height in m. The arrow points in the mean wave direction (a) 88110412 (b) 88110512.

The time series for three buoys, 51001, 51002 and 51003 are shown for November in Appendix A.2. Buoy 51001 reported the highest waves, with a maximum significant wave height of 10 m. This was accompanied by an air-sea temperature difference of -5°C and strong, veering winds. The observed wind speed of 17.5 m/s would generate a windsea of about 7 m, indicating a swell energy of about 7 m. It is quite interesting to note that the WAM model wave height is 7 m. It is curious that the peak modeled wave height again appears to be limited by the equilibrium wave height in a growing situation, even though a significant level of additional northerly swell energy should have been present. Buoys 51002 and 51003 have swell energy in addition to the locally generated windsea, but unlike 51001, the wind speeds were not very high. The modeled wave heights at these two buoys are in better agreement to the observations.

3.3 East Coast of the US

3.3.1 Introduction

This is a challenging area for wave models. There are several reasons for this. As storm systems sweep west to east across the continental US and cross over to the Atlantic, fetch limitation can play a significant role in the modeling of waves near to the coastline. One of the superior features of the WAM model is that it models fetch limitation well, but the implementation on a grid with 3° resolution nullifies this ability. Hence, buoys have been chosen which are well away from shore. However, the Gulf stream along with accompanying rings and eddies plays a role in this region, too. Wave-current interactions are not modeled, so perturbations arising from this will show up as errors in the WAM model. Fig. 3.9 shows the eastern seaboard of the US, with the location of the Gulf stream and rings in 1975, and also the position of the buoys used in this study. Two buoys are north of the Gulf stream while three are east of it. Another interesting feature is the large, negative air-sea temperature differences which can arise, sometimes of the order of -10°C to -15°C. This points to a strongly unstable atmosphere at times, which is known to increase the rate at which waves grow. The WAM model does not take this into account, but assumes neutral stability. A hurricane is a sub-grid scale effect which would not be resolved properly.

3.3.2 Wave heights and winds

In Fig. 3.10(a) is again presented a collocation plot of modeled and observed wave heights, this time off the east coast of the US. 4284 points have been plotted. The buoys show the same preference already discussed, of reporting in .5 m intervals, with gaps more or less in-between. The WAM model is showing what we have seen before in the Gulf of Alaska and Hawaii, that is, a tendency to overpredict the low waves and underpredict the high waves.

Fig. 3.10(b) shows the model winds to be rather good, with no particular bias evident, although the degree of scatter is high.

In Table 3.7, the wind and wave statistics for this area are presented. The mean, standard deviation about the mean and maximum value show what we have noted already in other areas, that the observed values are higher than the modeled values. The bias is -.38 m and the RMS error is .66 m. The scatter index of .37 is rather high. The Y-on-X slope and intercept of the least squares fit imply a lack of dynamic response of the WAM model in this region.

The wind statistics show the winds driving the WAM model to be of reasonable quality. There is practically no bias in the wind speed. The vector and scalar RMS errors are respectively 2.90 and 1.89 m/s. The wind statistics are quite similar to those obtained in the Gulf of Alaska.

As in the previous two areas, the modeled wave heights were rounded to the nearest .5 m, so that these numbers would be more in keeping with the digitization of the buoy observations, and the statistics were recomputed. The effect was to change the statistics very little from those in Table 3.6, only to make them insignificantly worse and the results will not be presented.

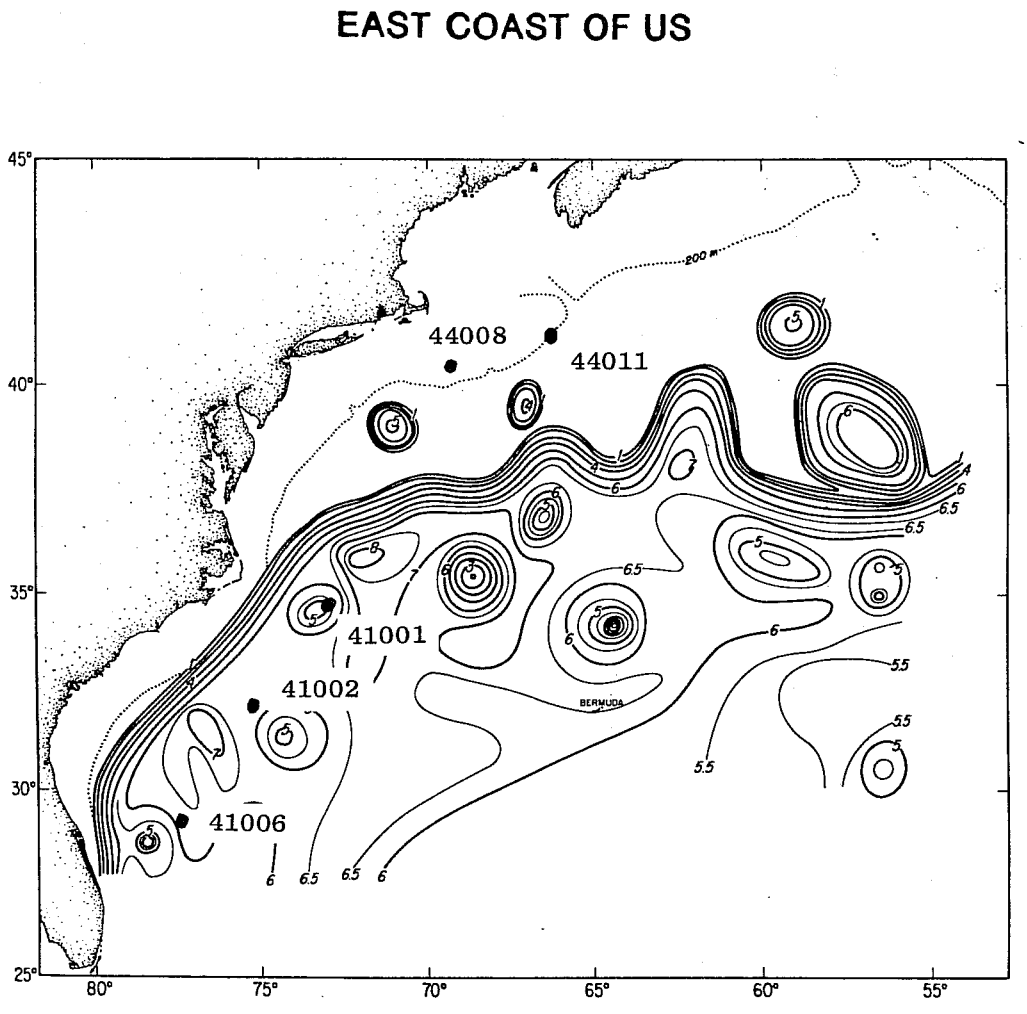

Fig. 3.9 Location of buoys in relation to the Gulf Stream. The contours indicate the topography (hectometers) of the 15° isothermal surface in 1975 (Robinson, 1983).

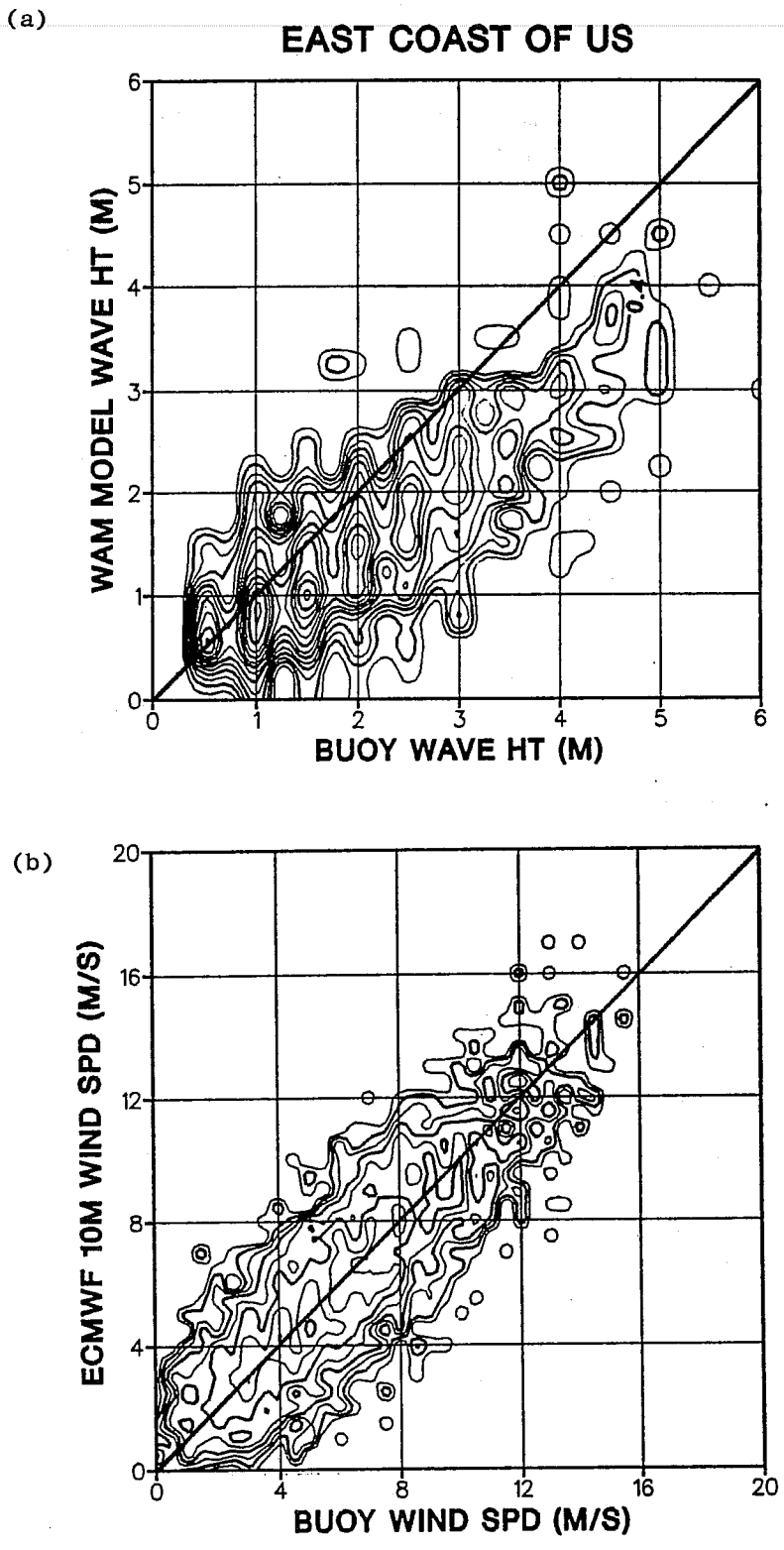

Fig. 3.10 Contour plot of the log of the number of collocations of (a) modeled wave heights and buoy wave heights (b) modeled wind speeds and buoy wind speeds off the eastern seaboard of the US.

Table 3.7

Annual wave height and wind field verification statistics off the east coast of the United States

Area: East coast of the United States		
Buoys: 41001 41002 41006 44008 44011		
Wave height (meters)		
Number of reports 4284		
	OBS	MODEL
Mean	1.80	1.42
Stdev about mean	0.96	0.75
Max value	7.80	6.10
Bias	-0 .38	
Stdev	0.54	
Rmse	0.66	
Rmse sys	0.51	
Rmse unsys	0.42	
Corr coef	0.83	
Scat index	0.37	
Least squares fit		
(Y=model X=obs)	Y-ON-X	X-ON-Y
Slope	0.64	1.07
Intercept	0.27	0.89
Wind speed (m/s)		
Number of reports 4229		
	VECTOR	SCALAR
Mean obs	1.20	6.32
Mean model	1.54	6.39
Bias	0.54	0.07
Stdev	2.85	1.89
Rmse	2.90	1.89
Corr coef	0.92	0.83
Scat index	0.46	0.30

3.3.3 Peak periods

Fig. 3.11 shows the contour plot of the log of the number of collocations of observed and modeled peak periods. The contouring has been done in the same manner as the prior plots of this kind. Altogether, 903 observations have been used.

Above 6 s, the WAM model has a strong tendency to have shorter peak periods than the buoys. This problem gets worse for higher periods. A 9 s peak by the buoy translates to a 7 s peak by the model. This corresponds to an observed deep water wavelength of 126 m and a modeled wavelength of 76 m, a substantial difference. For very short periods, the WAM model periods are biased high. For a buoy observation of 5 s, there is a high probability the modeled period will be 6 or 7 s.

The statistics presented in Table 3.8, confirm that the modeled values of the mean, standard deviation about the mean and maximum value are lower than those observed. The bias is -.71 s and the RMS error is 1.44 s. As a whole, the statistics demonstrate a lack of dynamic response of the WAM model in this area.

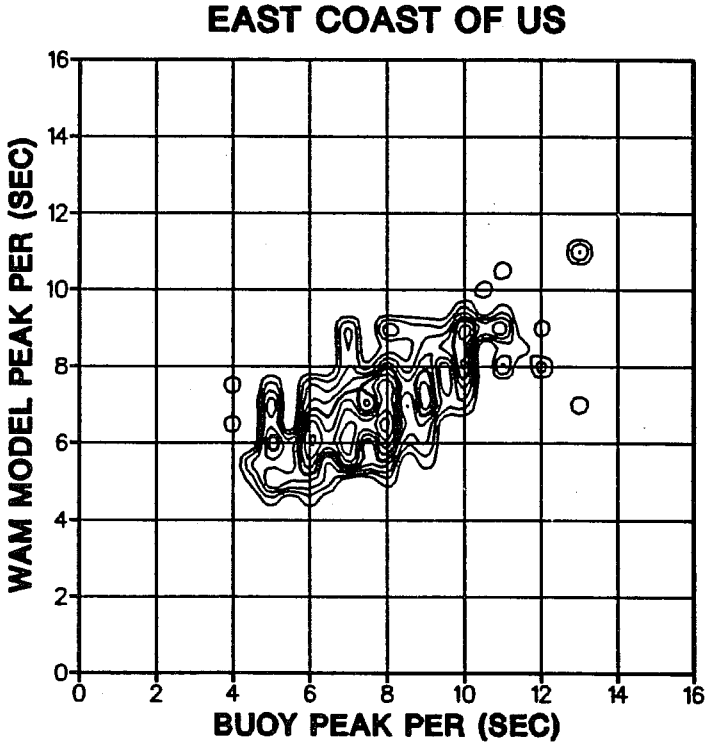

Fig. 3.11 Contour plot of the log of the number of collocations of modeled and observed peak periods off the east coast of the United Sates.

Table 3.8

Peak period statistics off the east coast of the United States

Area: East coast of the United States		
Buoys: 41001 41002 41003 41006 44008 44011		
Peak period (sec)		
Number of reports 903		
	OBS	MODEL
Mean	7.78	7.07
Stdev about mean	1.68	1.14
Max value	13.30	11.20
Bias	-0 .71	
Stdev	1.26	
Rmse	1.44	
Rmse sys	1.16	
Rmse unsys	0.86	
Corr coef	0.66	
Scat index	0.19	
Least squares fit		
(Y=model X=obs)	Y-ON-X	X-ON-Y
Slope	0.45	0.97
Intercept	3.55	4.58

3.3.4 Time series

The time series (Appendix A.3) exemplify many features of complexity in this region in contrast to an area of more settled climate like the Hawaiian Islands. Wind speed variability is high and the surface wind vector often rotates a full 360° over the period of a few days as storms pass through in succession. The November time series for buoys 41001, 41002 and 41006 are particularly striking in their depiction of this. Large negative air-sea temperature differences can also accompany high winds with the passage of cold fronts (January 44011: March 41002).

For the month of January at 44011, the modeled winds were biased high by 1.5 m/s, but the modeled waves had a low bias of .3 m. The observed peak near the 10th was not well predicted by the WAM model. On the 15th, the modeled winds were substantially higher than those observed, the atmosphere was highly unstable with an air-sea temperature difference of -14° C and the modeled waves properly estimated the observed peak in wave height. On the 27th, the observed wind speed of 14 m/s would have generated a maximum windsea of about 4.2 m, but the observed wave height was 6.2 m, indicating a substantial amount of swell was present. The modeled wind speeds were significantly overestimated, which helped to correct the WAM model tendency to underpredict the wave height.

In March, buoy 41002 experienced the passage of several weather systems, which is clearly evident from the wind speed and direction time series. On the 16th, the atmosphere was highly unstable with an air-sea temperature difference of -10° C. The observed peaks in wave height on 5, 11, 15 and 19 March were poorly predicted by the wave model. As the analysis of other time series has not revealed any difficulty in predicting the local windsea, the cause of the underprediction here is most likely due to the inability to model fetch limitation because of the coarse grid implementation. The veering wind would especially aggravate this limitation.

In April, the modeled wind speed and directions at buoy 44008 were good. The modeled wave heights were also fairly good although the two minor observed peaks on the 9th and 12th were not predicted.

The November time series for 41001, 41002, 41006, 44008 and 44011 are particularly interesting with the nearly periodic (3 day intervals) passage of cold fronts and the wind vector rotating a full 360°. Although the modeled wind speed and directions are on the whole well estimated, the WAM model underestimates nearly every peak. The observed peaks in wave height often occur when the winds are westerly, which indicates the WAM model is most likely having difficulty resolving fetch limited situations.

3.4 Northeast Atlantic

3.4.1 Introduction

This area often bears the brunt of storms sweeping across the Atlantic and is characterized by cold and wet winters. The winds are highly variable and the air-sea temperature differences can be large and negative, indicating a departure from neutral stability. There are four buoys which have been chosen for this study. Two lie north of the Outer Hebrides and two are west of the Shetland Islands. Fig. 3.12 shows where these buoys are situated.

3.4.2 Wave heights and winds

Fig. 3.13(a) presents the plot of the logarithm of the number of collocations of modeled and observed wave heights. Although these are the only buoys in this report which are not maintained by NOAA, they show the same preference to report wave height to the nearest .5 m, as in the other three areas already discussed. The WAM model makes here a better estimation of the low waves, in contrast to the other areas where it was overpredicting the low waves. However, the tendency to underpredict the high waves remains.

The collocation plot of modeled and observed winds, Fig. 3.13(b), shows that the winds driving the wave model are rather good and have only a slight negative bias.

In Table 3.8 are presented the statistics for the area. There were 2825 wave height observations available. As for the first three areas, the observed mean, standard deviation about the mean and the maximum value are higher than those modeled. The modeled wave heights have a bias of -.40 m and an RMS error of .82 m. The correlation coefficient is .85 and the scatter index is .29.

The wind statistics show the wind speeds to be higher on average than in the Gulf of Alaska, but the modeled wind speeds are slightly underpredicted with a -.54 m/s bias. Both the scalar and vector RMS errors are higher here. The scalar scatter index of .28 is rather good, but the vector scatter index of .57 indicates difficulty in pointing the modeled winds in the correct direction.

NORTHEAST ATLANTIC

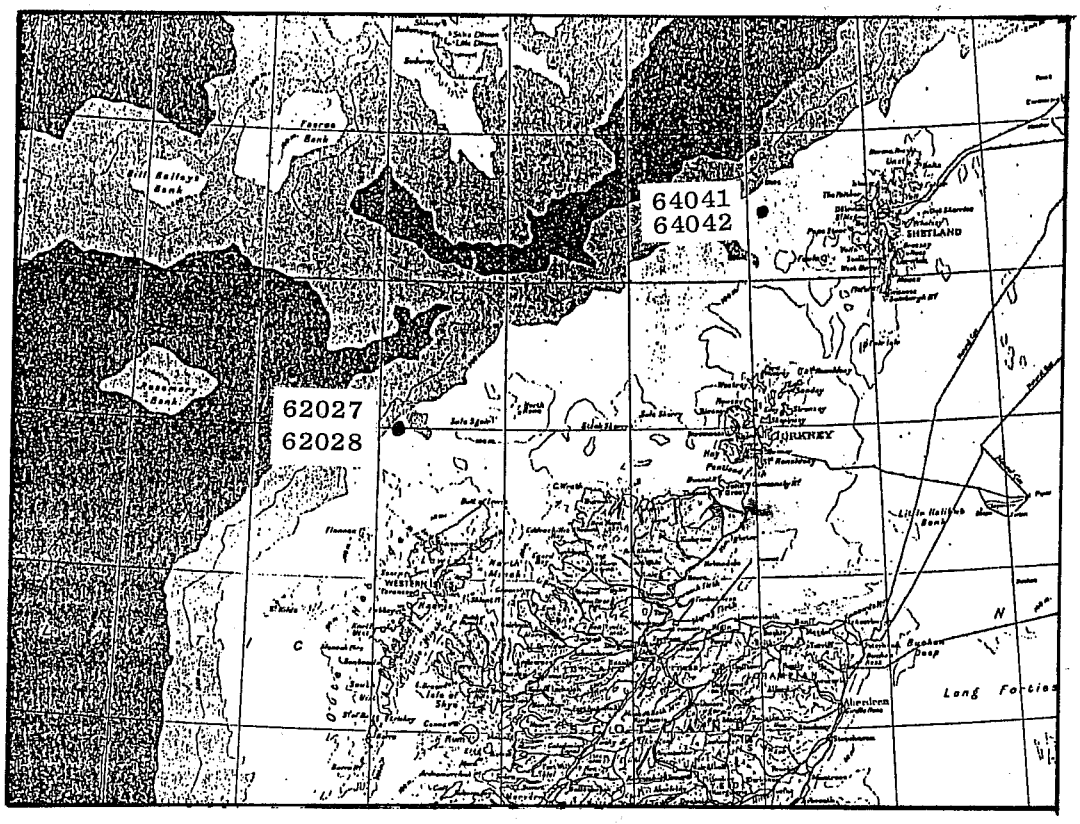

Fig. 3.12 Location of buoys in the northeast Atlantic Ocean.

(a)

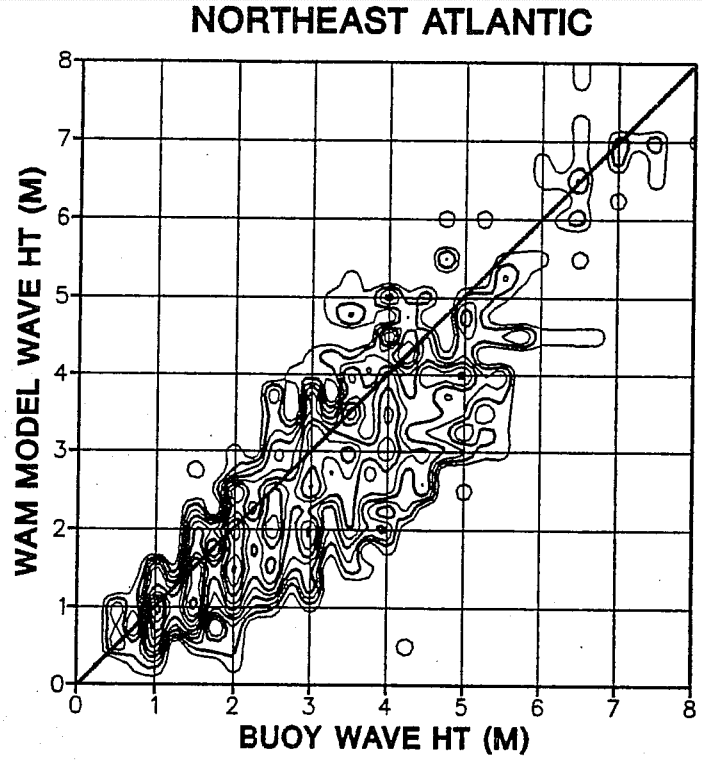

(b)

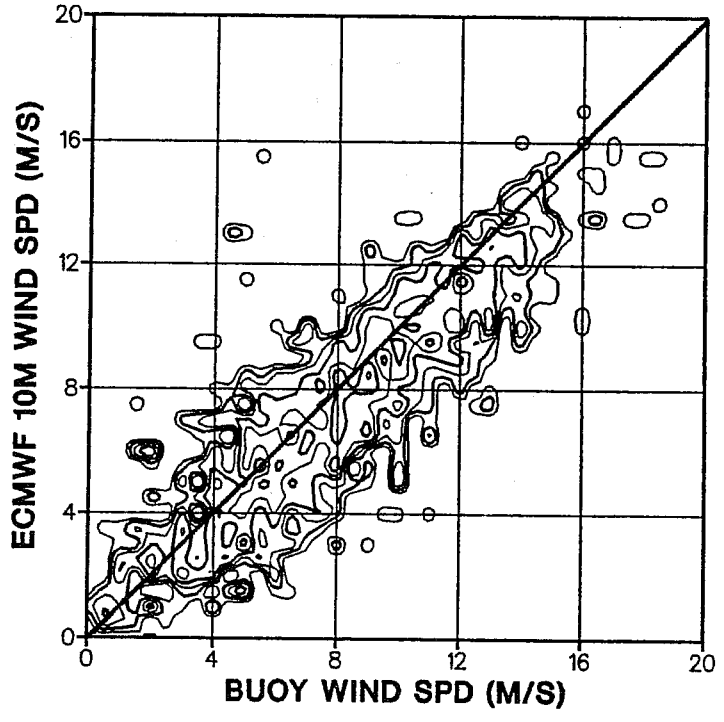

Fig. 3.13 Contour plot of the log of the number of collocations of (a) modeled wave heights and buoy wave heights (b) modeled wind speeds and buoy wind speeds north of the United Kingdom.

Table 3.9

Annual wave height and wind field verification statistics north of the United Kingdom

Area: Northeast Atlantic		
Buoys: 64041 64042 62027 62028		
Wave height (meters)		
Number of reports 2825		
	OBS	MODEL
Mean	2.88	2.48
Stdev about mean	1.36	1.26
Max value	13.00	8.30
Bias	-0 .40	
Stdev	0.72	
Rmse	0.82	
Rmse sys	0.49	
Rmse unsys	0.66	
Corr coef	0.85	
Scat index	0.29	
Least squares fit		
(Y=model X=obs)	Y-ON-X	X-ON-Y
Slope	0.79	0.92
Intercept	0.20	0.92
Wind speed (m/s)		
Number of reports 2455		
	VECTOR	SCALAR
Mean obs	2.01	8.47
Mean model	1.42	7.93
Bias	0.73	-0 .54
Stdev	4.73	2.35
Rmse	4.79	2.41
Corr coef	0.86	0.81
Scat index	0.57	0.28

3.4.3 Time series

In March, the significant wave height time series for buoy 64042 is particularly good. Over the month, the wind speeds were highly variable but have no bias and the bias in wave height was only .2 m. The peak wave heights were most likely due to locally generated windsea as none of the peaks in wave height exceeded the equilibrium value for those wind speeds. In this situation, the WAM model impressively predicted peaks in wave height. For the Gulf of Alaska buoy 46001 in April, the time series was also excellent and it was concluded that the peak wave energy was mainly local windsea. Therefore, this is further confirmation that for the situations where the WAM model underpredicted peaks in wave height, the peaks contained energy in addition to what could have been generated by the local wind, and it was this difference that was unaccounted for by the modeled waves.

In April, for the same buoy 64042, the WAM model was not as successful. The highest peak near to the 9th was underestimated. The fully developed windsea would have had a value of about 4.8 m, which is close to what the WAM model is showing. There should have been about 4.8 m of swell. This swell is apparently missing from the modeled wave height.

The November wave height time series for buoy 64041 is not impressive, although the WAM model succeeded in estimating the two peaks on the 9th and 12th correctly. These two peak modeled wave heights did not exceed the equilibrium wave heights corresponding to the modeled wind speeds. This is consistent with our prior observations that the WAM model correctly estimates peak wave heights when these peaks are mainly windsea energy containing little swell.

4. COMPARISON BETWEEN COARSE AND FINE MESH HINDCASTS

The tendency of the WAM model to underpredict peaks in wave height may result from the implementation on a geographical grid which is too coarse. In order to investigate this matter, two special hindcasts were done for a severe storm in the north Atlantic, one on the coarse global 3° x 3° grid and a second on a 1° x 1° limited area fine mesh grid. Both hindcasts were begun with a zero sea state on 86120812 and were allowed to execute for nine days until 86121712.

In both cases, the winds were held constant for periods of six hours and were identical apart from their adaptation to respective grids. The source term integration time step for the fine mesh hindcast was 900s and the propagation time step was 1800s. For the global hindcast, these two numbers were 1200s and 3600s, respectively. The total number of active grid points (sea points) in each case was roughly the same. This led to a nearly identical amount of CPU on the CRAY X-MP of ECMWF of 150s/day required for each hindcast. Therefore, roughly the same amount of CPU was needed for the fine mesh north Atlantic implementation of the model as for the coarse mesh global implementation.

Fig. 4.1 presents the wave height charts for the two hindcasts at two times, on Dec 13 at 00 UT and on Dec 15 at 18 UT. The isolines are significant wave height in one meter intervals and the arrows point in the mean wave direction.

There are some obvious differences between the two hindcasts. One is in the resolution of islands and coastal effects. The fine mesh hindcast nicely resolves Iceland, whereas the coarse mesh hindcast does not know Iceland exists! Also, the resolution along the southeast coast of Greenland and the European coastline, including the North Sea, is much better with the fine mesh grid.

Another detail which is different in the two hindcasts is the resolution on Dec 13 of the small 5-7 m wave system just south of Nova Scotia. The fine mesh hindcast has a peak wave height of 7 m, but the coarse mesh hindcast has only 5 m. The magnitude of these waves and the difference between the two hindcasts are suspiciously similar to the underprediction of peaks in wave height by the WAM model in the Gulf of Alaska.

However, in support of implementing wave models on coarse global grids, it will be noticed that the dominant wave system on Dec 13 of 11-12 m and on Dec 15 of 18-19 m is well represented and only slightly intensified by the fine mesh model. We can conclude that the finer grid improves the resolution of smaller wave systems which occur frequently in nature, land masses and coastal effects, but has little or no additional benefit in representing moderate to large wave systems.

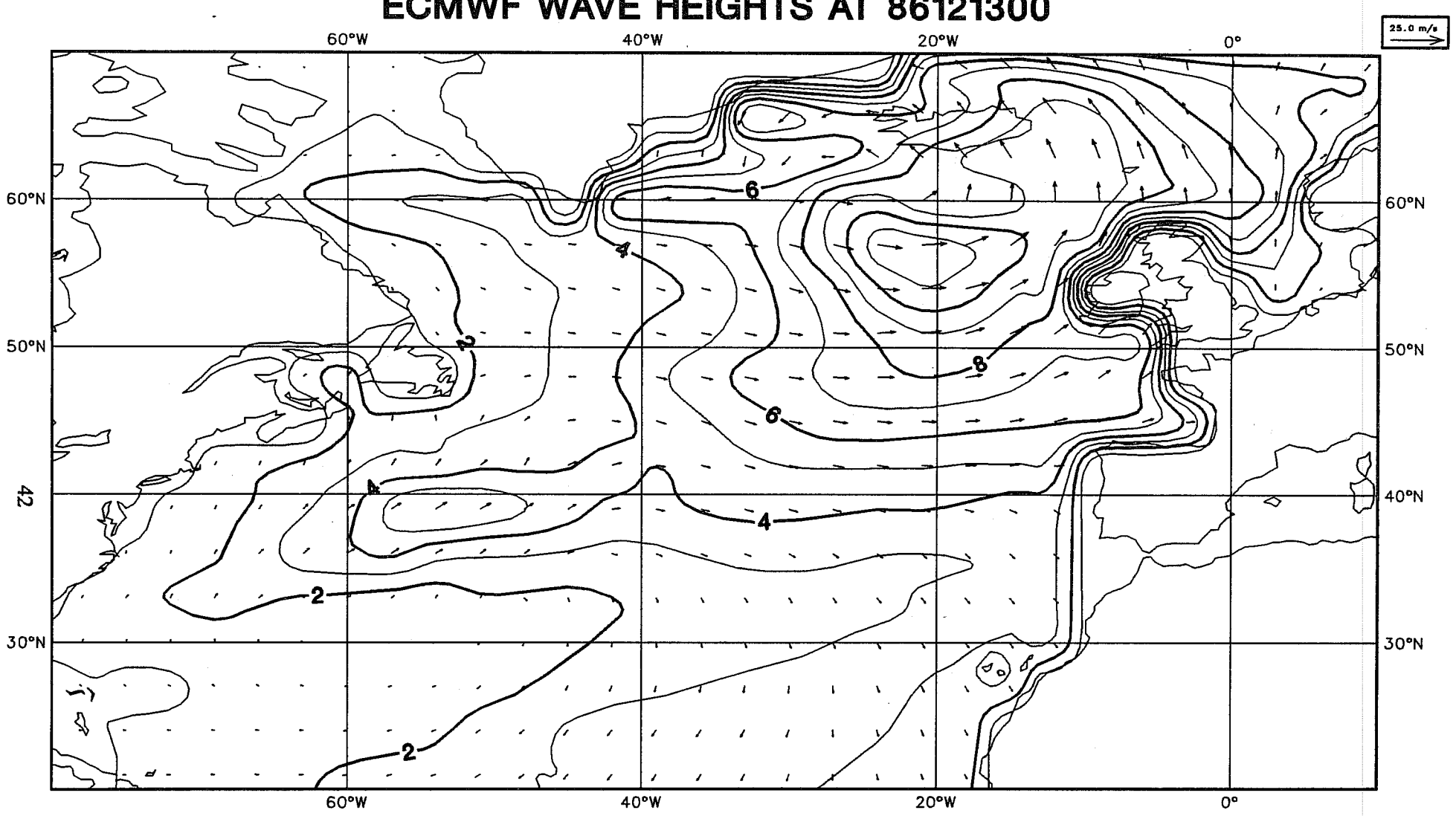

Fig. 4.1a A comparison of significant wave heights between coarse (3°x3°) and fine (1°x1°) mesh hindcasts. Coarse mesh hindcast at 86121300.

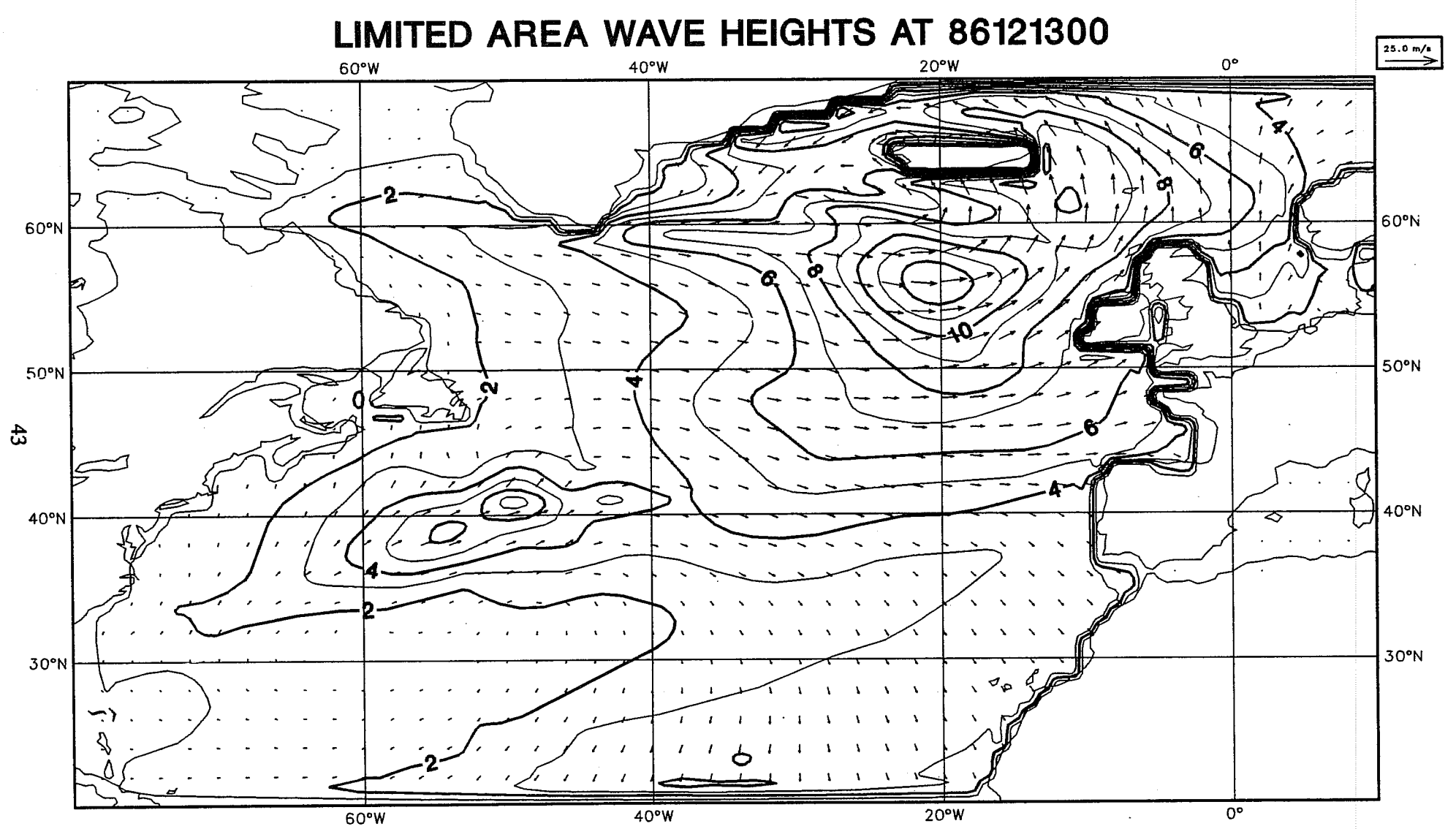

Fig. 4.1b Fine mesh hindcast at 86121300.

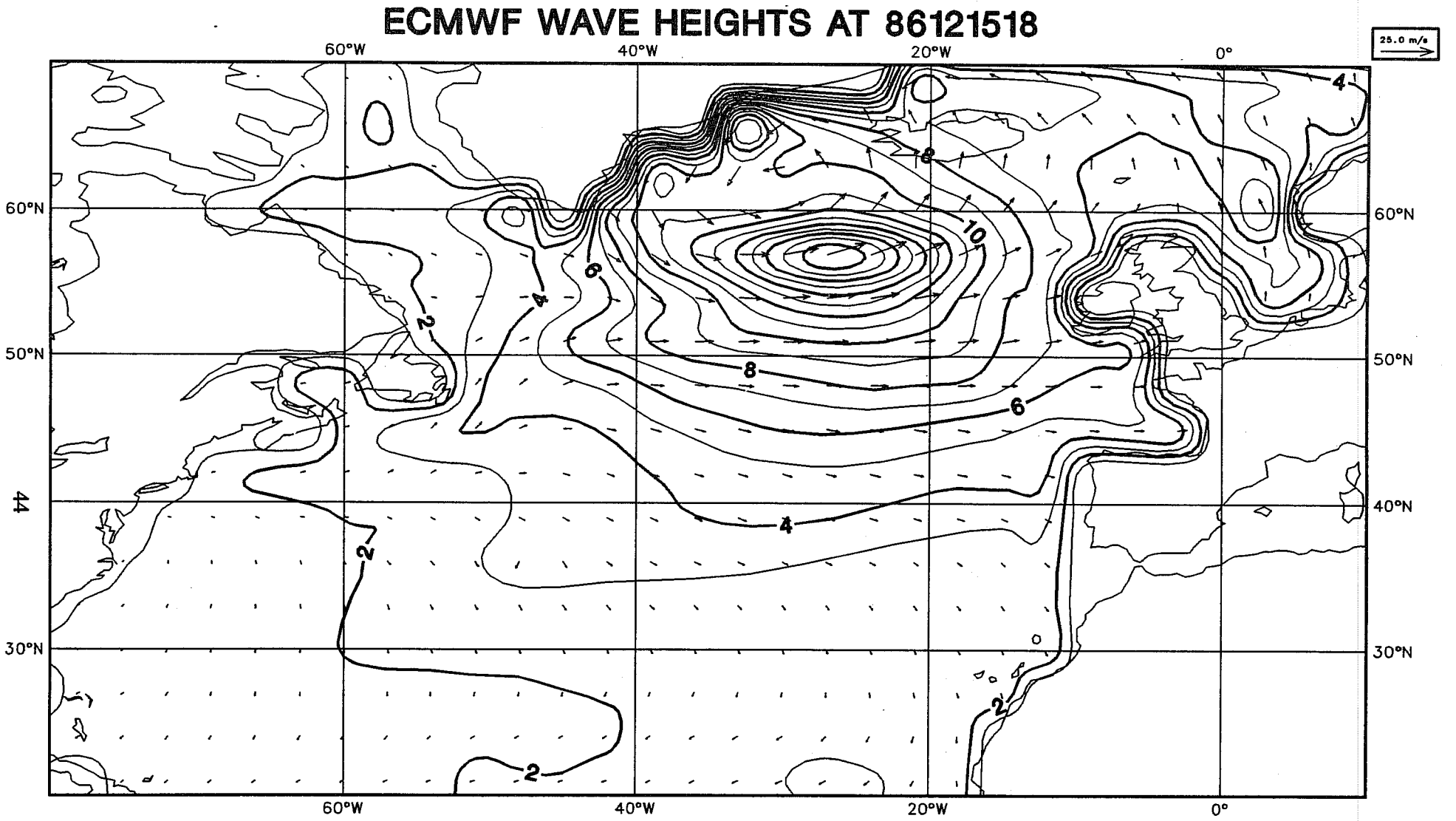

Fig. 4.1c Coarse mesh hindcast at 86121518.

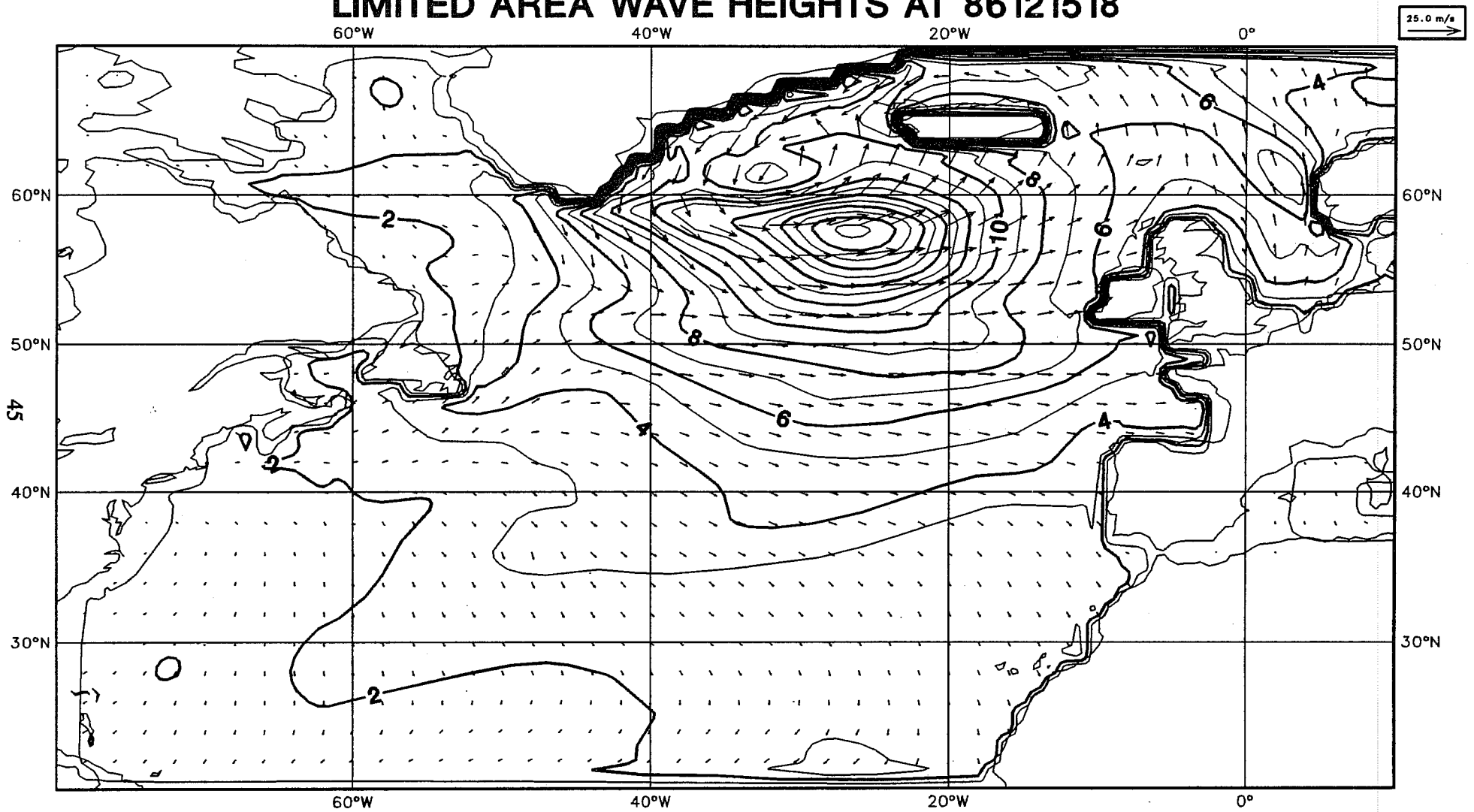

Fig. 4.1d Fine mesh hindcast at 86121518.

5. SUMMARY

A verification of wave heights and peak periods of the global WAM model and the ECMWF 10 m surface winds by moored buoys in four parts of the world has been carried out. The wind and wave height verification was for the period of one year, December 1987 - November 1988, while the peak period verification was only for 1 1/2 months, the later half of October and November of 1988. The major conclusions can be summarized as follows:

1. With seasonal and annual RMS errors well under 1 m, the WAM model predicts wave height with a high degree of accuracy. However, the current implementation of the model indicates a frequent tendency to underpredict the peak wave heights of wave systems in each of the four areas investigated. This usually manifests itself as an ability to do well in the lower two-thirds of the wave height regime, but with an underprediction of maxima by 1 or 2 m. As the greatest value of a wave model is to estimate the highest waves, this needs correction. Off the east coast of the US, the WAM model is particularly unresponsive, probably due to the inability to resolve sub-grid scale coastal effects.

   The detailed analysis of time series revealed that the failure of the WAM model to predict peaks in wave height appears to be related to a mechanism limiting wave energy in a growing situation when the combination of sea and swell exceeds the Pierson-Moskowitz equilibrium wave height. This suggests as hypotheses a problem either with windsea-swell interactions or with too much dissipation. This issue needs more investigation through some carefully chosen case studies.

2. In the Gulf of Alaska, the Hawaiian Islands and off the east coast of the US, the WAM model underpredicts the period of the spectral peak. This can make a substantial difference in the prediction of the peak wavelength. In the Hawaiian area, the model sometimes shows the swell peak to be dominant, whereas this is rarely the case with the buoys. No evaluation of periods was done in the northeast Atlantic area.

   There is other evidence in support of the conclusion that the WAM model underpredicts the peak period or wavelength. Numerical Synthetic Aperture Radar (SAR) simulations using WAM model spectra as input for the Seasat and Labrador Extreme Waves Experiment (LEWEX) time periods showed that peak wavelengths of simulated SAR spectra were too short (personal communication from C. Bruening). The LEWEX hindcasts were done on a grid of 1° resolution in latitude and longitude. Therefore the underprediction of peak period or wavelength may not be a problem related to grid resolution.

3. The ECMWF 10 m surface winds used to drive the WAM model have reasonable RMS errors and no major shortcomings were found. A few comments can be made however about details. In the Gulf of Alaska, the higher wind speeds above 8 m/s are biased slightly high. In the Hawaiian area, starting at about 6 m/s, they are biased low. At 10 m/s, the bias is 1 m/s too low. Off the east coast of the US, there is no bias present whatsoever, although there is a substantial amount of scatter. In the northeast Atlantic, the 10 m winds are biased .5 m/s too low over the entire regime. A comparison between vector and scalar errors for this region indicate some difficulty in pointing the wind vector in the right direction.

4. A comparison was made between coarse and fine mesh WAM model hindcasts. It was found that the fine mesh implementation has little or no additional benefit in representing moderate to large wave systems. However, smaller wave systems, which frequently occur in nature, have higher significant wave heights by 1-2 m when they are modeled on the finer grid. This tends to correct the underprediction of peak wave heights which was identified in the coarse grid implementation of the WAM model. Also, islands, coastlines and fetch limitation are better determined by the fine mesh grid, which supports the notion that the coarse grid implementation hinders the ability to correctly resolve coastal effects, as evident by the rather lackluster performance of the WAM model off the eastern seaboard of the US.

REFERENCES

Komen, G.J., and L. Zambresky, 1986: A third generation ocean wave model, Proceedings of the International Workshop on Wave Hindcasting and Forecasting, Halifax, Nova Scotia, September 23-26, 1986. Environmental Studies Revolving Funds, Report Series No. 065. Ottawa, pp 233-241.

Robinson, A.R., 1983: Eddies in Marine Science. Springer Verlag, p. 29.

WAMDIG: S. Hasselmann, K. Hasselmann, E. Bauer, P.A.E.M. Janssen, G.J. Komen, L. Bertotti, P. Lionello, A. Guillaume, V.C. Cardone, J.A. Greenwood, M. Reistad, L. Zambresky and J.A. Ewing, 1988: The WAM Model - a third generation ocean wave prediction model. JPO, Vol. 18, No. 12.

APPENDIX A.1

Time series in the Gulf of Alaska

Conventions:

—— model
- - - observation

Wind direction

0°	Southerly
90°	Westerly
180°	Northerly
270°	Easterly

BUOY 46001 (56.3N,148.3W)
JANUARY 1988

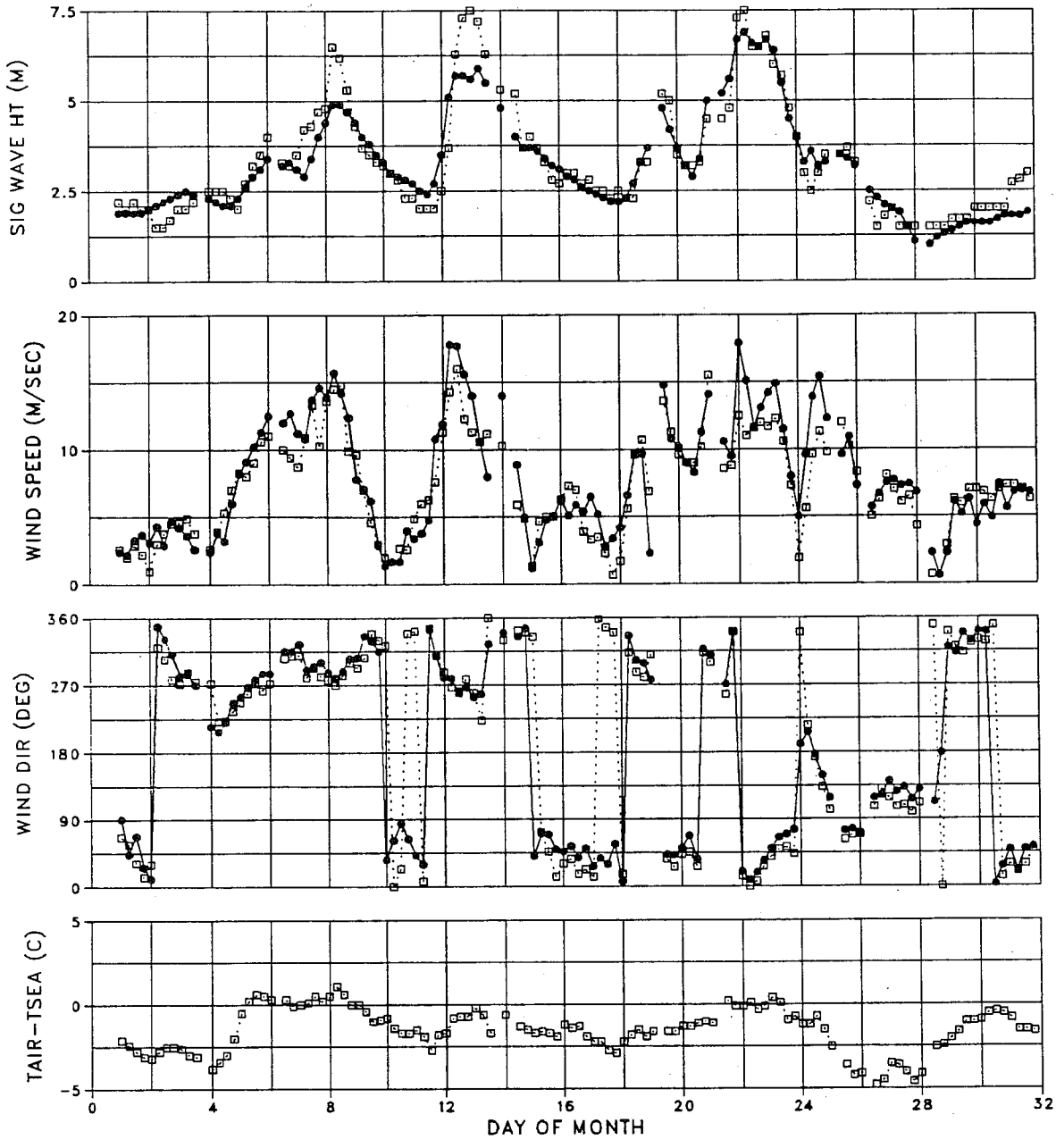

WAVES

MODEL MEAN = 3.2 STDEV = 1.4
OBS MEAN = 3.4 STDEV = 1.6
LSQ FIT: SLOPE = 0.83 INTR = 0.45
RMSE = 0.56
CORR COEF = 0.94 SI = 0.17

WINDS

MODEL MEAN = 8.0 STDEV = 4.3
OBS MEAN = 7.4 STDEV = 3.7
LSQ FIT: SLOPE = 1.07 INTR = 0.11
RMSE = 1.78
CORR COEF = 0.91 SI = 0.24

BUOY 46004 (50.9N,135.9W)
JANUARY 1988

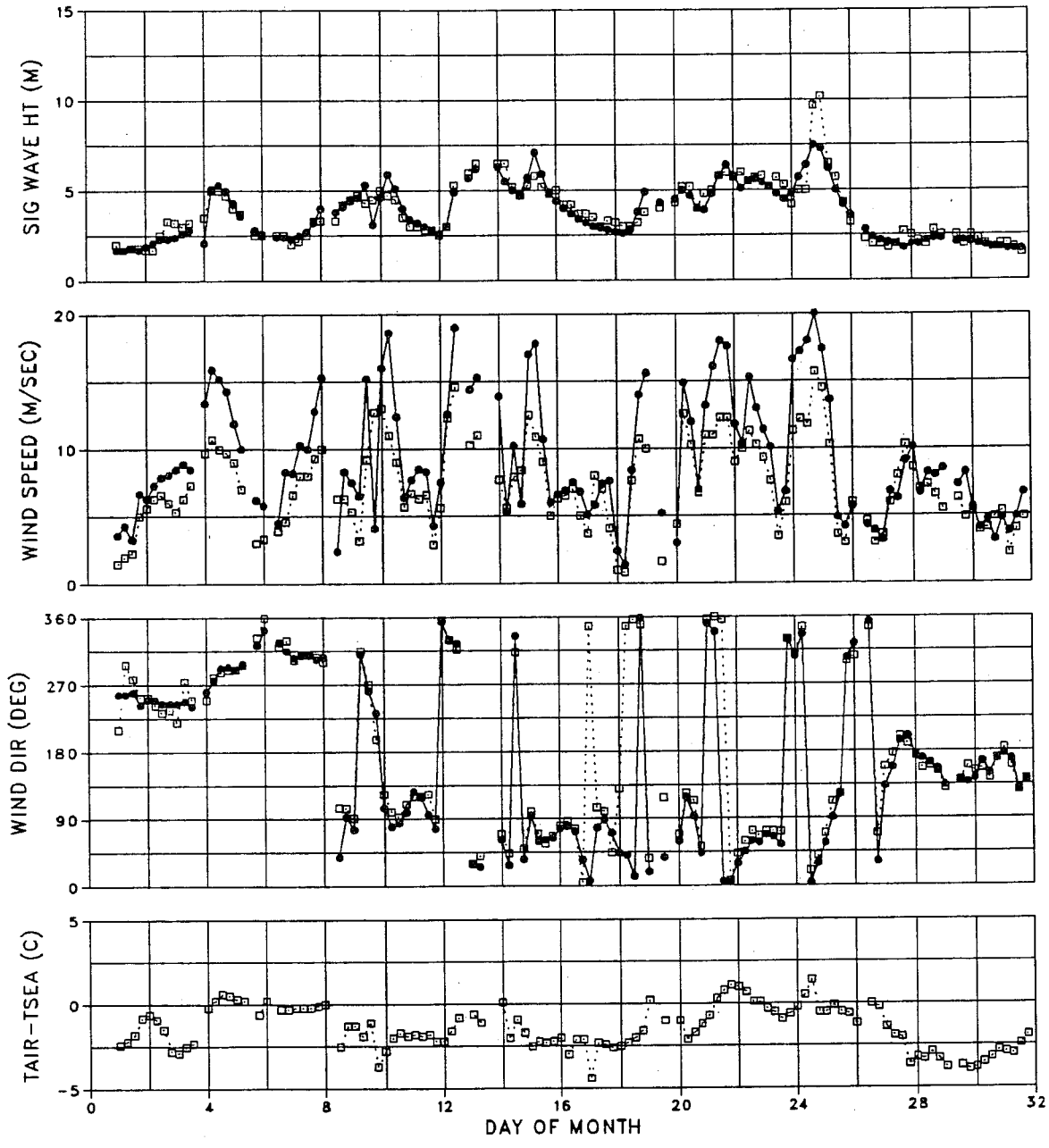

WAVES

MODEL MEAN = 3.7 STDEV = 1.5
OBS MEAN = 3.8 STDEV = 1.6
LSQ FIT: SLOPE = 0.87 INTR = 0.39
RMSE = 0.60
CORR COEF = 0.93 SI = 0.16

WINDS

MODEL MEAN = 9.3 STDEV = 4.6
OBS MEAN = 7.3 STDEV = 3.3
LSQ FIT: SLOPE = 1.24 INTR = 0.22
RMSE = 2.29
CORR COEF = 0.88 SI = 0.31

BUOY 46005 (46.1N,131.0W)
JANUARY 1988

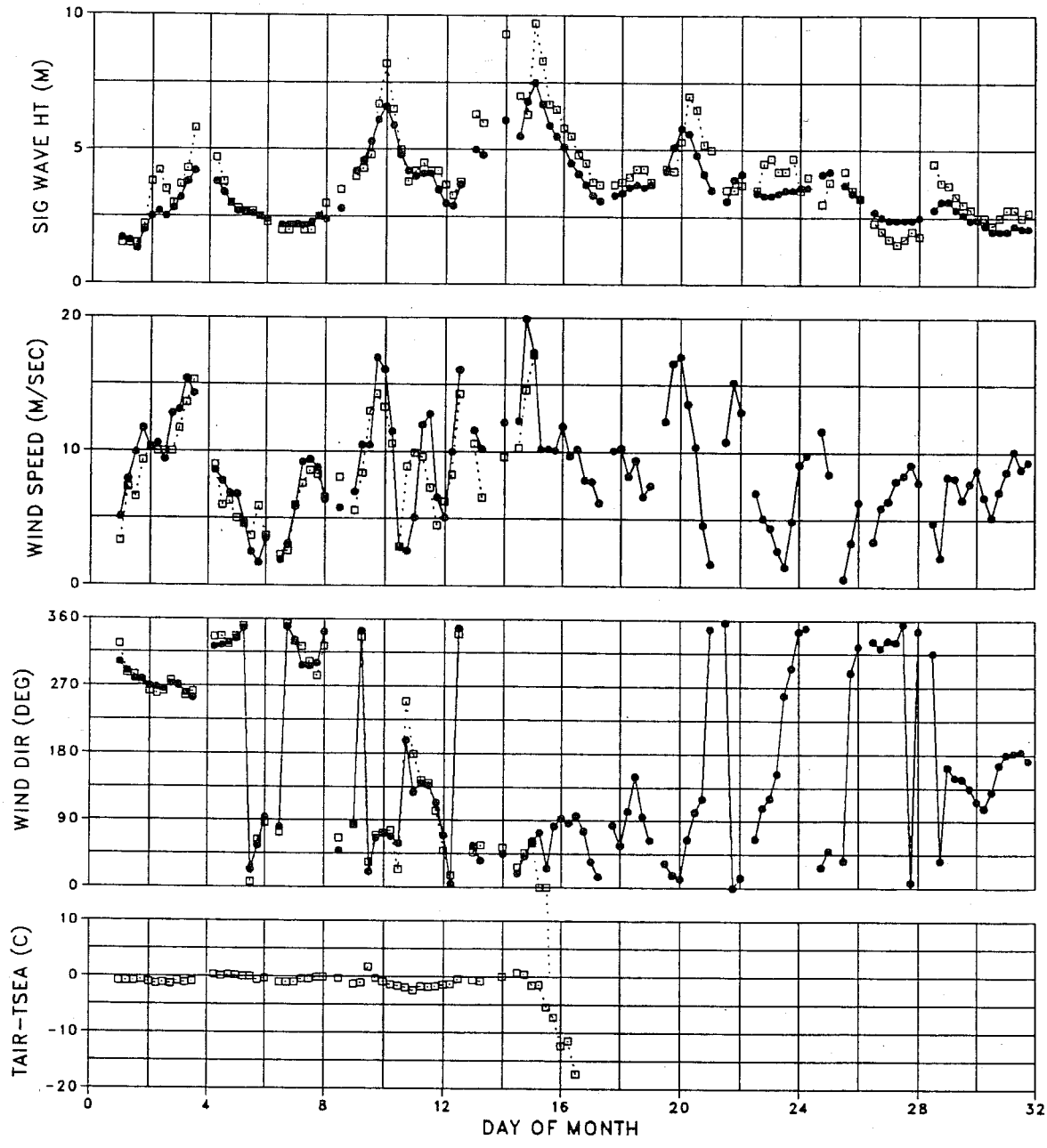

WAVES

MODEL MEAN = 3.5 STDEV = 1.3
OBS MEAN = 3.9 STDEV = 1.7
LSQ FIT: SLOPE = 0.70 INTR = 0.76
RMSE = 0.71
CORR COEF = 0.92 SI = 0.18

WINDS

MODEL MEAN = 9.2 STDEV = 4.5
OBS MEAN = 8.5 STDEV = 3.6
LSQ FIT: SLOPE = 1.07 INTR = 0.12
RMSE = 2.22
CORR COEF = 0.87 SI = 0.26

BUOY 46003 (51.9N,155.9W)
MARCH 1988

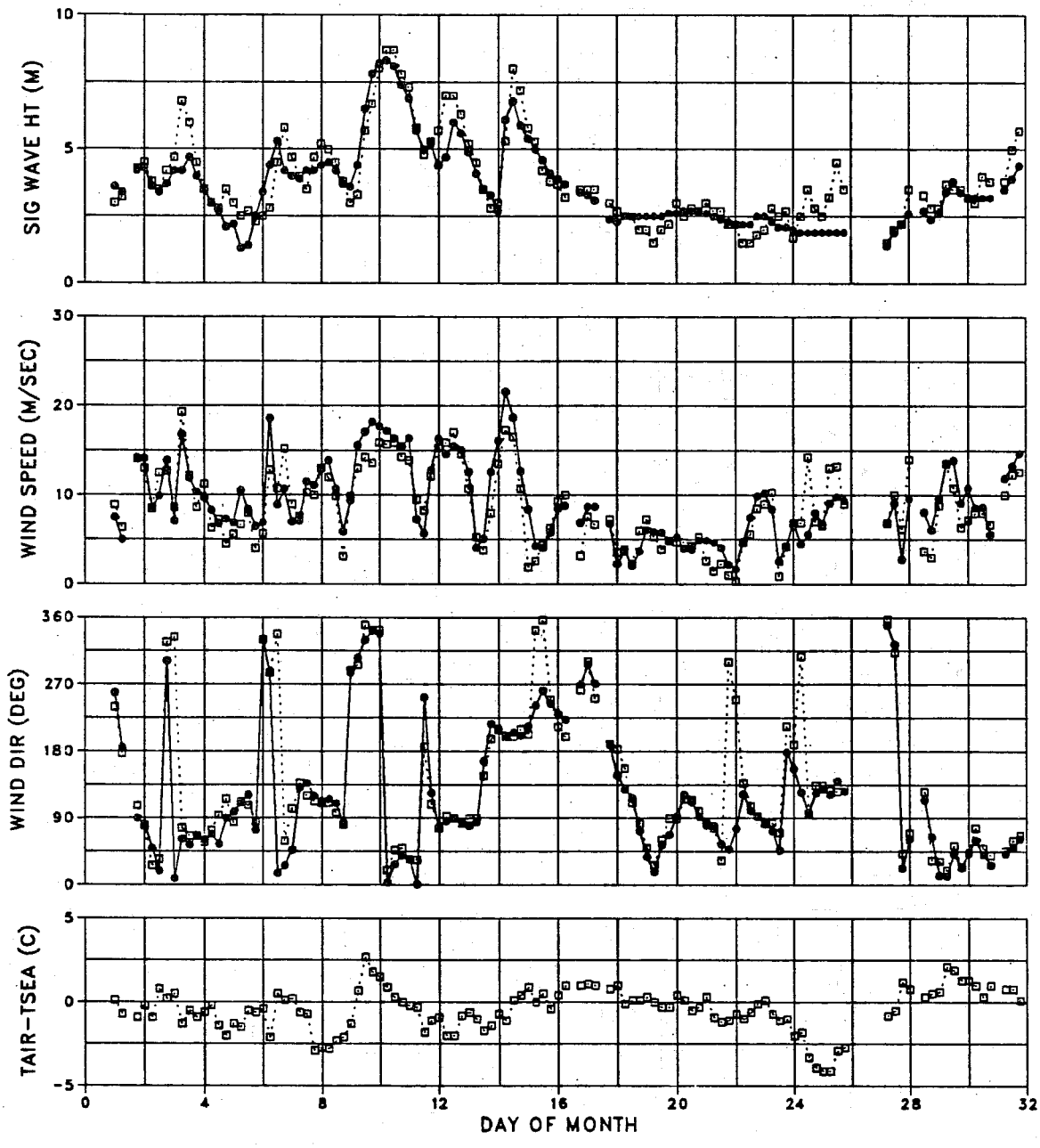

WAVES

MODEL MEAN = 3.6 STDEV = 1.5
OBS MEAN = 3.9 STDEV = 1.7
LSQ FIT: SLOPE = 0.83 INTR = 0.40
RMSE = 0.73
CORR COEF = 0.90 SI = 0.19

WINDS

MODEL MEAN = 9.3 STDEV = 4.4
OBS MEAN = 8.7 STDEV = 4.3
LSQ FIT: SLOPE = 0.90 INTR = 1.44
RMSE = 2.22
CORR COEF = 0.87 SI = 0.26

BUOY 46004 (50.9N,135.9W)
MARCH 1988

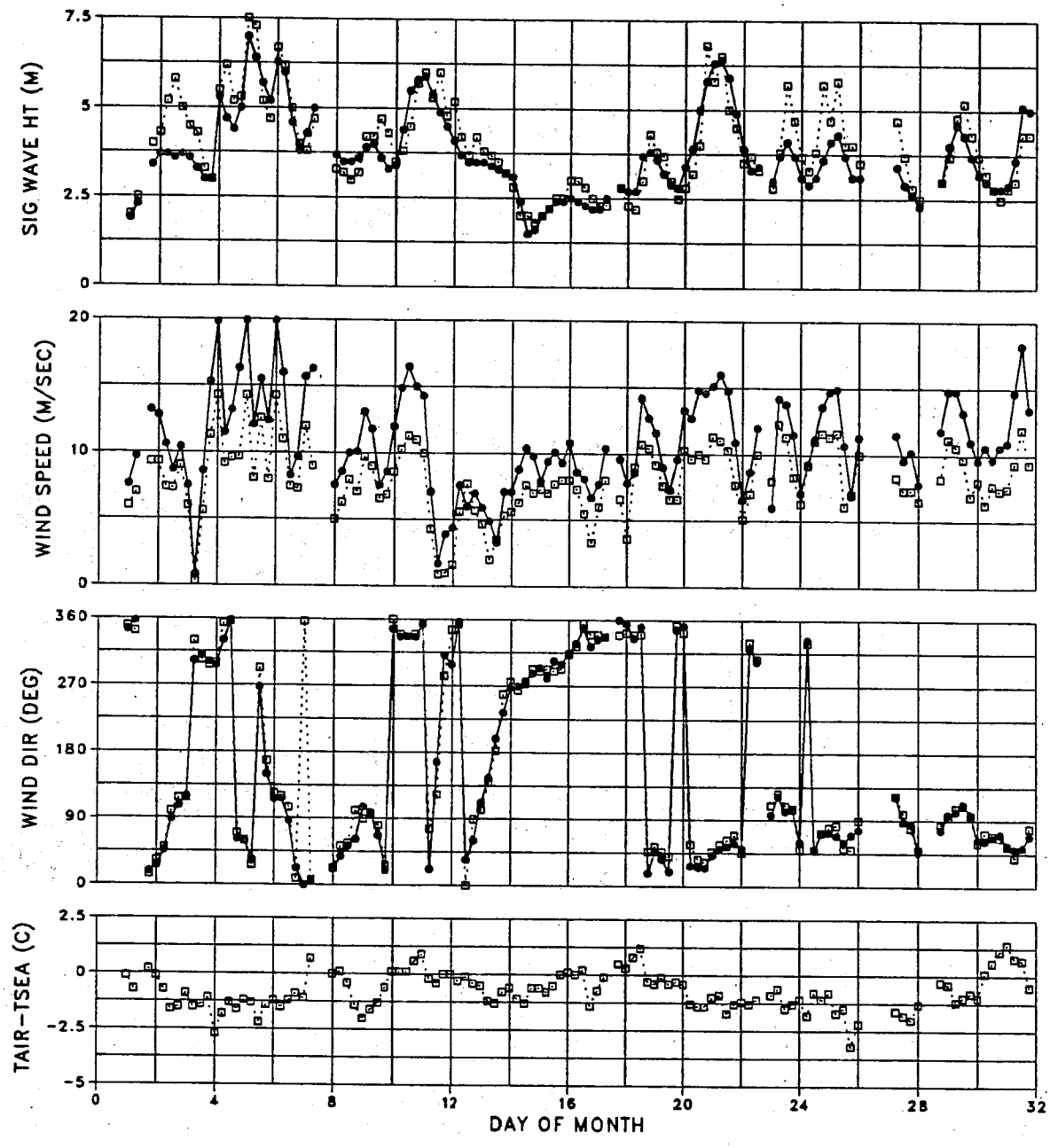

WAVES

MODEL MEAN = 3.7 STDEV = 1.2
OBS MEAN = 4.0 STDEV = 1.3
LSQ FIT: SLOPE = 0.79 INTR = 0.60
RMSE = 0.62
CORR COEF = 0.87 SI = 0.16

WINDS

MODEL MEAN = 10.8 STDEV = 3.7
OBS MEAN = 8.1 STDEV = 2.7
LSQ FIT: SLOPE = 1.25 INTR = 0.75
RMSE = 1.61
CORR COEF = 0.92 SI = 0.20

BUOY 46001 (56.3N,148.3W)
APRIL 1988

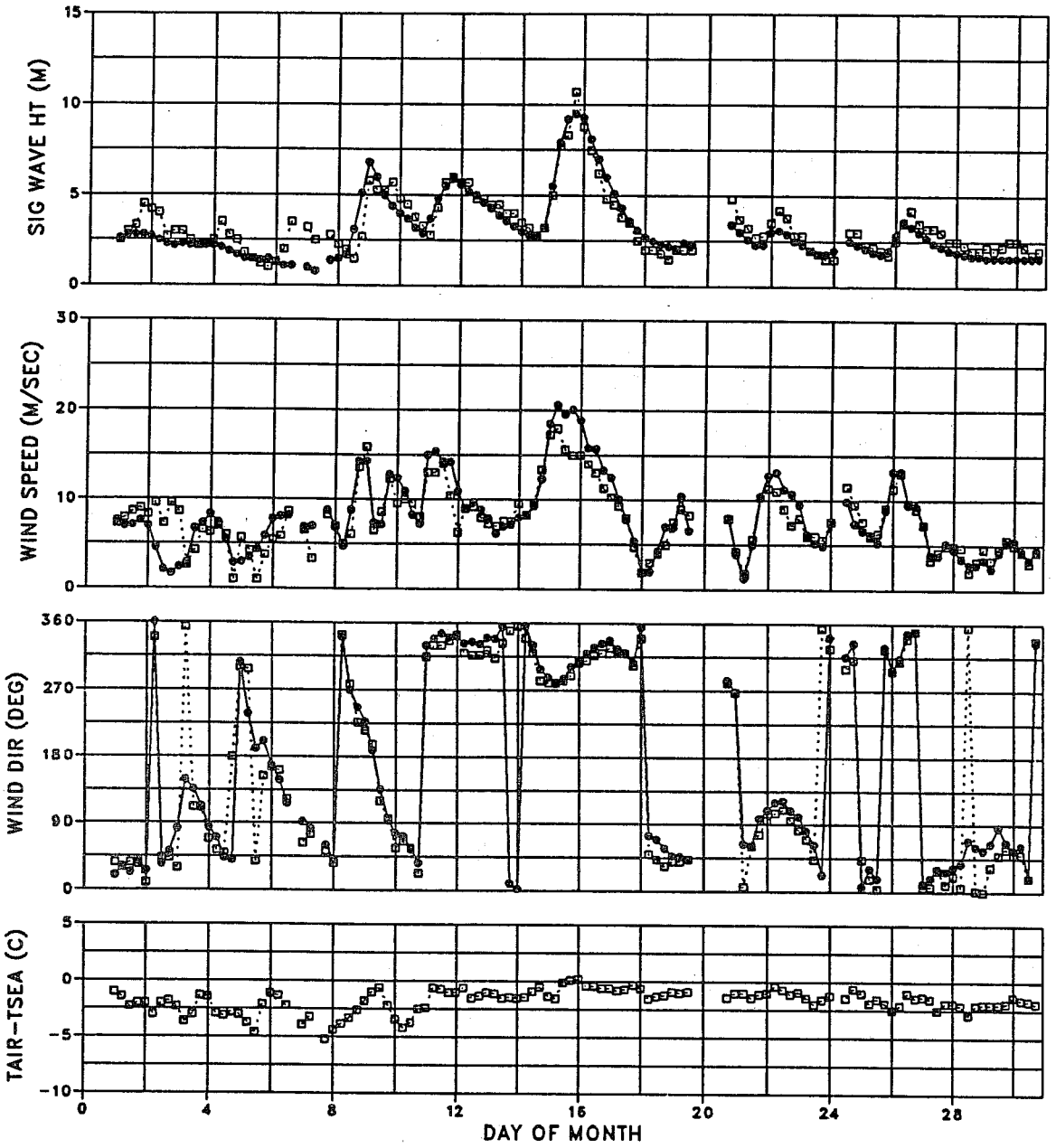

WAVES

MODEL MEAN = 3.1 STDEV = 1.8
OBS MEAN = 3.4 STDEV = 1.7
LSQ FIT: SLOPE = 0.99 INTR =-0.23
RMSE = 0.73
CORR COEF = 0.91 SI = 0.22

WINDS

MODEL MEAN = 8.1 STDEV = 4.3
OBS MEAN = 7.8 STDEV = 3.6
LSQ FIT: SLOPE = 1.07 INTR =-0.27
RMSE = 1.95
CORR COEF = 0.89 SI = 0.25

BUOY 46003 (51.9N,155.9W)
APRIL 1988

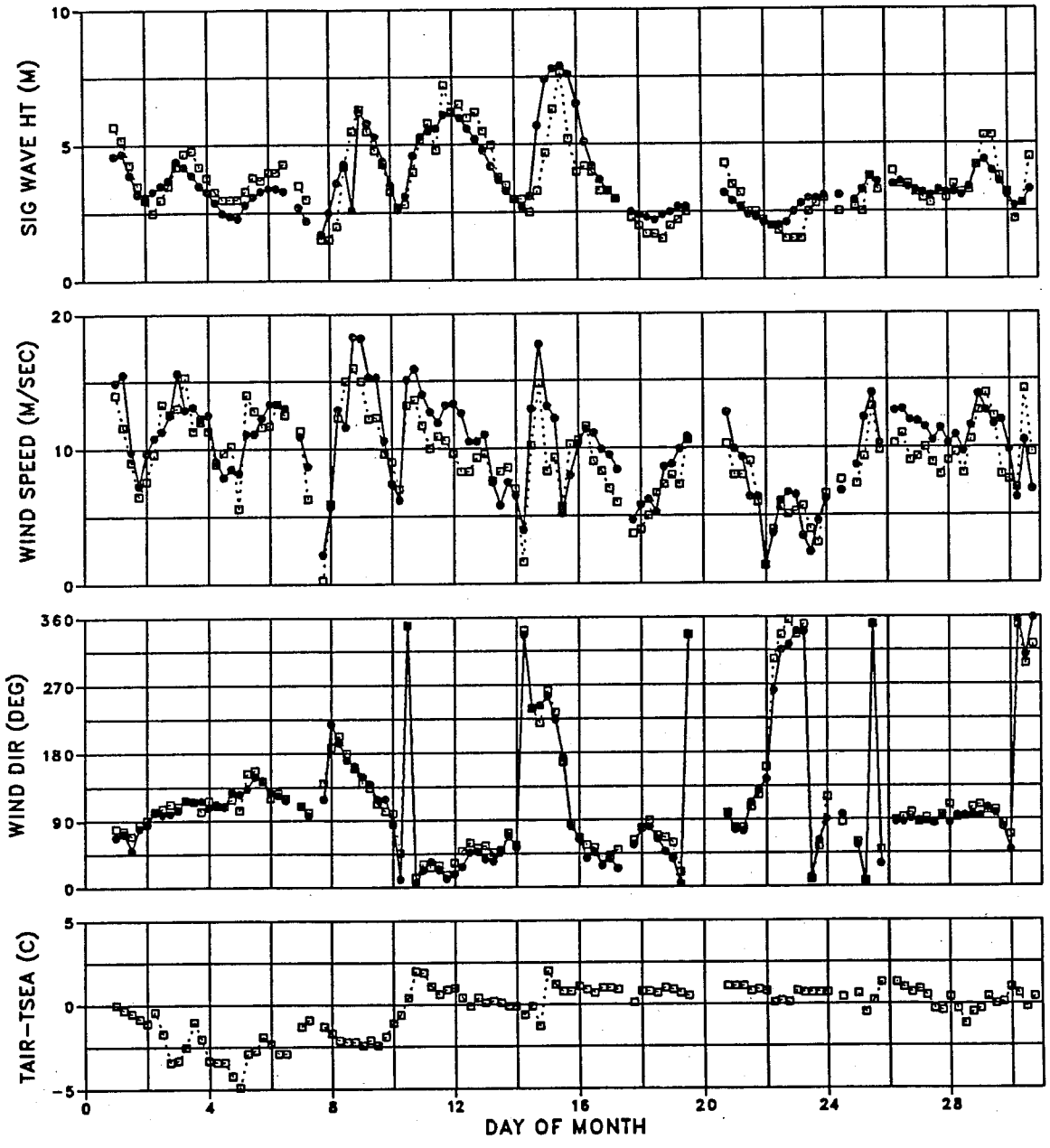

WAVES

MODEL MEAN = 3.7 STDEV = 1.3
OBS MEAN = 3.6 STDEV = 1.3
LSQ FIT: SLOPE = 0.81 INTR = 0.72
RMSE = 0.79
CORR COEF = 0.82 SI = 0.22

WINDS

MODEL MEAN = 10.2 STDEV = 3.5
OBS MEAN = 9.3 STDEV = 3.2
LSQ FIT: SLOPE = 0.94 INTR = 1.41
RMSE = 1.80
CORR COEF = 0.86 SI = 0.19

BUOY 46004 (50.9N,135.9W)
APRIL 1988

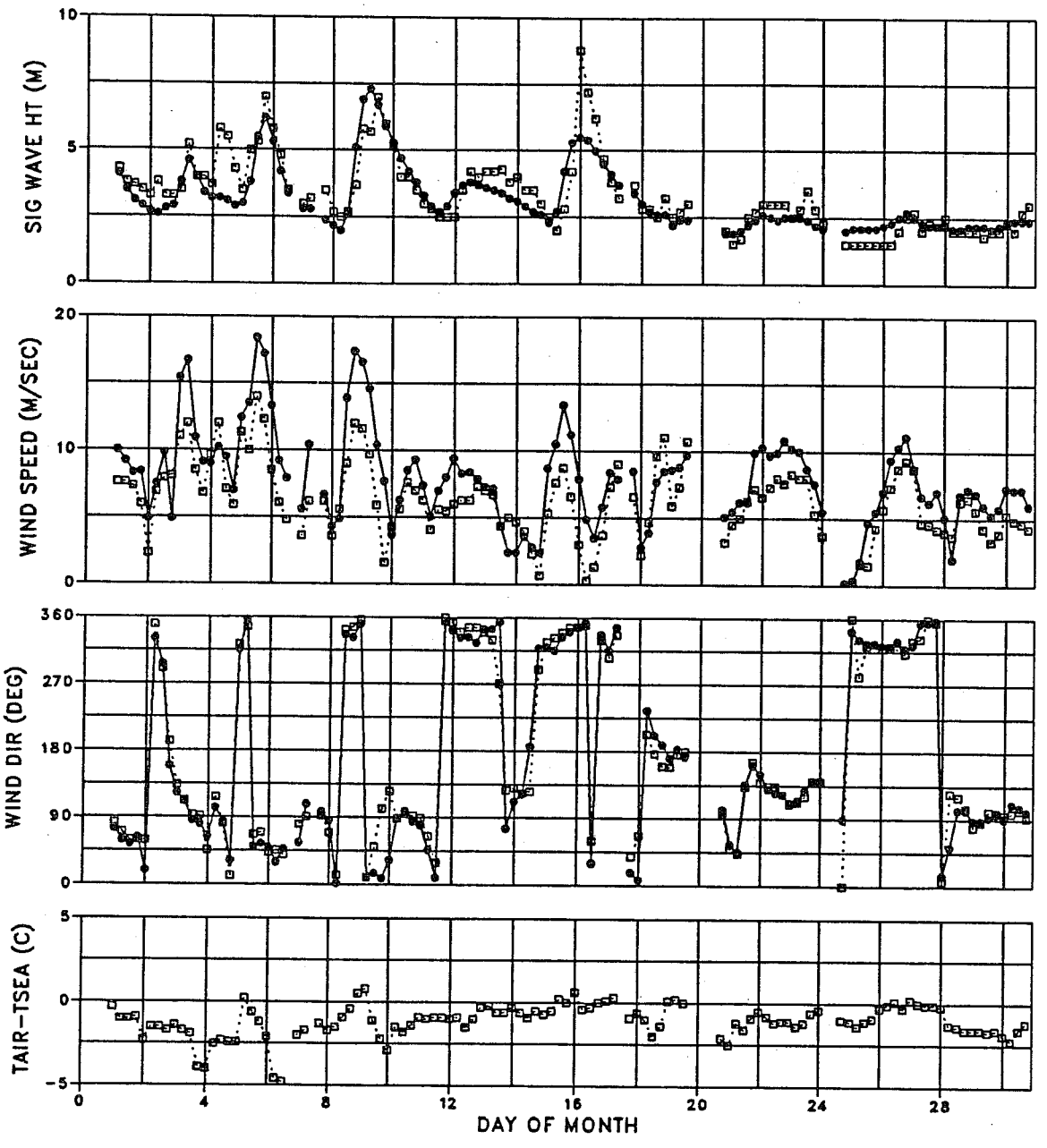

WAVES

MODEL MEAN = 3.2 STDEV = 1.2
OBS MEAN = 3.4 STDEV = 1.4
LSQ FIT: SLOPE = 0.72 INTR = 0.74
RMSE = 0.73
CORR COEF = 0.85 SI = 0.22

WINDS

MODEL MEAN = 8.0 STDEV = 3.5
OBS MEAN = 6.3 STDEV = 2.8
LSQ FIT: SLOPE = 1.07 INTR = 1.33
RMSE = 1.86
CORR COEF = 0.85 SI = 0.30

BUOY 46001 (56.3N,148.3W)
MAY 1988

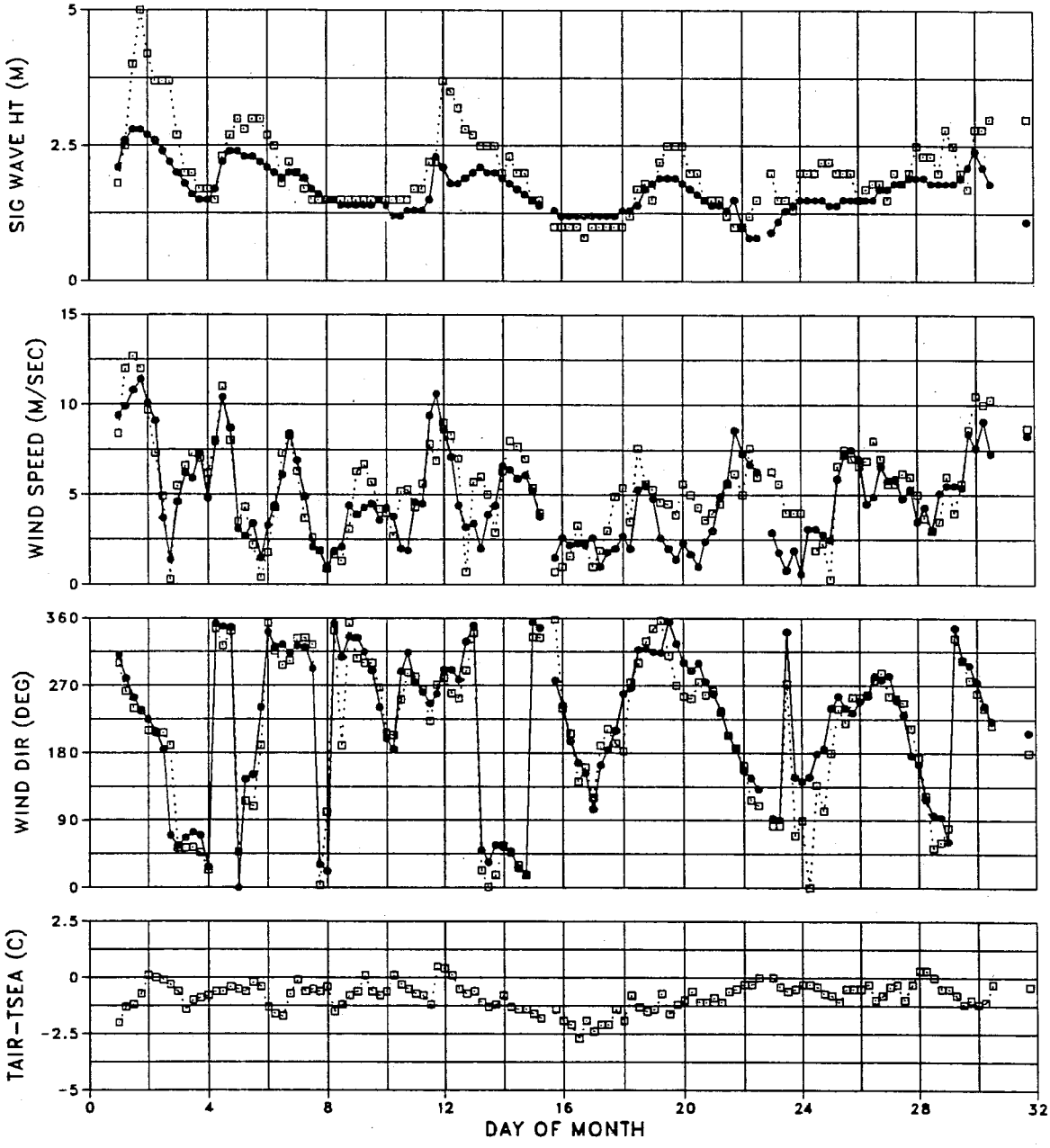

WAVES

MODEL MEAN = 1.7 STDEV = 0.4
OBS MEAN = 2.0 STDEV = 0.8
LSQ FIT: SLOPE = 0.43 INTR = 0.81
RMSE = 0.50
CORR COEF = 0.79 SI = 0.25

WINDS

MODEL MEAN = 4.8 STDEV = 2.6
OBS MEAN = 5.4 STDEV = 2.6
LSQ FIT: SLOPE = 0.81 INTR = 0.45
RMSE = 1.59
CORR COEF = 0.82 SI = 0.30

BUOY 46001 (56.3N,148.3W)
NOVEMBER 1988

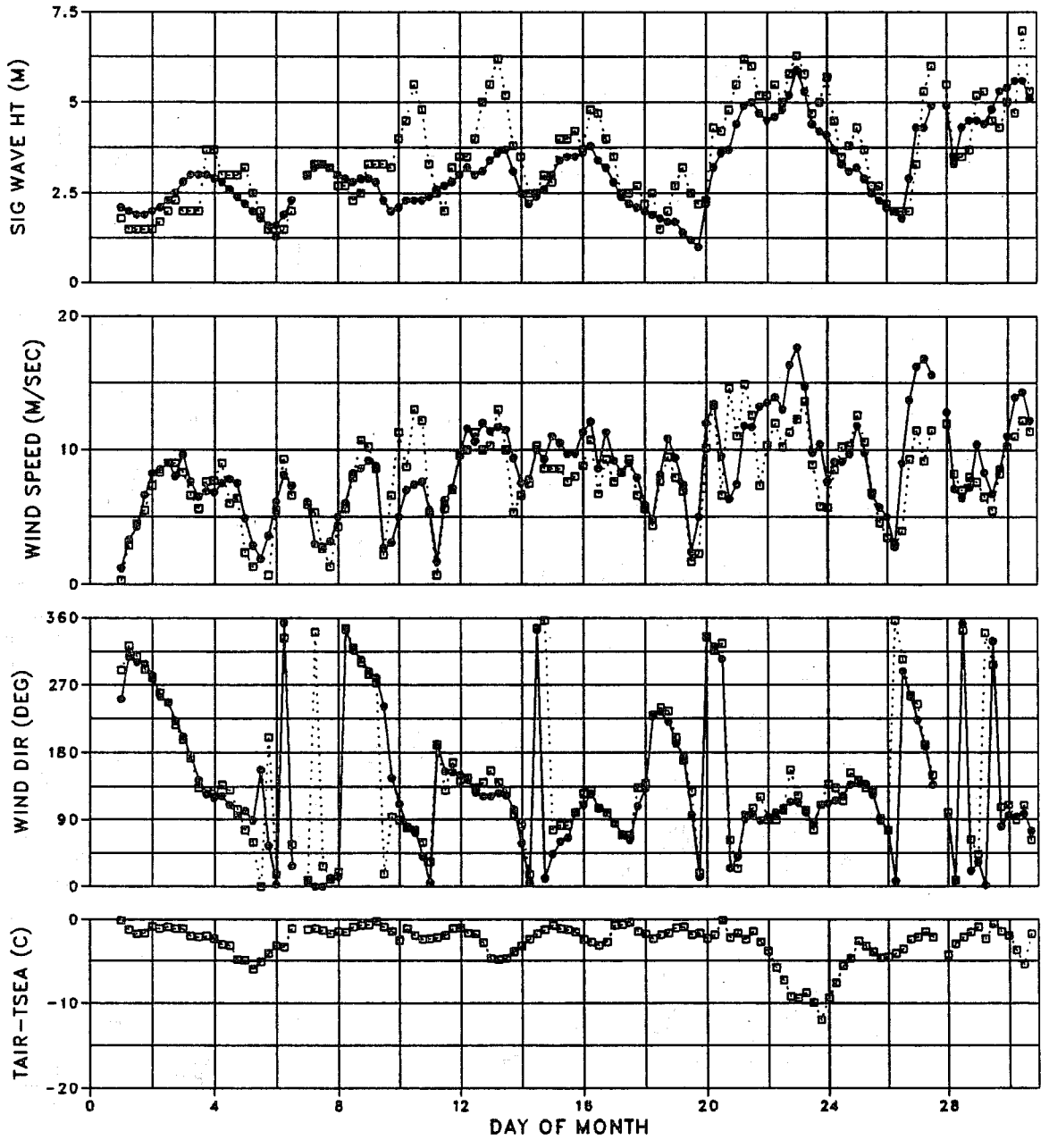

WAVES

MODEL MEAN = 3.1 STDEV = 1.1
OBS MEAN = 3.6 STDEV = 1.4
LSQ FIT: SLOPE = 0.66 INTR = 0.78
RMSE = 0.79
CORR COEF = 0.81 SI = 0.22

WINDS

MODEL MEAN = 8.7 STDEV = 3.4
OBS MEAN = 7.9 STDEV = 3.2
LSQ FIT: SLOPE = 0.83 INTR = 2.09
RMSE = 2.25
CORR COEF = 0.77 SI = 0.28

BUOY 46002 (42.5N,130.4W)
NOVEMBER 1988

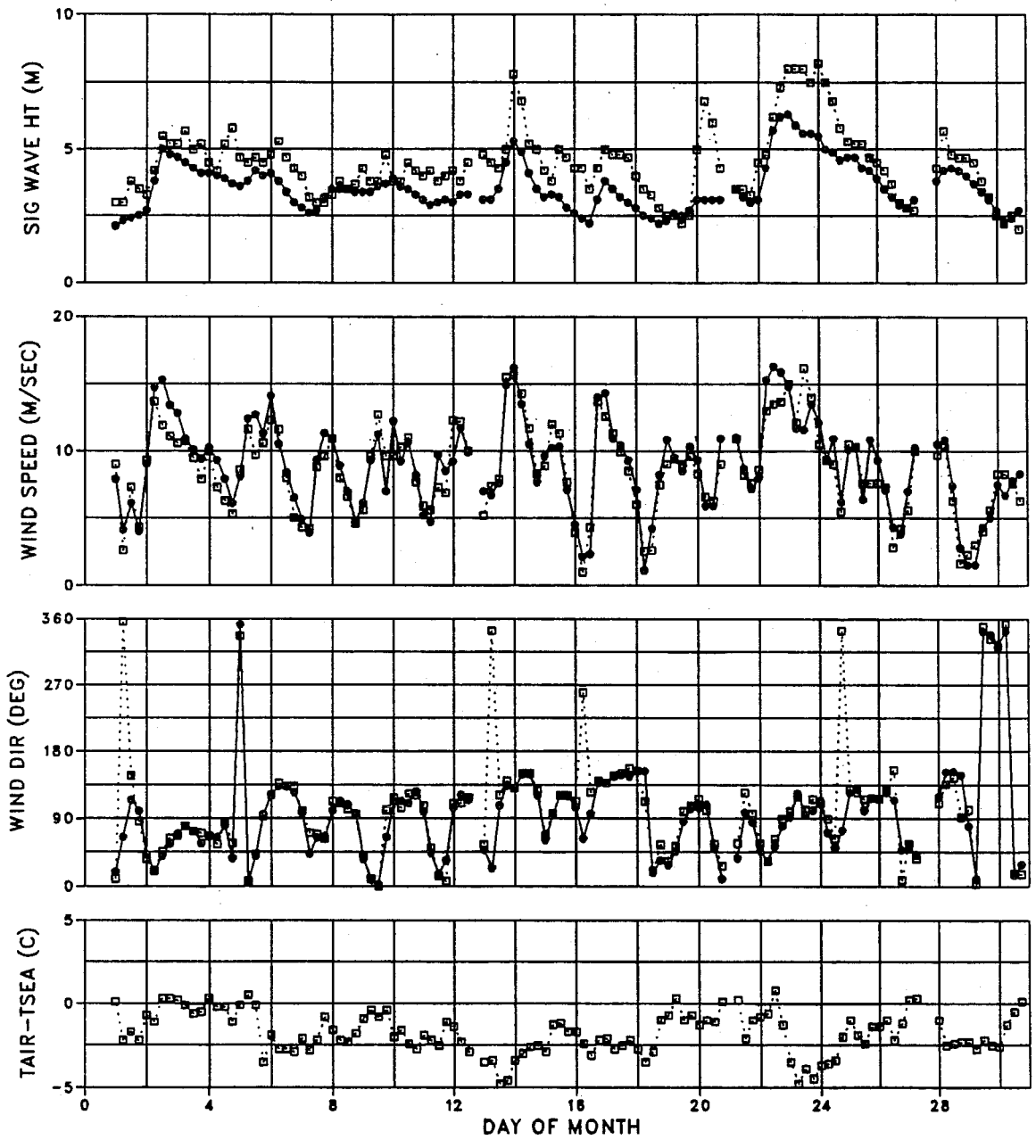

WAVES

MODEL MEAN = 3.6 STDEV = 0.9
OBS MEAN = 4.5 STDEV = 1.3
LSQ FIT: SLOPE = 0.58 INTR = 0.99
RMSE = 0.75
CORR COEF = 0.84 SI = 0.17

WINDS

MODEL MEAN = 8.9 STDEV = 3.4
OBS MEAN = 8.6 STDEV = 3.3
LSQ FIT: SLOPE = 0.96 INTR = 0.65
RMSE = 1.32
CORR COEF = 0.92 SI = 0.15

BUOY 46006 (40.8N,137.6W)
NOVEMBER 1988

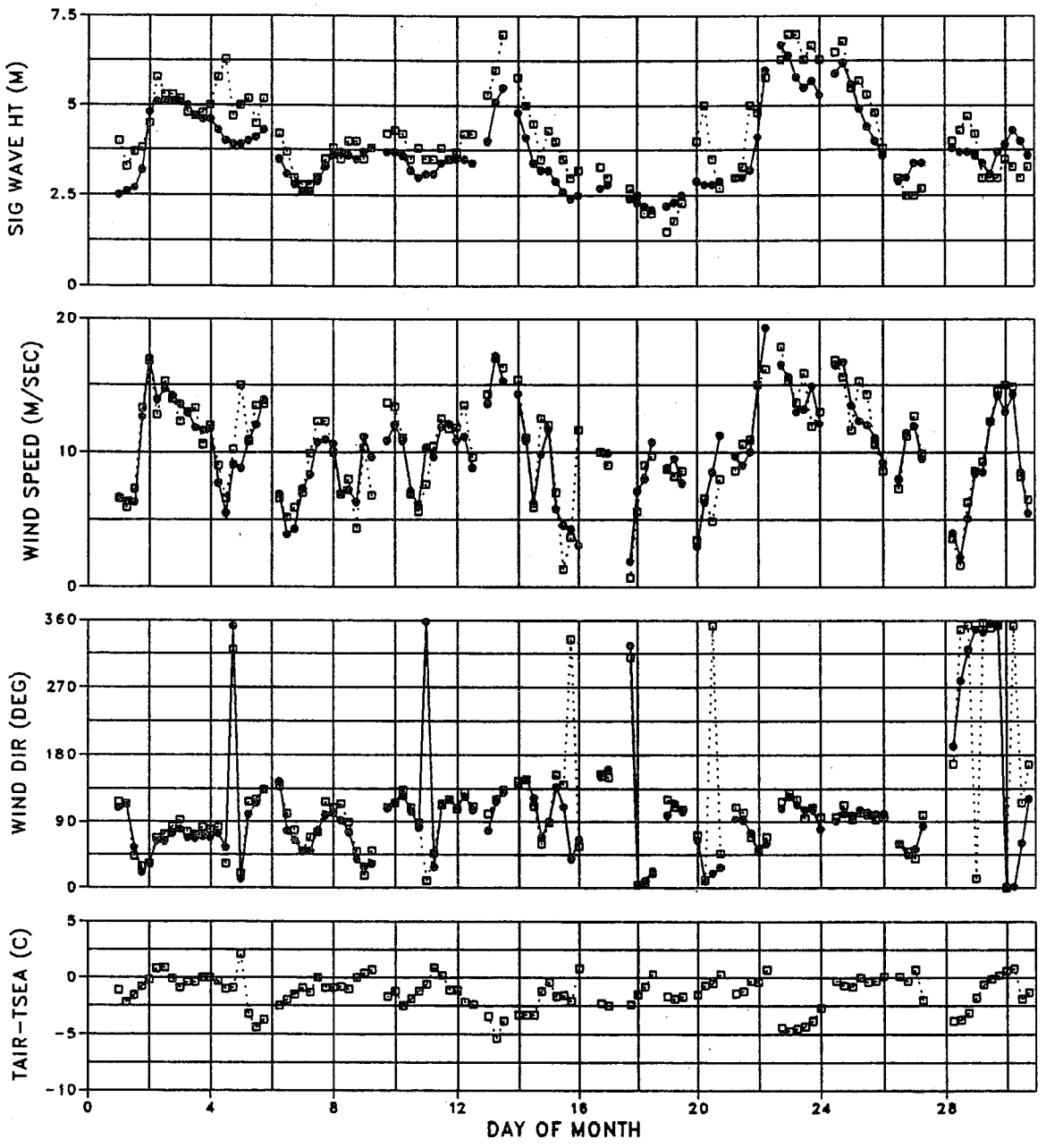

WAVES

MODEL MEAN = 3.8 STDEV = 1.0
OBS MEAN = 4.2 STDEV = 1.3
LSQ FIT: SLOPE = 0.72 INTR = 0.75
RMSE = 0.63
CORR COEF = 0.87 SI = 0.15

WINDS

MODEL MEAN = 10.1 STDEV = 3.6
OBS MEAN = 10.4 STDEV = 3.8
LSQ FIT: SLOPE = 0.85 INTR = 1.27
RMSE = 1.67
CORR COEF = 0.90 SI = 0.16

APPENDIX A.2

Time series in the Hawaiian area

Conventions:

—— model
- - - observation

Wind direction

0°	Southerly
90°	Westerly
180°	Northerly
270°	Easterly

BUOY 51002 (17.2N,157.8W)
JANUARY 1988

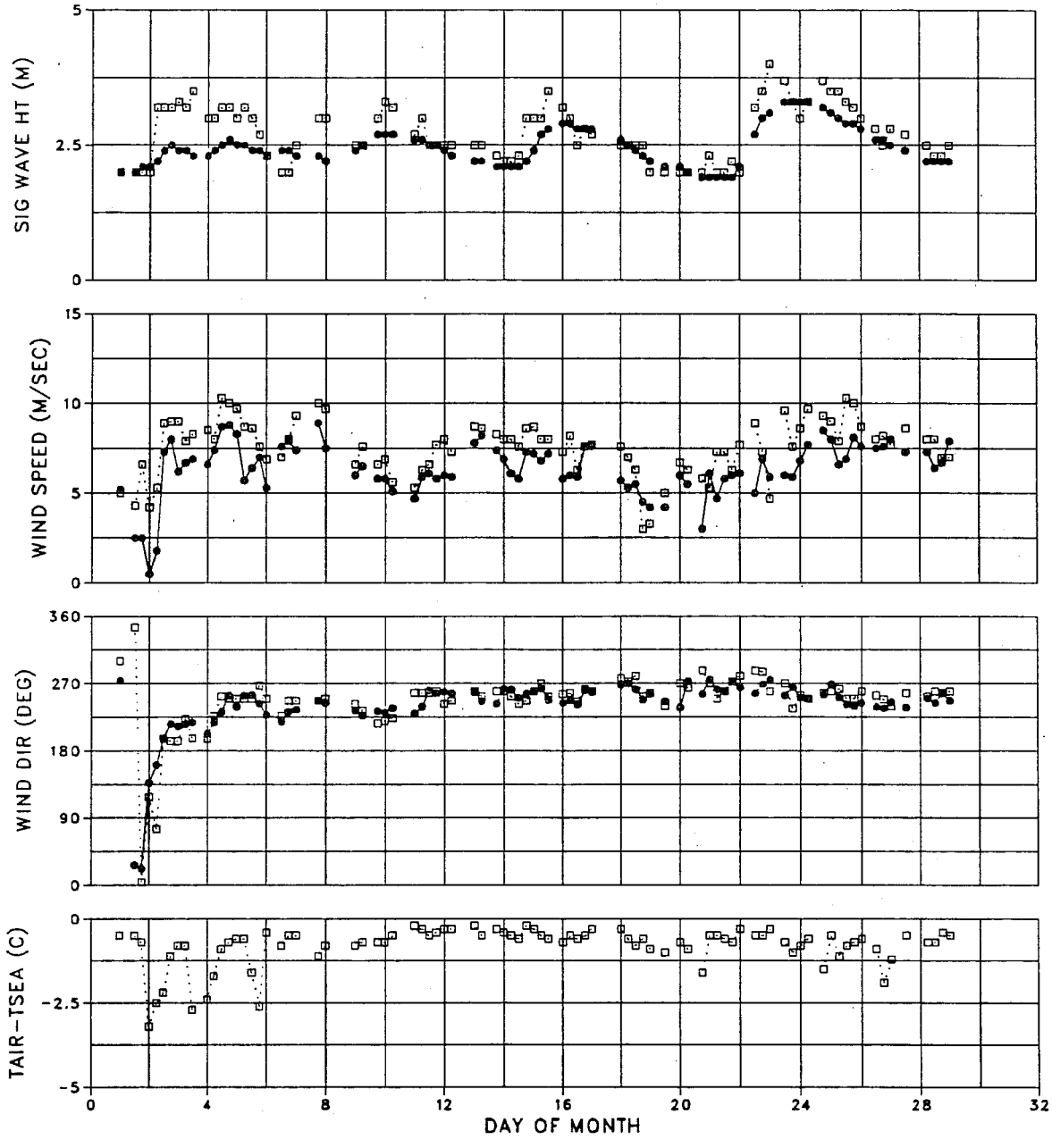

WAVES

MODEL MEAN = 2.5 STDEV = 0.4
OBS MEAN = 2.7 STDEV = 0.5
LSQ FIT: SLOPE = 0.53 INTR = 1.01
RMSE = 0.33
CORR COEF = 0.76 SI = 0.12

WINDS

MODEL MEAN = 6.3 STDEV = 1.5
OBS MEAN = 7.6 STDEV = 1.5
LSQ FIT: SLOPE = 0.73 INTR = 0.80
RMSE = 1.11
CORR COEF = 0.74 SI = 0.15

BUOY 51001 (23.4N,162.3W)
MAY 1988

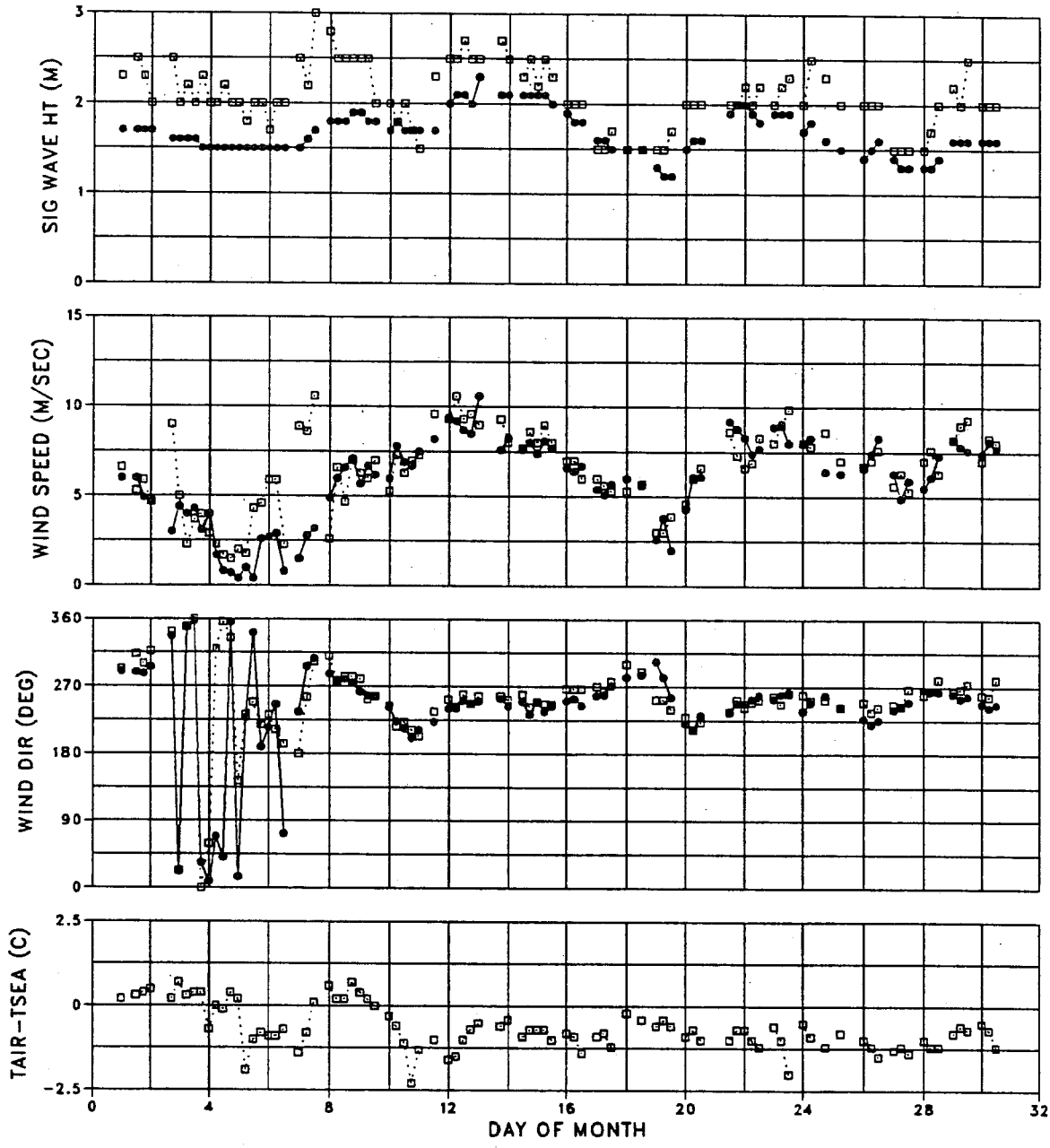

WAVES

MODEL MEAN = 1.7 STDEV = 0.2
OBS MEAN = 2.1 STDEV = 0.3
LSQ FIT: SLOPE = 0.44 INTR = 0.76
RMSE = 0.27
CORR COEF = 0.63 SI = 0.13

WINDS

MODEL MEAN = 5.9 STDEV = 2.4
OBS MEAN = 6.5 STDEV = 2.2
LSQ FIT: SLOPE = 0.79 INTR = 0.77
RMSE = 1.72
CORR COEF = 0.72 SI = 0.26

BUOY 51003 (19.2N,160.8W)
MAY 1988

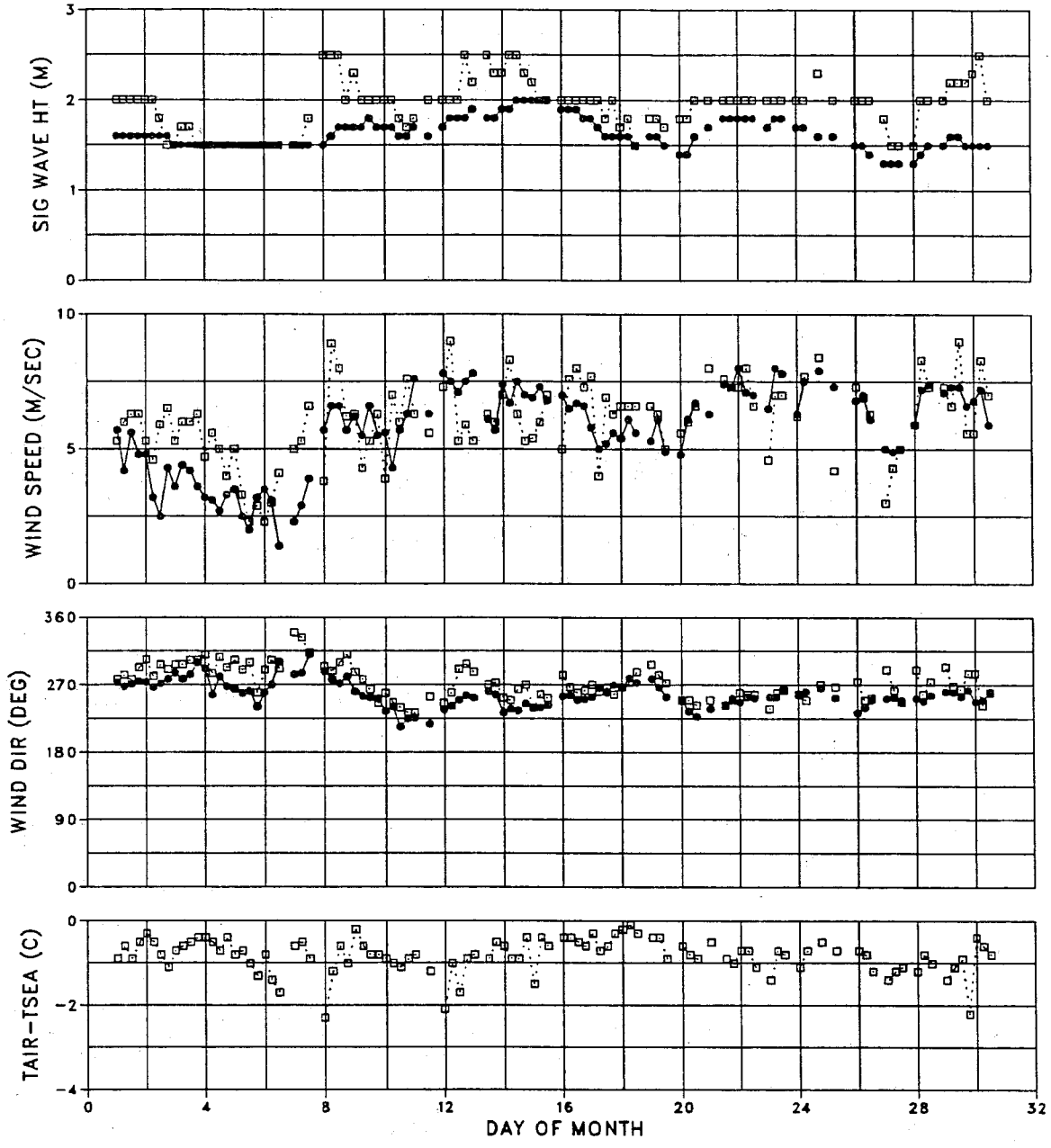

WAVES

MODEL MEAN = 1.6 STDEV = 0.2
OBS MEAN = 1.9 STDEV = 0.3
LSQ FIT: SLOPE = 0.32 INTR = 1.02
RMSE = 0.24
CORR COEF = 0.55 SI = 0.12

WINDS

MODEL MEAN = 5.7 STDEV = 1.6
OBS MEAN = 6.1 STDEV = 1.5
LSQ FIT: SLOPE = 0.67 INTR = 1.63
RMSE = 1.36
CORR COEF = 0.61 SI = 0.22

BUOY 51001 (23.4N,162.3W)
JULY 1988

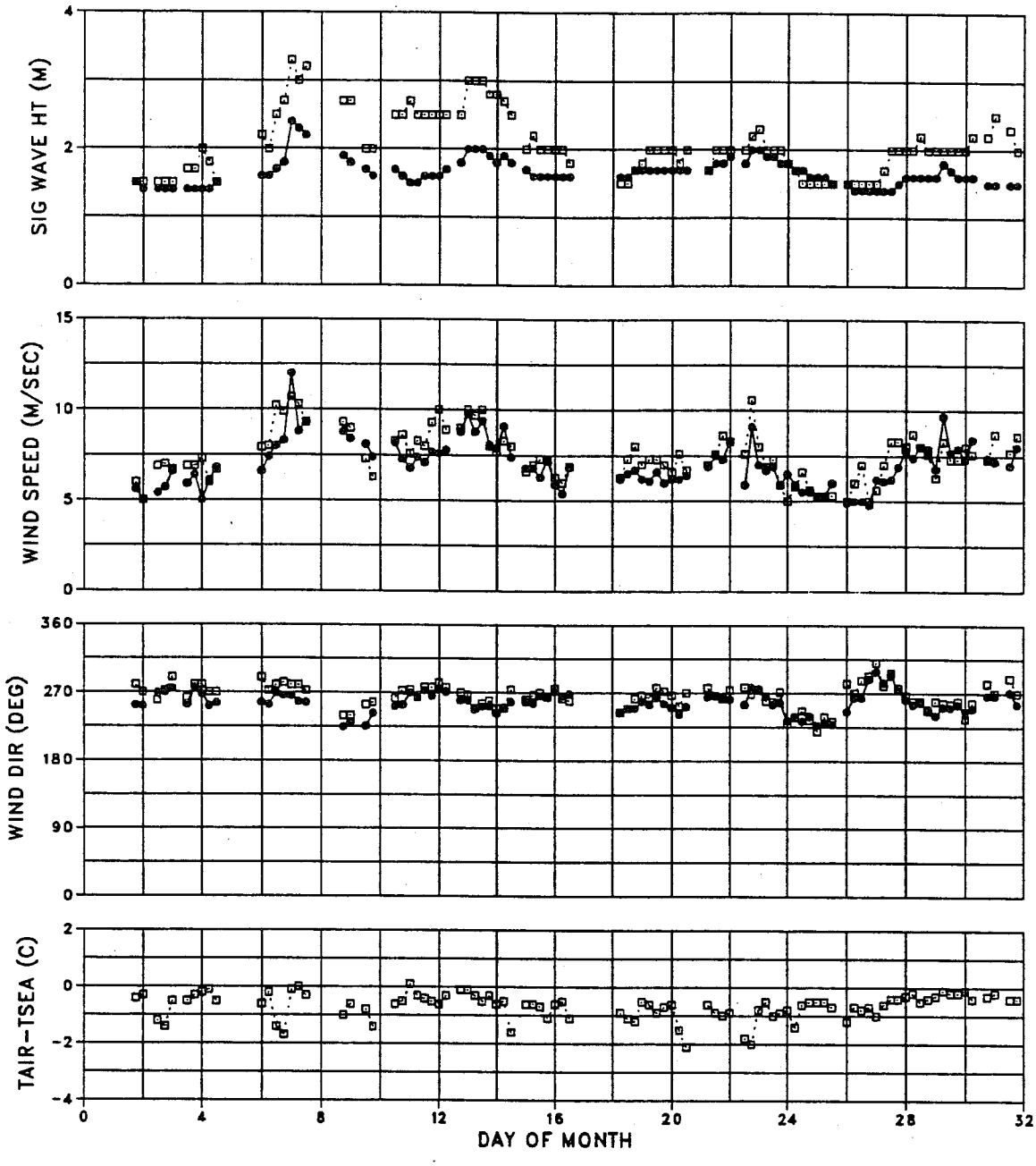

WAVES

MODEL MEAN = 1.7 STDEV = 0.2
OBS MEAN = 2.1 STDEV = 0.5
LSQ FIT: SLOPE = 0.30 INTR = 1.04
RMSE = 0.35
CORR COEF = 0.67 SI = 0.17

WINDS

MODEL MEAN = 7.0 STDEV = 1.3
OBS MEAN = 7.5 STDEV = 1.4
LSQ FIT: SLOPE = 0.77 INTR = 1.22
RMSE = 0.82
CORR COEF = 0.81 SI = 0.11

BUOY 51003 (19.2N,160.8W)
JULY 1988

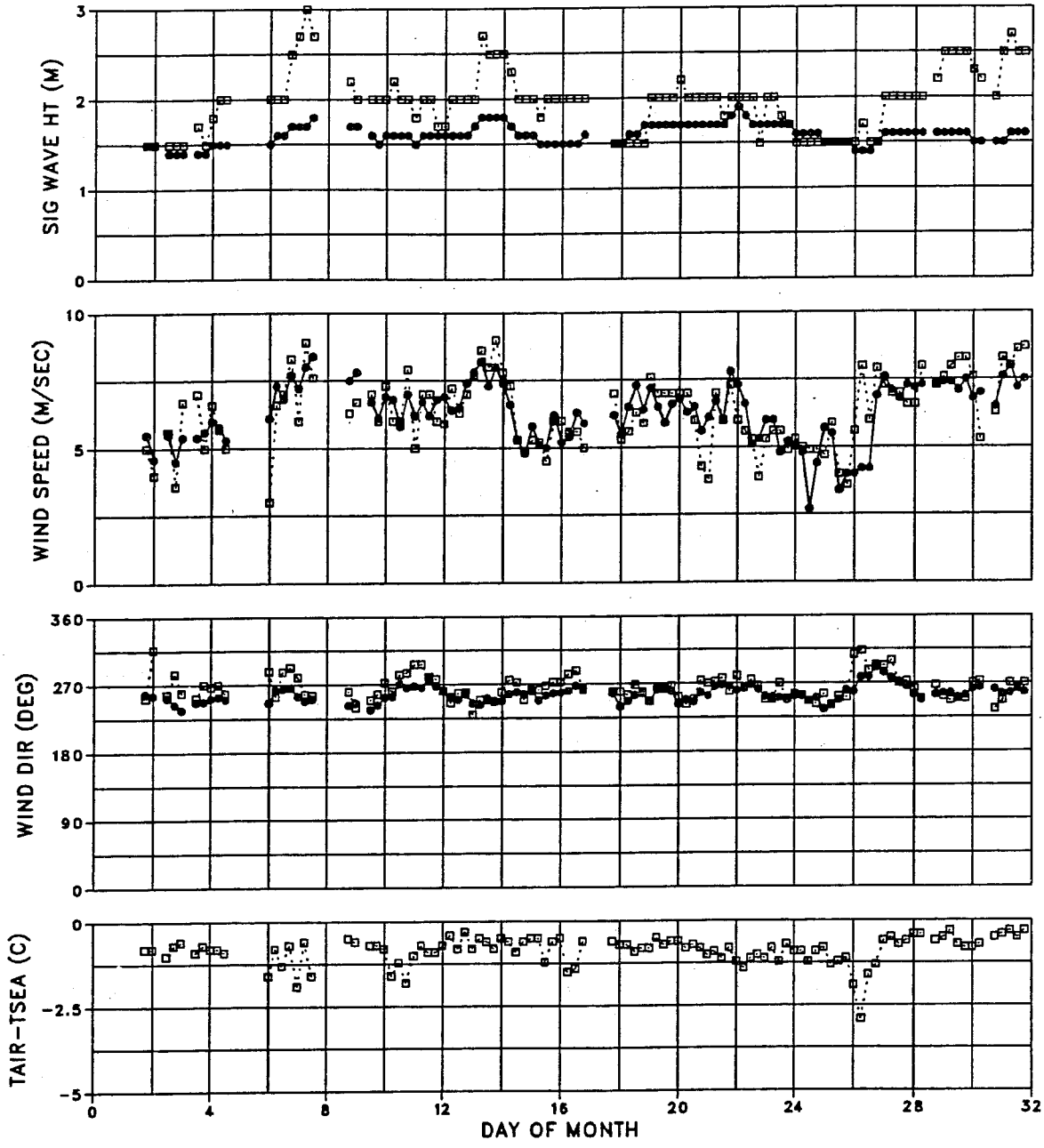

WAVES

MODEL MEAN = 1.6 STDEV = 0.1
OBS MEAN = 2.0 STDEV = 0.3
LSQ FIT: SLOPE = 0.15 INTR = 1.31
RMSE = 0.31
CORR COEF = 0.48 SI = 0.16
MEAN REL ERR = 0.18 STDEV = 0.11

WINDS

MODEL MEAN = 6.3 STDEV = 1.1
OBS MEAN = 6.3 STDEV = 1.3
LSQ FIT: SLOPE = 0.61 INTR = 2.45
RMSE = 0.94
CORR COEF = 0.71 SI = 0.15
MEAN REL ERR = 0.12 STDEV = 0.14

BUOY 51001 (23.4N,162.3W)
NOVEMBER 1988

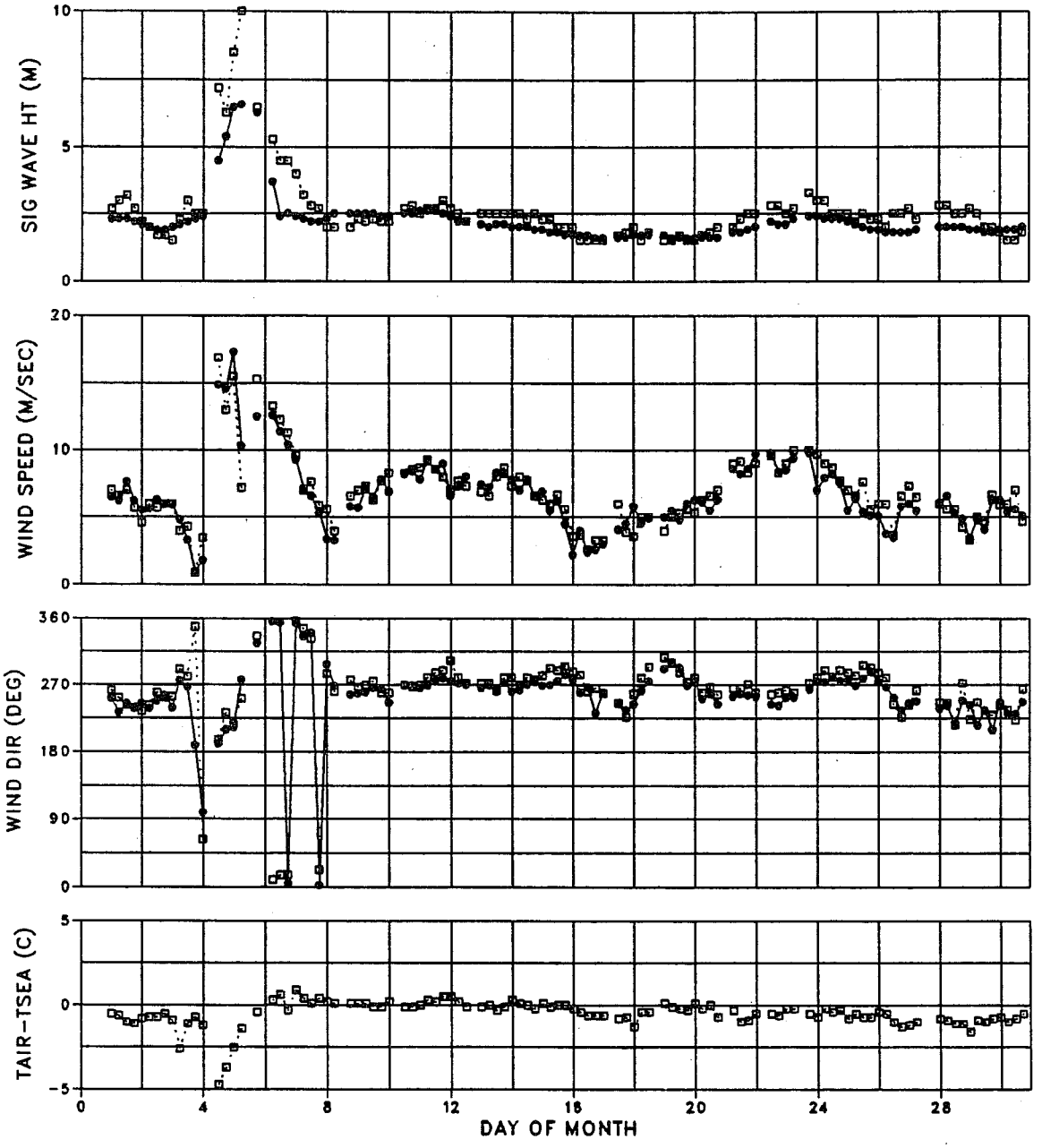

WAVES

MODEL MEAN = 2.2 STDEV = 0.9
OBS MEAN = 2.6 STDEV = 1.3
LSQ FIT: SLOPE = 0.62 INTR = 0.63
RMSE = 0.61
CORR COEF = 0.92 SI = 0.23

WINDS

MODEL MEAN = 6.7 STDEV = 2.6
OBS MEAN = 6.9 STDEV = 2.6
LSQ FIT: SLOPE = 0.94 INTR = 0.14
RMSE = 0.94
CORR COEF = 0.94 SI = 0.14

BUOY 51002 (17.2N,157.8W)
NOVEMBER 1988

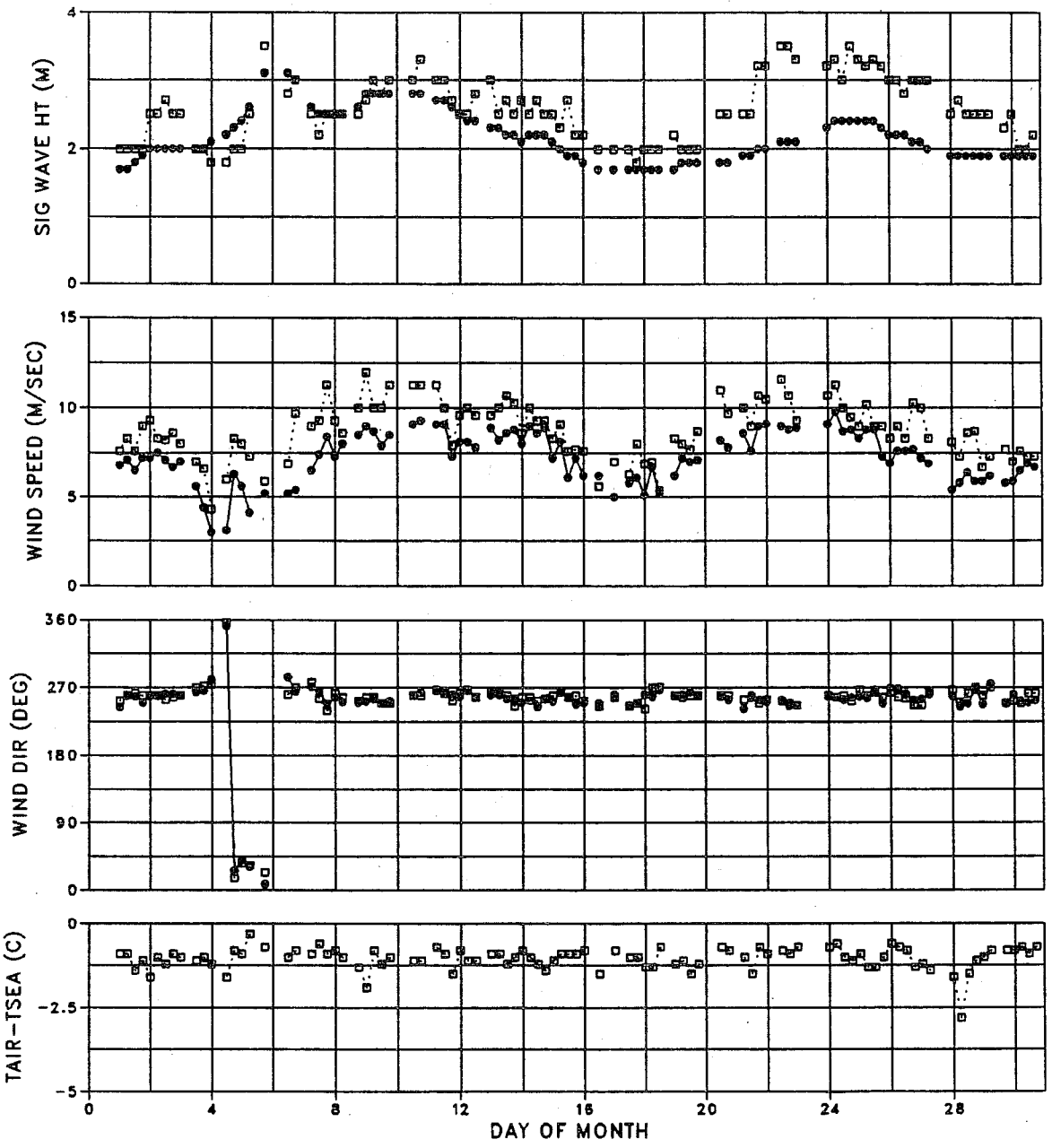

WAVES

MODEL MEAN = 2.2 STDEV = 0.4
OBS MEAN = 2.6 STDEV = 0.5
LSQ FIT: SLOPE = 0.43 INTR = 1.06
RMSE = 0.39
CORR COEF = 0.55 SI = 0.15

WINDS

MODEL MEAN = 7.2 STDEV = 1.4
OBS MEAN = 8.8 STDEV = 1.6
LSQ FIT: SLOPE = 0.79 INTR = 0.32
RMSE = 0.81
CORR COEF = 0.85 SI = 0.09

BUOY 51003 (19.2N,160.8W)
NOVEMBER 1988

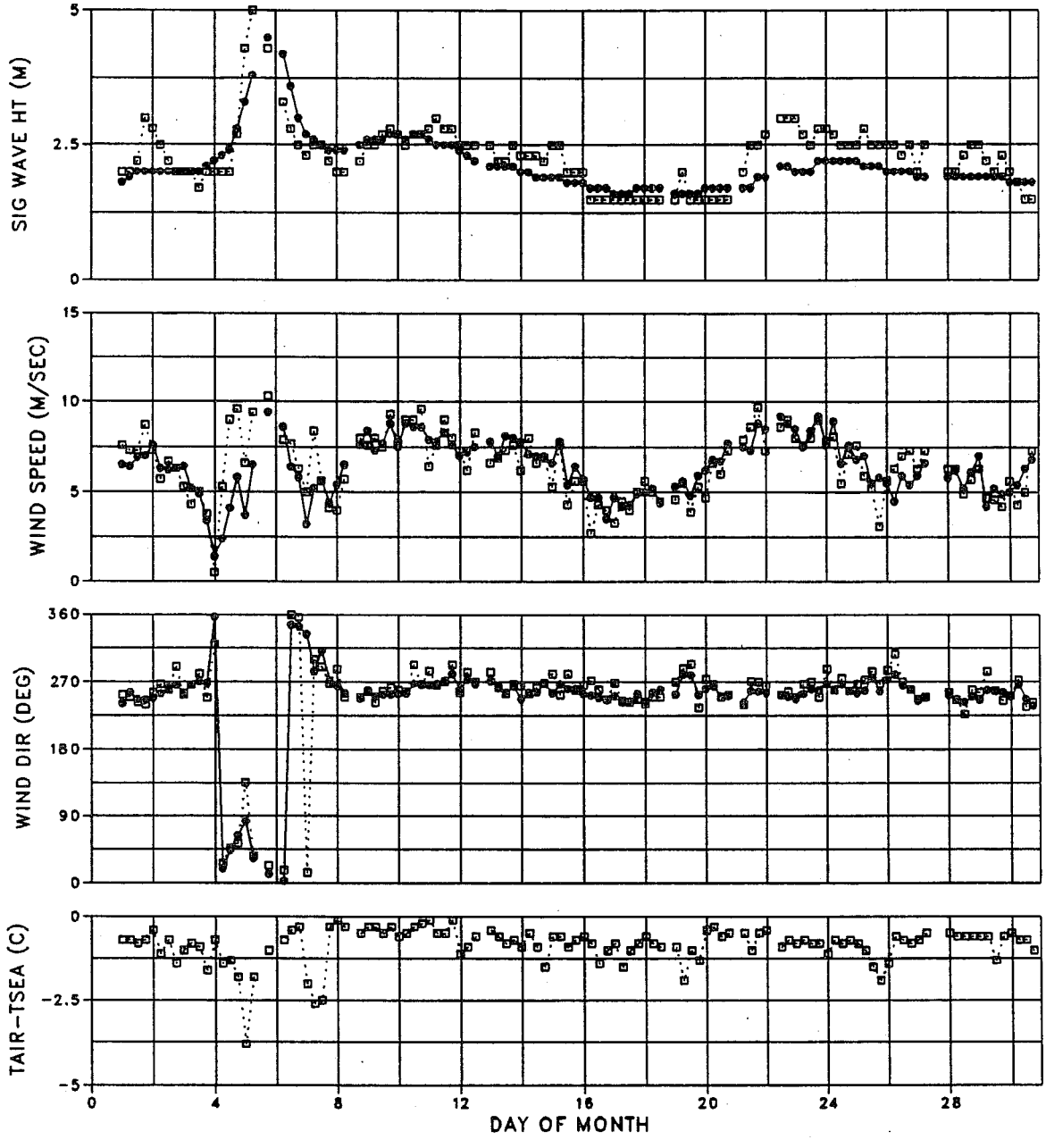

WAVES

MODEL MEAN = 2.1 STDEV = 0.5
OBS MEAN = 2.3 STDEV = 0.6
LSQ FIT: SLOPE = 0.65 INTR = 0.65
RMSE = 0.39
CORR COEF = 0.75 SI = 0.17

WINDS

MODEL MEAN = 6.4 STDEV = 1.6
OBS MEAN = 6.5 STDEV = 1.8
LSQ FIT: SLOPE = 0.68 INTR = 2.03
RMSE = 1.16
CORR COEF = 0.76 SI = 0.18

APPENDIX A.3

Time series off the east coast of the US

Conventions:

—— model
- - - observation

Wind direction

0°	Southerly
90°	Westerly
180°	Northerly
270°	Easterly

BUOY 44011 (41.1N, 66.6W)
JANUARY 1988

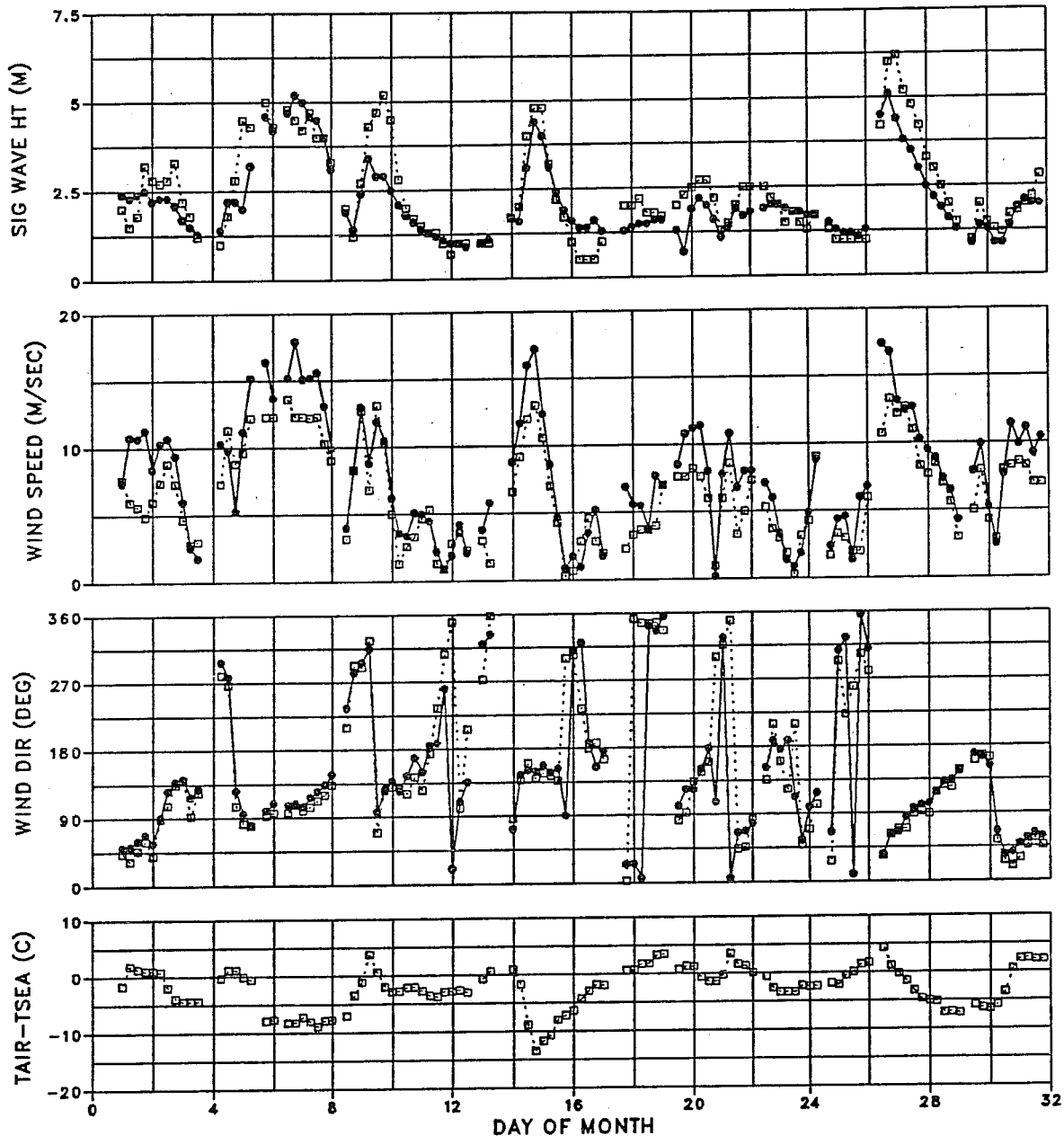

WAVES

MODEL MEAN = 2.1 STDEV = 1.1
OBS MEAN = 2.4 STDEV = 1.3
LSQ FIT: SLOPE = 0.71 INTR = 0.43
RMSE = 0.65
CORR COEF = 0.88 SI = 0.27

WINDS

MODEL MEAN = 7.9 STDEV = 4.4
OBS MEAN = 6.4 STDEV = 3.6
LSQ FIT: SLOPE = 1.12 INTR = 0.81
RMSE = 1.78
CORR COEF = 0.92 SI = 0.28

BUOY 41002 (32.2N, 75.3W)
MARCH 1988

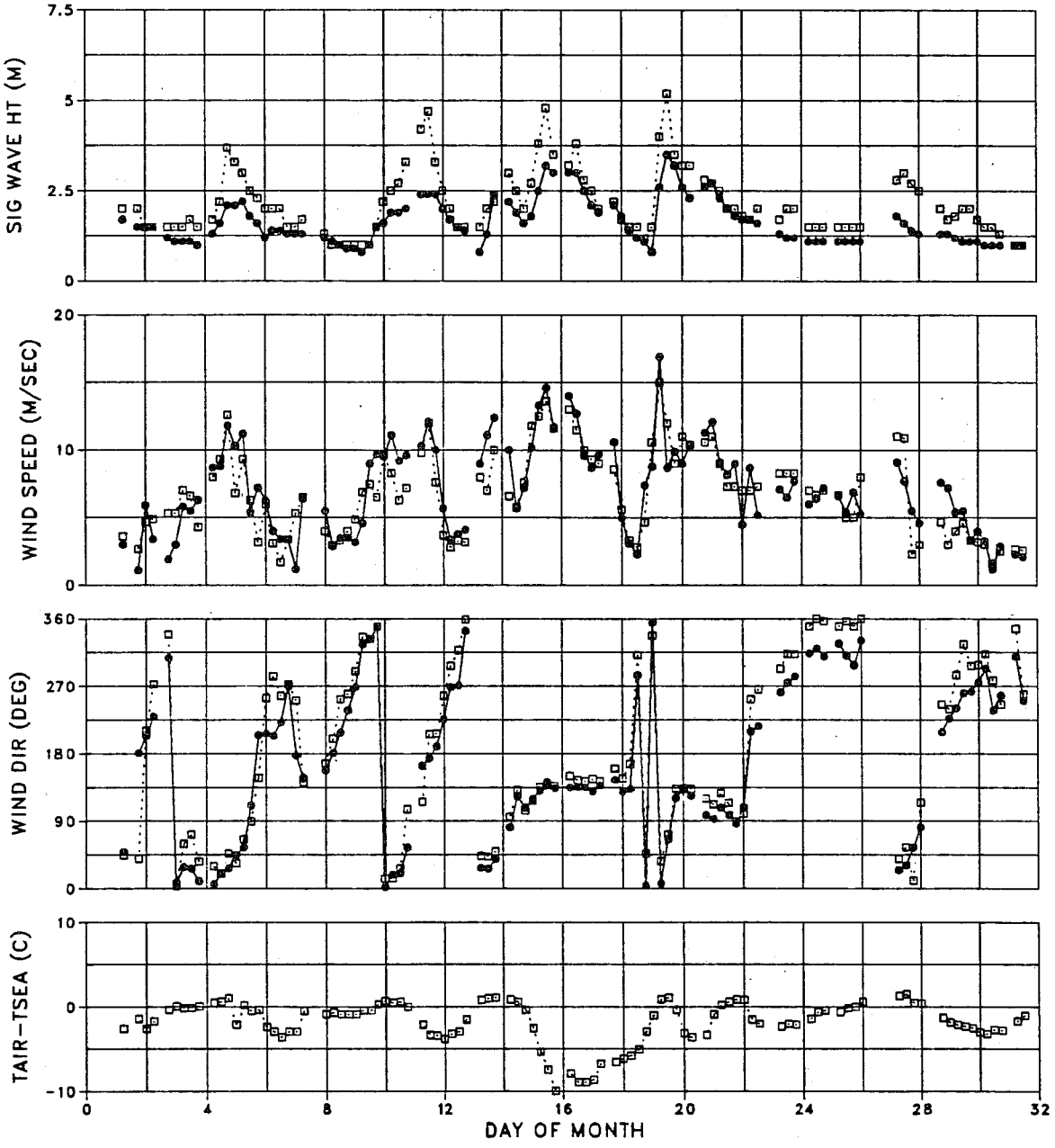

WAVES

MODEL MEAN = 1.6 STDEV = 0.6
OBS MEAN = 2.2 STDEV = 0.9
LSQ FIT: SLOPE = 0.60 INTR = 0.33
RMSE = 0.47
CORR COEF = 0.87 SI = 0.22

WINDS

MODEL MEAN = 7.1 STDEV = 3.4
OBS MEAN = 6.8 STDEV = 3.1
LSQ FIT: SLOPE = 0.92 INTR = 0.87
RMSE = 1.74
CORR COEF = 0.86 SI = 0.26

BUOY 44008 (40.5N, 69.5W)
APRIL 1988

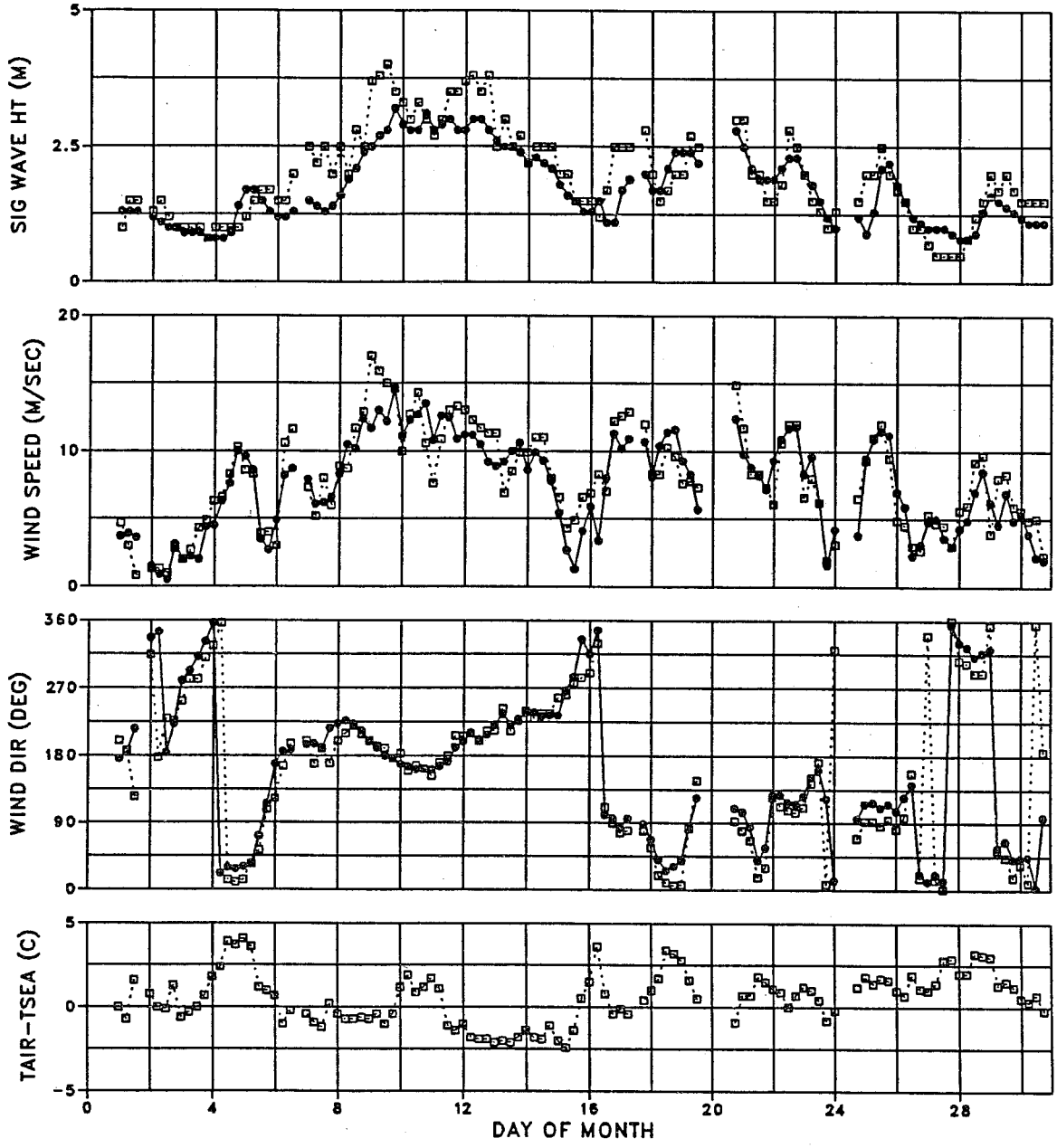

WAVES

MODEL MEAN = 1.7 STDEV = 0.7
OBS MEAN = 2.0 STDEV = 0.9
LSQ FIT: SLOPE = 0.69 INTR = 0.38
RMSE = 0.42
CORR COEF = 0.87 SI = 0.21

WINDS

MODEL MEAN = 7.5 STDEV = 3.5
OBS MEAN = 8.0 STDEV = 3.7
LSQ FIT: SLOPE = 0.85 INTR = 0.72
RMSE = 1.64
CORR COEF = 0.90 SI = 0.21

BUOY 41001 (34.9N, 72.9W)
NOVEMBER 1988

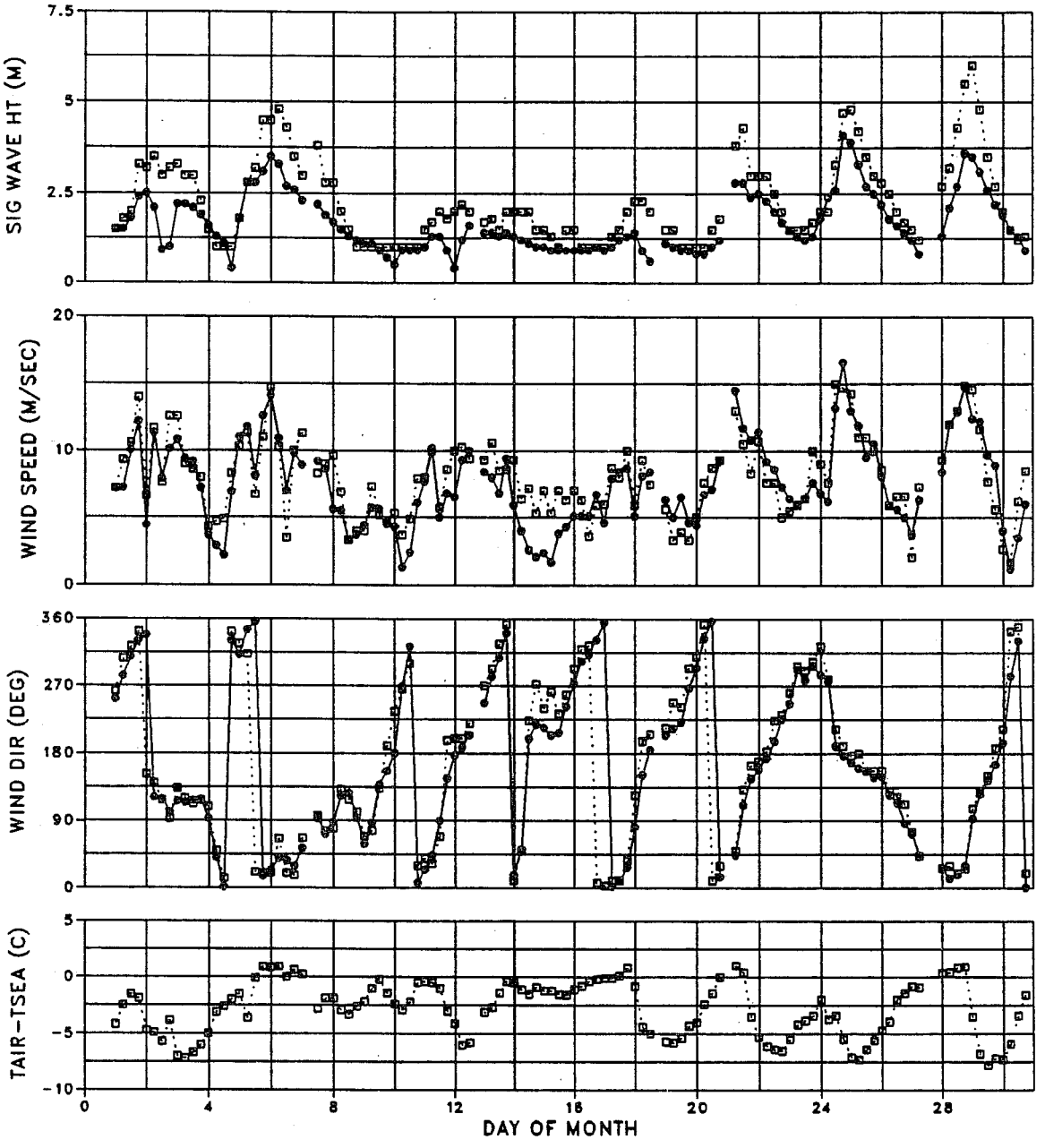

WAVES

MODEL MEAN = 1.7 STDEV = 0.8
OBS MEAN = 2.3 STDEV = 1.2
LSQ FIT: SLOPE = 0.64 INTR = 0.22
RMSE = 0.55
CORR COEF = 0.90 SI = 0.24

WINDS

MODEL MEAN = 7.5 STDEV = 3.2
OBS MEAN = 8.1 STDEV = 3.0
LSQ FIT: SLOPE = 0.93 INTR =-0.01
RMSE = 1.64
CORR COEF = 0.86 SI = 0.20

BUOY 41002 (32.2N, 75.3W)
NOVEMBER 1988

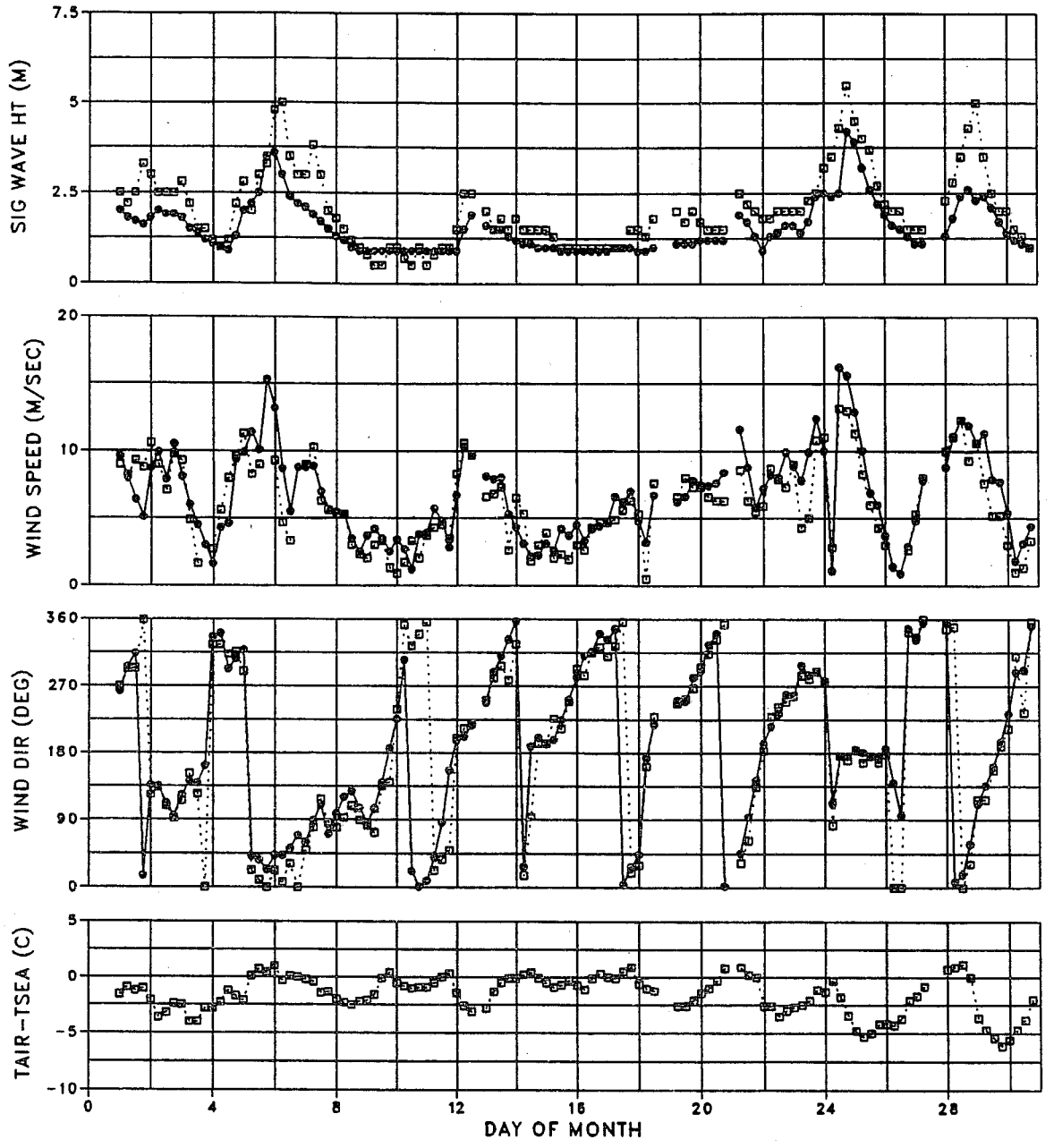

WAVES

MODEL MEAN = 1.5 STDEV = 0.7
OBS MEAN = 2.1 STDEV = 1.1
LSQ FIT: SLOPE = 0.60 INTR = 0.31
RMSE = 0.52
CORR COEF = 0.91 SI = 0.25

WINDS

MODEL MEAN = 6.7 STDEV = 3.2
OBS MEAN = 6.1 STDEV = 3.1
LSQ FIT: SLOPE = 0.90 INTR = 1.25
RMSE = 1.60
CORR COEF = 0.87 SI = 0.26

BUOY 41006 (29.3N, 77.4W)
NOVEMBER 1988

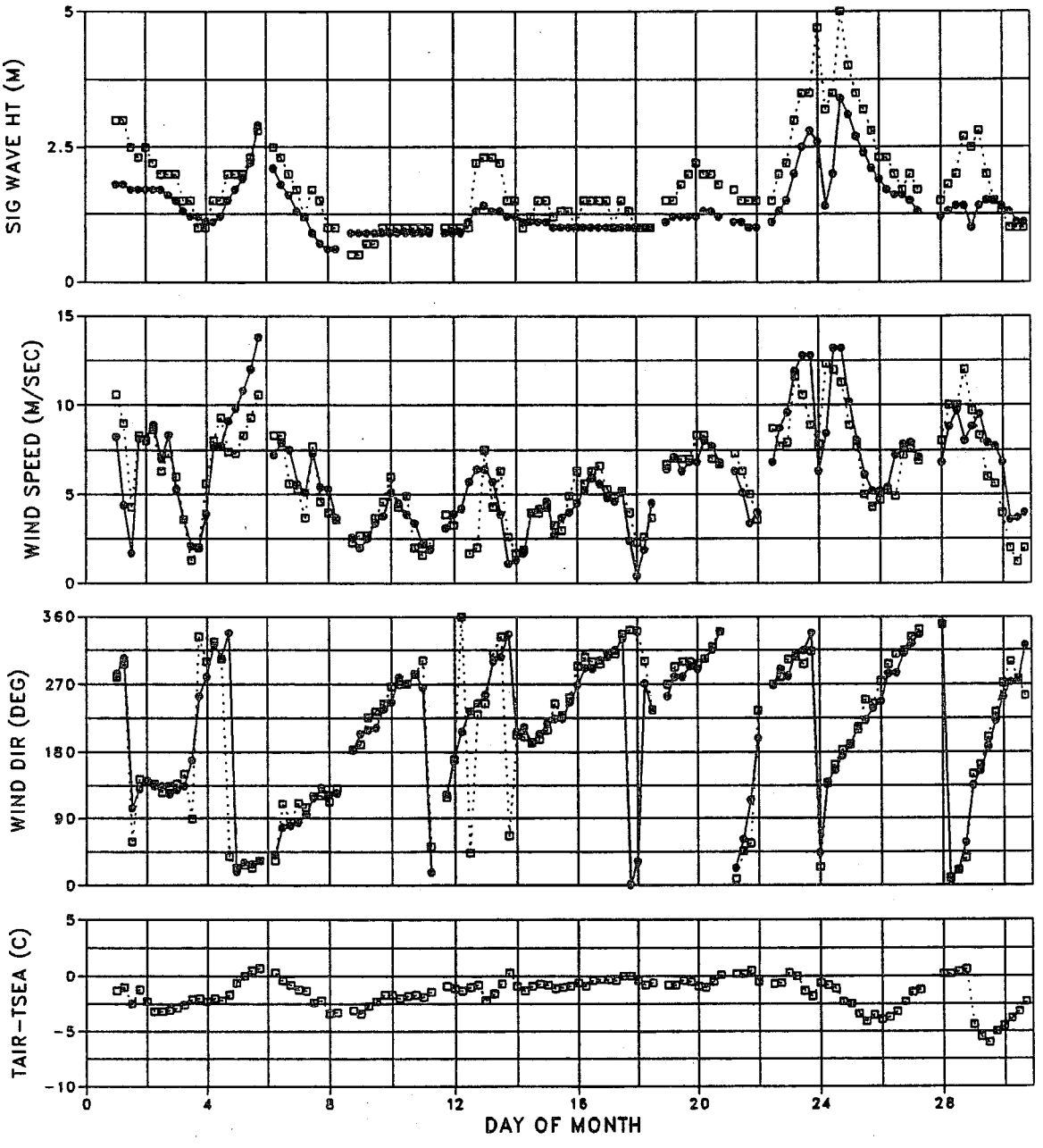

WAVES

MODEL MEAN = 1.4 STDEV = 0.5
OBS MEAN = 1.8 STDEV = 0.8
LSQ FIT: SLOPE = 0.55 INTR = 0.37
RMSE = 0.45
CORR COEF = 0.87 SI = 0.25

WINDS

MODEL MEAN = 6.1 STDEV = 2.9
OBS MEAN = 6.0 STDEV = 2.7
LSQ FIT: SLOPE = 0.89 INTR = 0.74
RMSE = 1.56
CORR COEF = 0.85 SI = 0.26

BUOY 44008 (40.5N, 69.5W)
NOVEMBER 1988

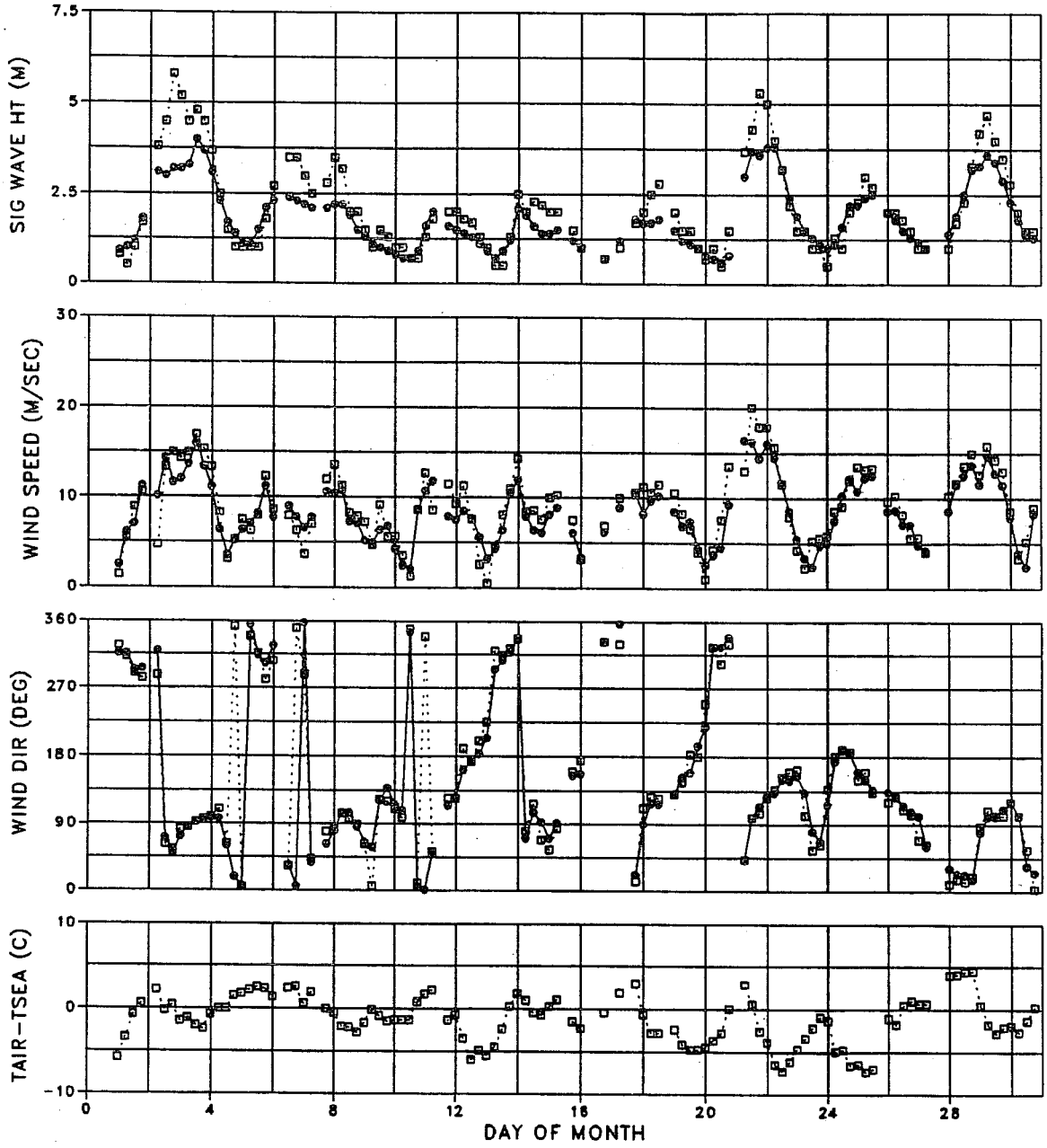

WAVES

MODEL MEAN = 1.8 STDEV = 0.9
OBS MEAN = 2.1 STDEV = 1.3
LSQ FIT: SLOPE = 0.64 INTR = 0.46
RMSE = 0.55
CORR COEF = 0.93 SI = 0.26

WINDS

MODEL MEAN = 8.4 STDEV = 3.5
OBS MEAN = 9.1 STDEV = 4.1
LSQ FIT: SLOPE = 0.78 INTR = 1.28
RMSE = 1.65
CORR COEF = 0.92 SI = 0.18

BUOY 44011 (41.1N, 66.6W)
NOVEMBER 1988

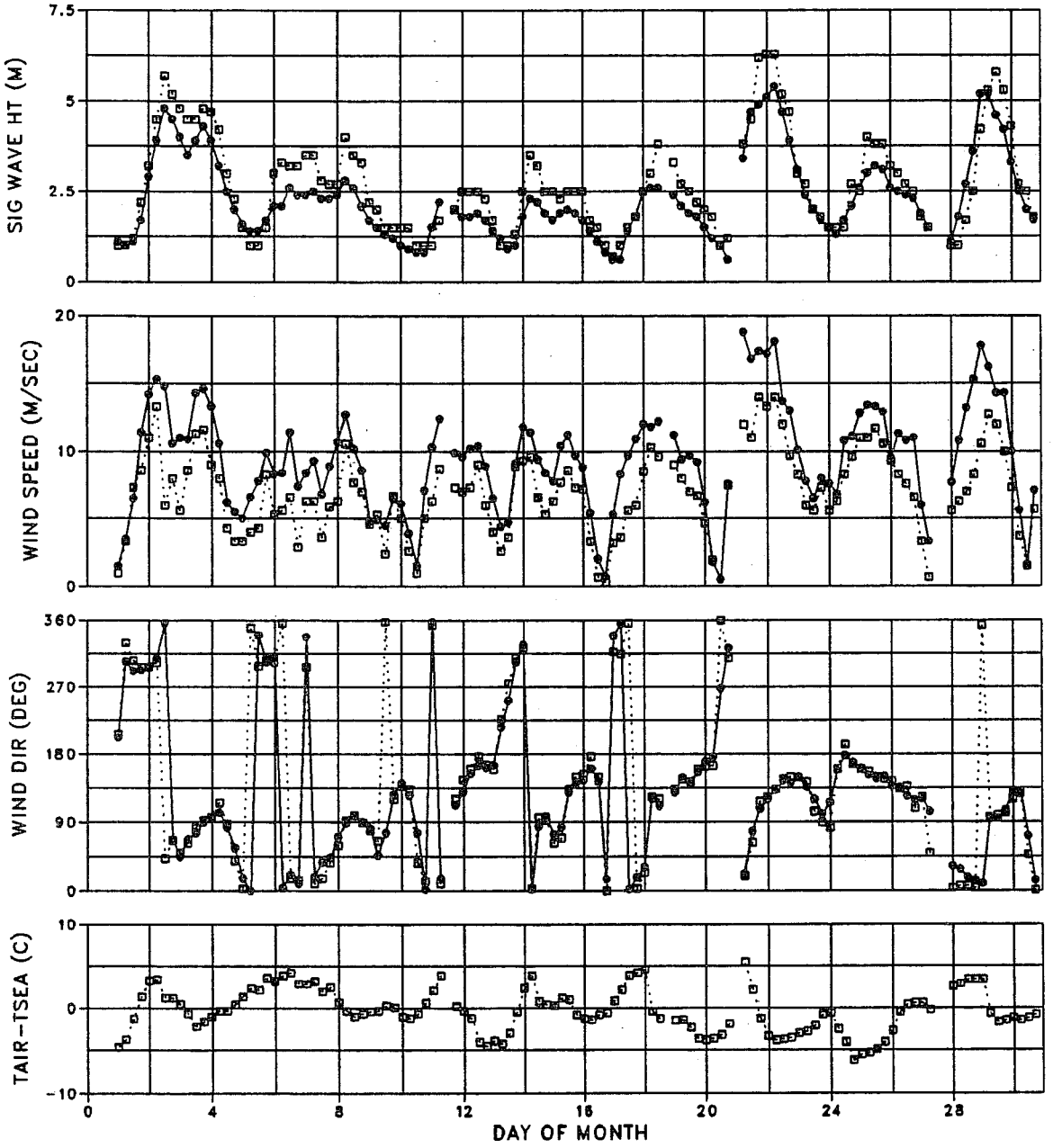

WAVES

MODEL MEAN = 2.3 STDEV = 1.2
OBS MEAN = 2.7 STDEV = 1.4
LSQ FIT: SLOPE = 0.79 INTR = 0.17
RMSE = 0.49
CORR COEF = 0.94 SI = 0.18

WINDS

MODEL MEAN = 9.5 STDEV = 3.9
OBS MEAN = 7.0 STDEV = 3.1
LSQ FIT: SLOPE = 1.14 INTR = 1.55
RMSE = 1.63
CORR COEF = 0.91 SI = 0.23

APPENDIX A.4

Time series in the northeast Atlantic

Conventions:

—— model
- - - observation

Wind direction

0°	Southerly
90°	Westerly
180°	Northerly
270°	Easterly

BUOY 64042 (60.5N, 2.9W)
MARCH 1988

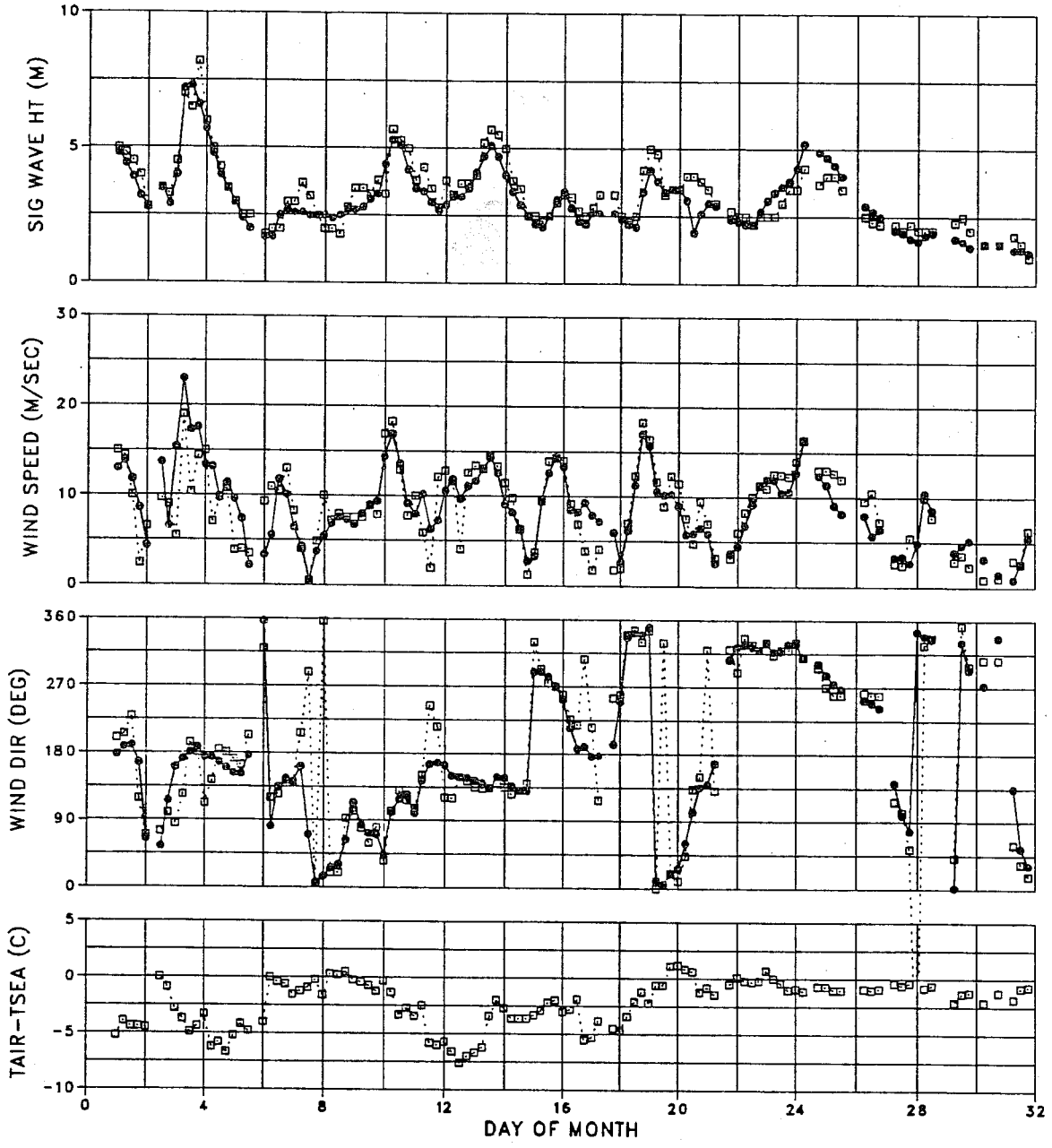

WAVES

MODEL MEAN = 3.1 STDEV = 1.2
OBS MEAN = 3.3 STDEV = 1.2
LSQ FIT: SLOPE = 0.88 INTR = 0.21
RMSE = 0.53
CORR COEF = 0.90 SI = 0.16

WINDS

MODEL MEAN = 8.8 STDEV = 4.2
OBS MEAN = 8.8 STDEV = 4.5
LSQ FIT: SLOPE = 0.76 INTR = 2.14
RMSE = 2.69
CORR COEF = 0.81 SI = 0.31

BUOY 64042 (60.5N, 2.9W)
APRIL 1988

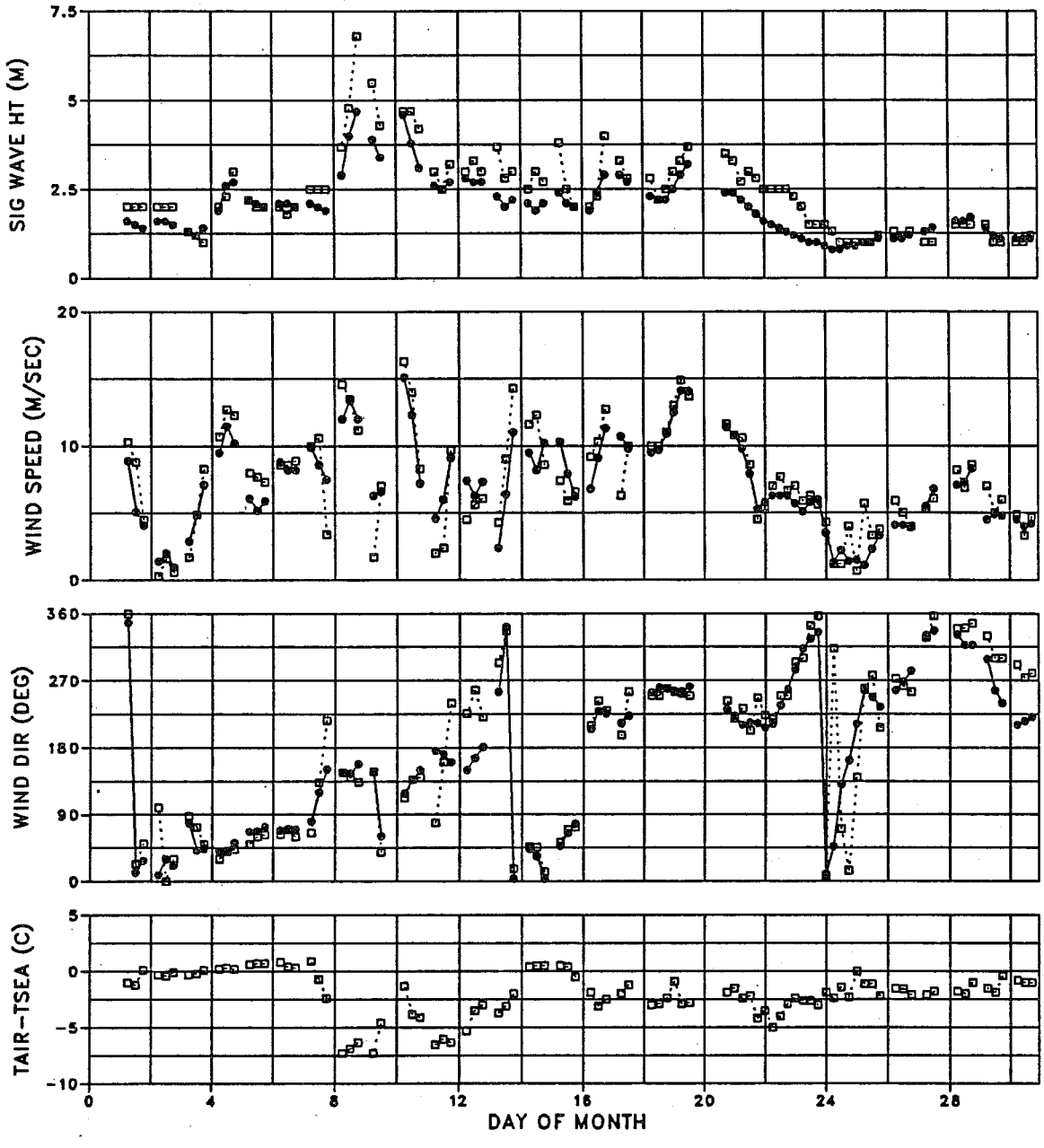

WAVES

MODEL MEAN = 2.0 STDEV = 0.8
OBS MEAN = 2.4 STDEV = 1.1
LSQ FIT: SLOPE = 0.68 INTR = 0.35
RMSE = 0.49
CORR COEF = 0.92 SI = 0.20

WINDS

MODEL MEAN = 7.1 STDEV = 3.3
OBS MEAN = 7.5 STDEV = 3.7
LSQ FIT: SLOPE = 0.80 INTR = 1.14
RMSE = 1.68
CORR COEF = 0.89 SI = 0.23

BUOY 64041 (60.5N, 2.9W)
NOVEMBER 1988

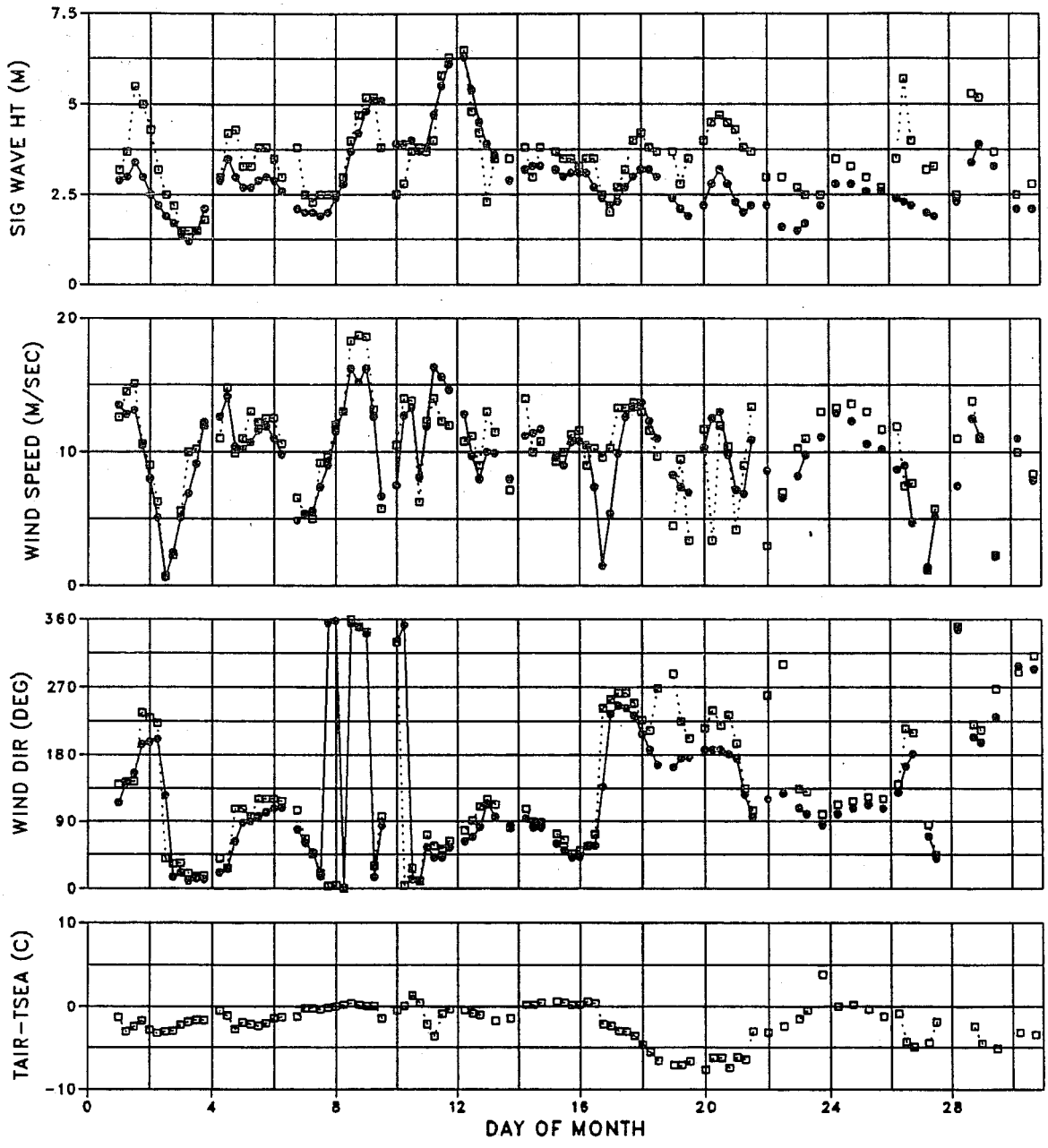

WAVES

MODEL MEAN = 2.9 STDEV = 1.0
OBS MEAN = 3.5 STDEV = 1.0
LSQ FIT: SLOPE = 0.69 INTR = 0.47
RMSE = 0.79
CORR COEF = 0.69 SI = 0.22

WINDS

MODEL MEAN = 9.8 STDEV = 3.4
OBS MEAN = 10.3 STDEV = 3.6
LSQ FIT: SLOPE = 0.75 INTR = 2.11
RMSE = 2.19
CORR COEF = 0.81 SI = 0.21

TECHNICAL REPORTS

No. 1 A case study of a ten day prediction.
K. Arpe, L. Bengtsson, A. Hollingsworth and Z. Janjic. September, 1976

No. 2 The effect of arithmetic precision on some meteorological integrations.
A.P.M. Baede, D. Dent and A. Hollingsworth. December, 1976

No. 3 Mixed-radix fourier transforms without reordering.
C. Temperton. February, 1977

No. 4 A model for medium range weather forecasts - adiabatic formulation.
D.M. Burridge and J. Haseler. March, 1977

No. 5 A study of some parameterisations of sub-grid processes in a baroclinic wave in a two dimensional model.
A. Hollingsworth. July, 1977

No. 6 The ECMWF analysis and data assimilation scheme: analysis of mass and wind field.
A. Lorenc, I. Rutherford and G. Larsen. December, 1977

No. 7 A ten-day high-resolution non-adiabatic spectral integration; a comparative study.
A.P.M. Baede and A.W. Hansen. October, 1977

No. 8 On the asymptotic behaviour of simple stochastic-dynamic systems.
A. Wiin-Nielsen. November, 1977

No. 9 On balance requirements as initial conditions.
A. Wiin-Nielsen. October, 1978

No. 10 ECMWF model parameterisation of sub-grid scale processes.
M. Tiedtke, J-F. Geleyn, A. Hollingsworth, and J-F. Louis. January, 1979

No. 11 Normal mode initialization for a multi-level grid-point model.
C. Temperton and D.L. Williamson. April, 1979

No. 12 Data assimilation experiments.
R. Seaman. October, 1978

No. 13 Comparison of medium range forecasts made with two parameterisation schemes.
A. Hollingsworth, K. Arpe, M. Tiedkte, M. Capaldo, H. Savijarvi, O. Akesson and J.A. Woods. October, 1978

No. 14 On initial conditions for non-hydrostatic models.
A.C. Wiin-Nielsen. November, 1978

No. 15 Adiabatic formulation and organization of ECMWF's spectral model.
A.P.M. Baede, M. Jarraud and U. Cubasch. November, 1979

No. 16 Model studies of a developing boundary layer over the ocean.
H. Okland. November, 1979

No. 17 The response of a global barotropic model to forcing by large scale orography.
J. Quiby. January 1980.

No. 18 Confidence limits for verification and energetic studies.
K. Arpe. May, 1980

No. 19 A low order barotropic model on the sphere with orographic and newtonian forcing.
E. Kallen. July, 1980

No. 20 A review of the normal mode initialization method.
Du Xing-yuan. August, 1980

No. 21 The adjoint equation technique applied to meteorological problems.
G. Kontarev. September, 1980

No. 22 The use of empirical methods for mesoscale pressure forecasts.
P. Bergthorsson. November, 1980

No. 23 Comparison of medium range weather forecasts made with models using spectral or finite difference techniques in the horizontal.
M. Jarraud, C. Girard and U. Cubasch. February, 1981

No. 24 On the average error of an ensemble of forecasts.
J. Derome. February, 1981

No. 25 On the atmospheric factors affecting the Levantine Sea.
E. Ozsoy. May, 1981

No. 26 Tropical influences on stationary wave motion in middle and high latitudes.
A.J. Simmons. August, 1981

No. 27 The energy budgets in North America, North Atlantic and Europe based on ECMWF analysis and forecasts.
H. Savijarvi. November, 1981

No. 28 An energy and angular momentum conserving finite-difference scheme, hybrid coordinates and medium range weather forecasts.
A.J. Simmons and R. Strüfing. November, 1981

No. 29 Orographic influences on Mediterranean lee cyclogenesis and European blocking in a global numerical model.
S. Tibaldi and A. Buzzi. February, 1982

No. 30 Review and re-assessment of ECNET - A private network with open architecture.
A. Haag, F. Konigshofer and P. Quoilin. May, 1982

No. 31 An investigation of the impact at middle and high latitudes of tropical forecast errors.
J. Haseler. August, 1982

No. 32 Short and medium range forecast differences between a spectral and grid point model. An extensive quasi-operational comparison. C. Girard and M. Jarraud
August, 1982

No. 33 Numerical simulations of a case of blocking: The effects of orography and land-sea contrast.
L.R. Ji and S. Tibaldi. September, 1982

No. 34 The impact of cloud track wind data on global analyses and medium range forecasts.
P. Kallberg, S. Uppala, N. Gustafsson and J. Pailleux. December, 1982

No. 35 Energy budget calculations at ECMWF. Part 1: Analyses 1980-81.
E. Oriol. December, 1982

No. 36 Operational verification of ECMWF forecast fields and results for 1980-1981.
R. Nieminen. February, 1983

No. 37 High resolution experiments with the ECMWF model: a case study.
L. Dell'Osso. September, 1983

No. 38 The response of the ECMWF global model to the El-Nino anomaly in extended range prediction experiments.
U. Cubasch. September, 1983

No. 39 On the parameterisation of vertical diffusion in large-scale atmospheric models.
M.J. Manton. December, 1983

No. 40 Spectral characteristics of the ECMWF objective analysis system.
R. Daley. December, 1983

No. 41 Systematic errors in the baroclinic waves of the ECMWF model.
E. Klinker and M. Capaldo. February, 1984

No. 42 On long stationary and transient atmospheric waves.
A.C. Wiin-Nielsen. August, 1984

No. 43 A new convective adjustment scheme.
A.K. Betts and M.J. Miller. October, 1984

No. 44 Numerical experiments on the simulation of the 1979 Asian summer monsoon.
U.C. Mohanty, R.P. Pearce and M. Tiedtke. October, 1984

No. 45 The effect of mechanical forcing on the formation of a mesoscale vortex.
G-X. Wu and S-J. Chen. October, 1984

No. 46 Cloud prediction in the ECMWF model.
J. Slingo and B. Ritter. January, 1985

No. 47 Impact of aircraft wind data on ECMWF analyses and forecasts during the FGGE period, 8-19 November, 1979.
A.P.M. Baede, P. Kallberg and S. Uppala. March, 1985

No. 48 A numerical case study of East Asian coastal cyclogenesis.
Shou-jun Chen and L. Dell'Osso. May, 1985

No. 49 A study of the predictability of the ECMWF operational forecast model in the tropics.
M. Kanamitsu. September, 1985

No. 50 On the development of orographic cyclones.
D. Radinovic. June, 1985

No. 51 Climatology and system error of rainfall forecasts at ECMWF.
F. Molteni and S. Tibaldi. October, 1985

No. 52 Impact of modified physical processes on the tropical simulation in the ECMWF model.
U.C. Mohanty, J.M. Slingo and M. Tiedtke. October, 1985

No. 53 The performance and systematic errors of the ECMWF tropical forecasts (1982-1984).
W.A. Heckley. November, 1985

No. 54 Finite element schemes for the vertical discretization of the ECMWF forecast model using linear elements.
D.M. Burridge, J. Steppeler and R. Strüfing. January, 1986

No. 55 Finite element schemes for the vertical discretization of the ECMWF forecast model using quadratic and cubic elements.
J. Steppeler. February, 1986

No. 56 Sensitivity of medium-range weather forecasts to the use of an envelope orography.
M. Jarraud, A.J. Simmons and M. Kanamitsu. September, 1986

No. 57 Zonal diagnostics of the ECMWF 1984-85 operational analyses and forecasts.
C. Brankovic. October, 1986

No. 58 An evaluation of the performance of the ECMWF operational forecasting system in analysing and forecasting tropical easterly wave disturbances. Part 1: Synoptic investigation.
R.J. Reed, A. Hollingsworth, W.A. Heckley and F. Delsol. September, 1986

No. 59 Diabatic nonlinear normal mode initialisation for a spectral model with a hybrid vertical coordinate.
W. Wergen. January, 1987

No. 60 An evaluation of the performance of the ECMWF operational forecasting system in analysing and forecasting tropical easterly wave disturbances. Part 2: Spectral investigation.
R.J. Reed, E. Klinker and A. Hollingsworth. January, 1987

No. 61 Empirical orthogonal function analysis in the zonal and eddy components of 500 mb height fields in the Northern extratropics.
F. Molteni. January, 1987

No. 62 Atmospheric effective angular momentum functions for 1986-1987.
G. Sakellarides. February 1989.